iScience

CellPress

Article

Pd-CuFe Catalyst for Transfer Hydrogenation of Nitriles: Controllable Selectivity to Primary Amines and Secondary Amines

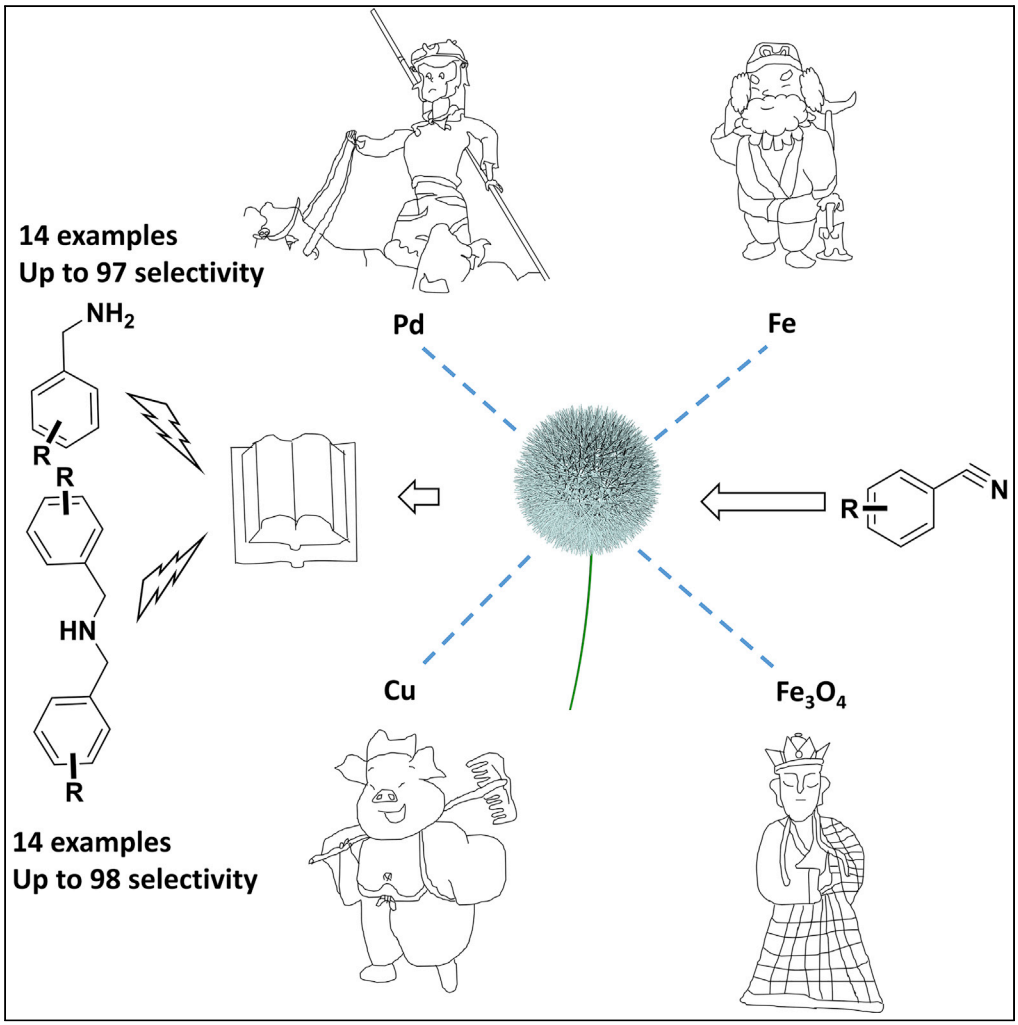

Lei Liu, Yuhong Liu, Yongjian Ai, ..., Yue Wang, Qionglin Liang, Hongbin Sun

liuyuhong@tsinghua.edu.cn (Y.L.)
liangql@mail.tsinghua.edu.cn (Q.L.)
sunhb@mail.neu.edu.cn (H.S.)

HIGHLIGHTS

The novel transfer hydrogenation of nitriles to primary or secondary amine

The dosage of Pd can be reduced to 139 ppm with a TOF of 3,597 hr^{-1}

The selectivity of products can be easily adjusted by electronic modulation

Liu et al., iScience 8, 61–73
October 26, 2018
https://doi.org/10.1016/j.isci.2018.09.010

iScience

CellPress

Article

Pd-CuFe Catalyst for Transfer Hydrogenation of Nitriles: Controllable Selectivity to Primary Amines and Secondary Amines

Lei Liu,[1,2] Yuhong Liu,[2,*] Yongjian Ai,[3] Jifan Li,[1] Junjie Zhou,[1] Zhibo Fan,[1] Hongjie Bao,[1] Ruihang Jiang,[1] Zenan Hu,[1] Jingting Wang,[1] Ke Jing,[1] Yue Wang,[2] Qionglin Liang,[3,*] and Hongbin Sun[1,4,*]

SUMMARY

A multicomponent nanocatalyst system was fabricated for the transfer hydrogenation of nitrile compounds. This catalyst system contains palladium, copper, and iron, which are supported on the magnetite nanospheres, and the loading of palladium could be at the parts per million level. Palladium and copper contribute to the transformation of nitrile, and the product distribution highly depends on the alloying of Fe to Cu. The nitriles could be converted to primary amine by the Pd-Cu catalyst in the absence of Fe, whereas in the presence of Fe the products are secondary amines with high selectivity. This could be attributed to the electronic modulation of iron to copper. A variety of nitriles have been transformed to the corresponding primary or secondary amines with high selectivity, and the TOF reaches 2,929 hr^{-1} for Pd. Furthermore, the catalyst could be recycled by an external magnetic field and reused five times without severe activity loss.

INTRODUCTION

Amines and their derivatives are manufactured on a large scale by the fine chemical industry every year, as they are important building blocks for the production of dyestuff, pesticides, and pharmaceuticals (Muller and Beller, 1998; Tang and Zhang, 2003; Pohlki and Doye, 2003; Severin and Doye, 2007; Mueller et al., 2008). They are generally prepared by reductive aminations (Storer et al., 2006; Gross et al., 2002), amination of aryl halides (Hartwig, 2006; Buchwald et al., 2006), the direct amination of alcohols (Gunanathan and Milstein, 2008; Ye et al., 2014; Pingen et al., 2010; Imm et al., 2010; Oldenhuis et al., 2014; Woeckel et al., 2014), and hydroamination (Muller and Beller, 1998; Mueller et al., 2008; Hartwig, 2008) of olefins. Beyond these, the catalytic reduction of nitriles is recognized as one of the most efficient and greenest one-step synthesis of these high-valued amine products (Werkmeister et al., 2014; Bagal and Bhanage, 2015). However, there are severe selectivity issues in the hydrogenation of nitrile so that mixtures of primary, secondary, and even tertiary amines via imine intermediates (Srimani et al., 2012; Chakraborty and Berke, 2014) are usually obtained (Scheme 1). Therefore, a catalyst that can selectively acquire any one of these products is being intensively pursuing. Within these possibilities, an interesting but challenging assignment is direct hydrogenation to form selectively either secondary or tertiary amines (Shao et al., 2016). The reason is that the reaction sequence involves at least four steps through nitrile reduction. Therefore, the activity and selectivity need to be precisely controlled.

Current researches about the reduction of nitriles are mostly conducted with pressurized hydrogen (Srimani et al., 2012; Tokmic et al., 2017; Chakraborty et al., 2017; Mukherjee et al., 2017; Adam et al., 2016, 2017; Cao et al., 2016; Elangovan et al., 2016; Chakraborty and Milstein, 2017; Ji et al., 2017; Yoshimura et al., 2018). However, direct hydrogenation is always labeled as a harsh synthetic process due to the explosive nature of hydrogen (Schafer et al., 2017). It is well known that catalytic hydrogenation with H_2 and transfer hydrogenation are two parallel pathways for hydrogenation reactions. Complementary to the traditional hydrogenation, transfer hydrogenation occurs at milder conditions (Gladiali and Alberico, 2006). The commonly applied H-donor molecules include hydrazine (Kumarraja and Pitchumani, 2004), isopropanol (Mohapatra et al., 2002), glycerol (Gawande et al., 2012), and formic acid (Prasad et al., 2005). In 2014, Beller's group achieved selective reduction of nitriles to primary amines in the presence of commercially available Pd/C with the $HCOOH/NEt_3$ system (Vilches-Herrera et al., 2014). In 2016, Li's group developed the transition metal alloy nanoparticles (NPs) (binary among Co, Ni, and Cu) that were embedded in N-doped carbon matrix and subsequently used in the transfer hydrogenation of nitriles in isopropanol to

[1]Department of Chemistry, Northeastern University, Shenyang 110819, People's Republic of China

[2]State Key Laboratory of Tribology, Tsinghua University, Beijing 100084, People's Republic of China

[3]Key Laboratory of Bioorganic Phosphorus Chemistry & Chemical Biology (Ministry of Education), Department of Chemistry, Tsinghua University, Beijing 100084, People's Republic of China

[4]Lead Contact

*Correspondence: liuyuhong@tsinghua.edu.cn (Y.L.), liangql@mail.tsinghua.edu.cn (Q.L.), sunhb@mail.neu.edu.cn (H.S.)

https://doi.org/10.1016/j.isci.2018.09.010

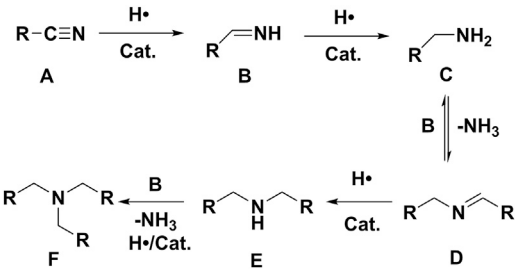

Scheme 1. The Probable Products in Nitrile Reduction: the Nature of Selectivity Issues

selectively yield the imines (Long et al., 2016). In 2017, Li's group designed a bifunctional N-doped Co@C catalyst system (Co@NC) for the transfer hydrogenation of nitriles under base-free conditions with isopropyl alcohol as the proton donor to realize the selective synthesis of imines or amines (Long et al., 2017).

Recently, ammonia borane (AB, $NH_3 \cdot BH_3$) has become a promising hydrogen source because of its high hydrogen density (hydrogen content of 19.6 wt %), nontoxicity, and high solubility in water and alcohol (Peng and Chen, 2008; Demirci and Miele, 2009; Rossin and Peruzzini, 2016; Metin et al., 2010; Koepke et al., 2016; Gutowska et al., 2005). In 2014–2017, Sun's group continuously reported the facile synthesis of bimetal NPs (NiPd, FePd, and CuNi) and their assembly on graphene to catalyze the tandem AB dehydrogenation and hydrogenation of R-NO_2 and/or R-CN to R-NH_2 in aqueous methanol solutions (Goksu et al., 2014; Metin et al., 2016; Yu et al., 2017). Recently, Fu's group reported a heterogeneous Ni_2P catalytic system for the hydrogenation of nitriles to primary amines with AB as the hydrogen source (Zen et al., 2017). Actually, investigation on metal-catalyzed selective reduction of nitriles to secondary amines is rare, until Liu's group described the first homogeneous Co-pincer-catalyzed transfer hydrogenation of nitriles for the chemodivergent synthesis of primary and secondary amines with AB in 2016 (Shao et al., 2016). However, there are some problems with aforementioned the researches: the massive noble metal loading or ultralong reaction time. And to date, the facile synthesis of primary and secondary amines through selective hydrogenation of nitriles is endowed with significance and challenge.

As a continuation of our previous research in transfer hydrogenation (Sun et al., 2017; Ai et al., 2018a, 2018b; Zhou et al., 2017; Bao et al., 2018), we herein achieved a highly efficient heterogeneous catalytic reduction of nitriles to yield primary or secondary amines chemodiversely. This catalytic system holds an equilibrium point between low-loading palladium and short reaction time in the nitrile hydrogenation with the assistance of Cu sites. Moreover, the chemoselectivity could be precisely controlled by electronic modulation of metal alloying. The catalyst diagram and preparation flowchart are shown in Scheme 2.

RESULTS AND DISCUSSION

We employed the rough-edged Fe_3O_4 nanospheres as the support for the catalyst, and the reduction of benzonitrile was the model reaction. The conversion of benzonitrile and the selectivity of products over various catalysts are shown in Figure 1 (see Table S1 for more details). It is obvious that only copper can greatly enhance the catalytic effect of the low-loading palladium metal catalyst to complete the

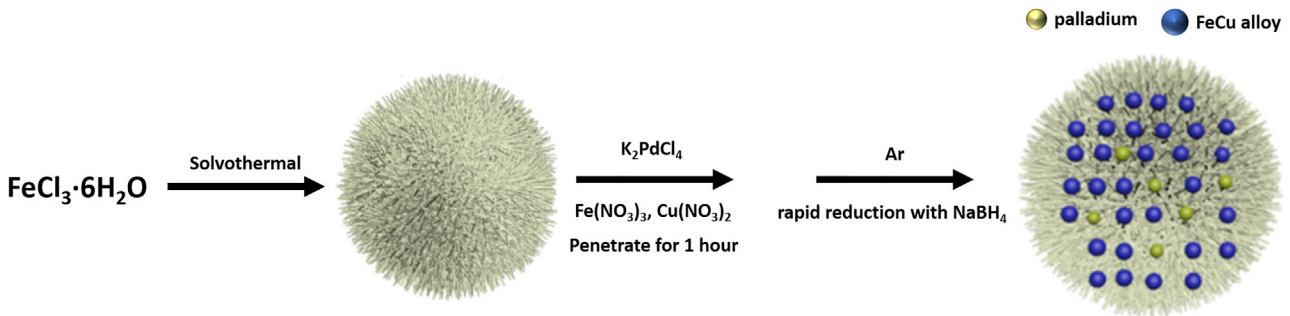

Scheme 2. The Flowchart for Preparation of the Catalyst

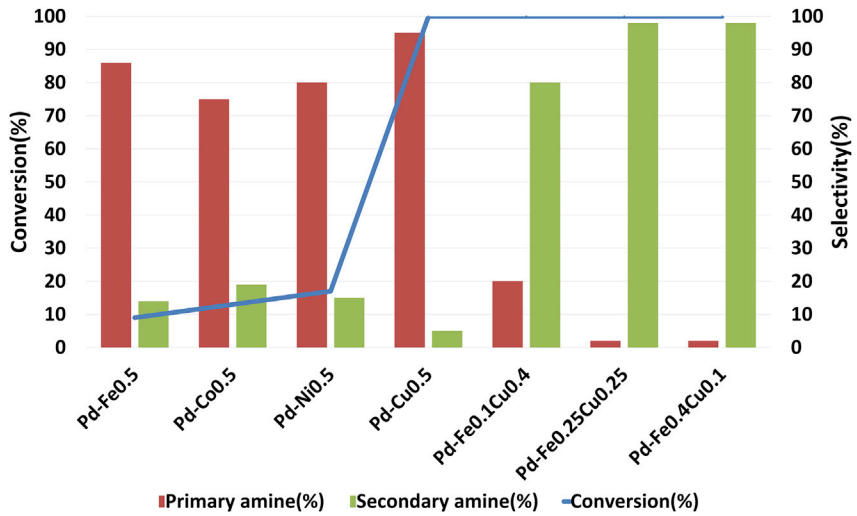

Figure 1. Screening of Catalysts

The catalysts that are expressed as Pd-$M1_xM2_y/Fe_3O_4$ are prepared with 0.5 mg $PdCl_2$, x and y mmol nitrate, and 100 mg Fe_3O_4.

See also Table S1.

transformation of benzonitrile to primary amines (Figure 1 and Table S1, entries 1–10). We believe that it is copper that activated the cyano group and made the triple bond easier to break through.

From the reduction pathway of nitriles (Scheme 1), we conclude that the selectivity of products is intensively determined by the lifetime of the intermediate imine. When it lives shortly, the product is a primary amine, otherwise secondary and tertiary amines are obtained. Applying the electronic modulation, which is a currently popular strategy (Guo et al., 2018; Bai et al., 2018), we modified the Pd-Cu catalyst with a third component to lessen the effect of copper so as to obtain secondary amines (Figure 1 and Table S1, entries 11–17). As expected, the secondary amines were selectively obtained when Fe, Co, or Ni was alloyed with copper, and the optimized catalyst was confirmed as Pd-$Fe_{0.25}Cu_{0.25}/Fe_3O_4$. The actual composition determined by inductively coupled plasma mass spectrometry (ICP-MS) is 0.24% Pd and 11.86% Cu; it means each reaction just needs 228 ppm Pd. The turnover of frequency (TOF) reached 2,929 hr^{-1} for Pd and 35.42 hr^{-1} for Fe or Cu. The reaction rate slowed down with the decline of palladium content (0.15% Pd determined by ICP-MS), but the TOF reached up to 3,597 hr^{-1} for a 139-ppm Pd catalyst (Table S1, entry 21). To verify the heterogeneity of the active center, a hot filtration test was performed. Once 30% of the benzonitrile was transformed (10 min, detected by gas chromatography [GC]), the Pd-$Fe_{0.25}Cu_{0.25}/Fe_3O_4$ catalyst was magnetically separated and the reaction was then continued in the tube for an additional 1 hr. There was no noticeable increase of conversion; this revealed that the amount of Pd(II), Cu(II), and Fe(III) ions leaching out was negligible and the catalyst was indeed heterogeneous in nature.

Characterization

The morphologies of Fe_3O_4 prepared by solvothermal method (Deng et al., 2005) and the optimum catalyst were investigated by transmission electron microscopy (TEM) and high-resolution TEM. As shown in Figure 2A, the Fe_3O_4 support is a relatively uniform pompon-like nanosphere with an average size of about 300 nm, and the external villi and the inner voids are distinguishable. It is also worth noting that the catalyst samples maintained similar shapes to those of their parent carrier material, and no large particles could be obviously observed on the surface of the catalysts (Figures 2B and S1). To demonstrate the form of active site, we selected a typical catalyst particle with more detailed characterization (Figures 2C–2I). The selected area electron diffraction (SAED) characterization presented high crystallinity of the catalyst (Figure 2E). The planes of the cubic phase of Fe_3O_4 were marked in parentheses, and the lattice spacing of 0.111, 0.173, 0.258, 0.301, and 0.495 nm correspond to the (553), (422), (311), (220), and (111) planes of the cubic phase of FeCu alloy, respectively (JCPDS No. 49-1399). Metallic palladium was confirmed due to the discovery of its (111) planes, 0.225 nm. No palladium alloy phase was detectable because the reduction potentials of Pd^{2+} to Fe^{3+} or Cu^{2+} were far apart, so the co-reduction of Pd with the two other metal ions is impossible in the absence of ligand

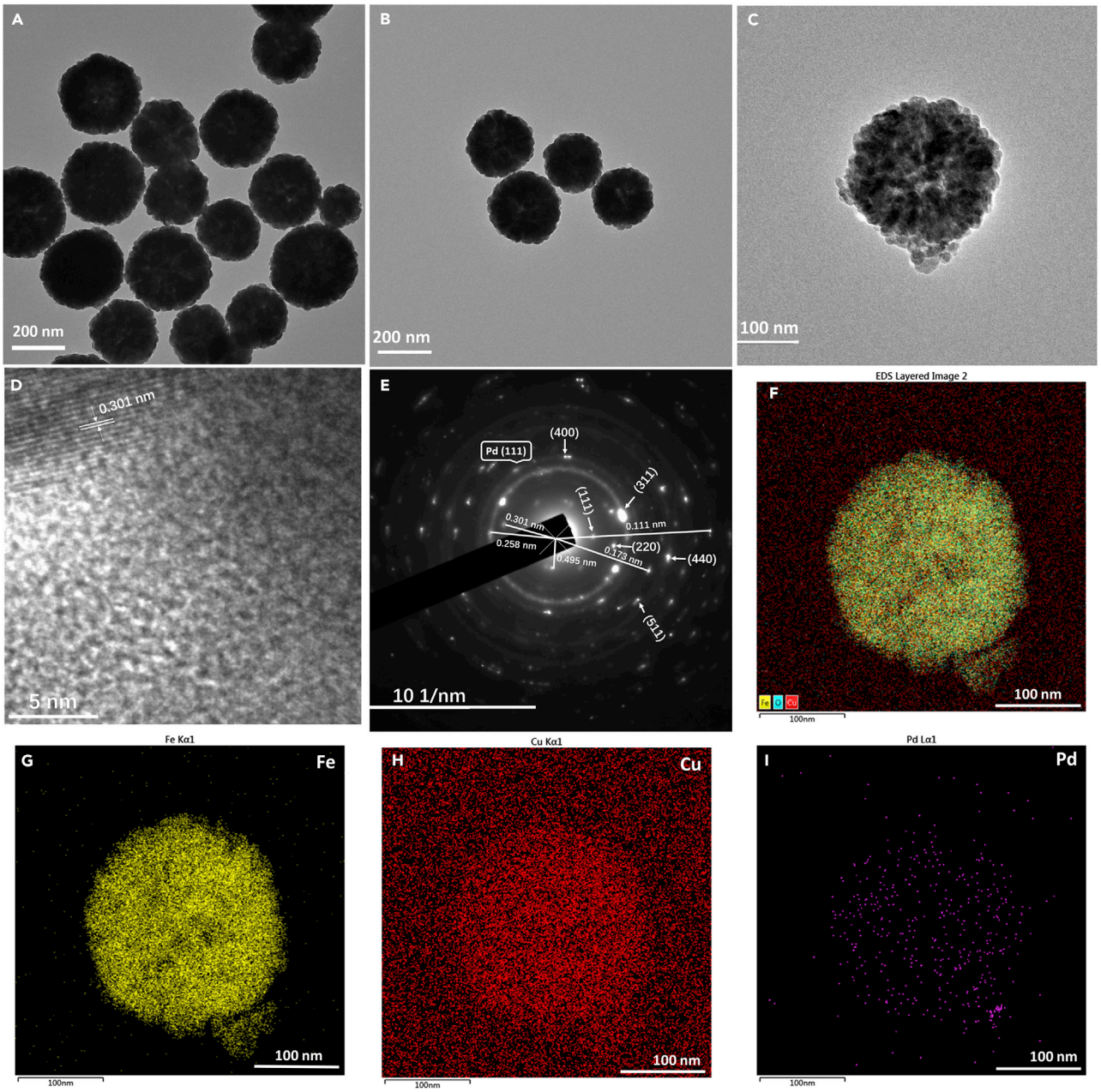

Figure 2. Characterization of Morphology

(A) Transmission electron microscopic (TEM) image of the Fe_3O_4 carrier. (B, C, and E–I) TEM image, high-resolution TEM (HRTEM) image, SEAD characterization, and EDS elemental mappings of the catalyst. (D) HRTEM image of a single Pd-FeCu NP.
See also Figure S1.

compound (Zhang et al., 2015; Diyarbakir et al., 2015). Figure 2D highlights a typical FeCu alloy nanoparticle with crystal lattice of 0.301 nm, which is discovered from the scattered particle in Figure 2F and assigned to the (220) interplanar spacing because the regular nanoparticles can only display the lattice stripes of ferric oxide (Figure S1). In addition, elemental mappings point out that Pd is evenly distributed in the catalysts (Figure 2I). All these evidences indicated that the active metal sites permeated into Fe_3O_4.

The structural information was further revealed by powder X-ray diffraction analysis (Figure 3). We initially characterized Pd-FeCu/Fe_3O_4, but the spectrum only displayed the diffraction peaks of magnetite

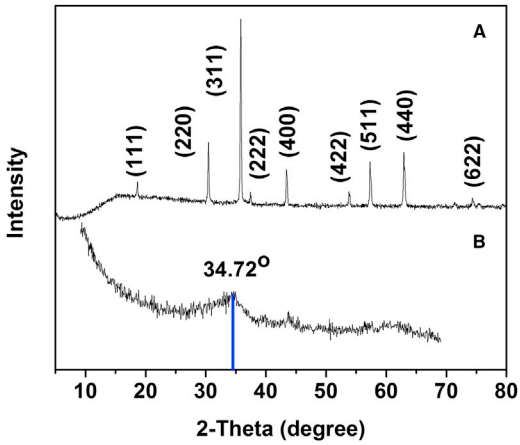

Figure 3. Characterization of Structure

X-ray diffraction pattern of optimal catalyst (A) and sole Pd-FeCu nanoparticles without carrier (B).

(Figure 3A). Suspecting that the high crystallinity of ferric oxide obscured the signal of alloy phase, we subsequently verified a carrier-free catalyst that was fabricated with a similar preparation process. The diffraction peaks at $2\theta = 34.72^{\circ}$ were assigned to the (311) plane of the cubic phase of FeCu alloy, and there was still no signal about the alloy phase of Pd (Figure 3B). Combining the energy dispersive X-ray spectroscopy (EDS) and SAED results, we believe that iron and copper existed as alloy in the catalyst, whereas palladium particles existed independently.

X-ray photoelectron spectroscopic characterization was further conducted to analyze the electronic modulation in the catalyst. For all materials, two main peaks around 932.6 and 706.7 eV are observable in the Cu 2p and Fe 2p regions (Figures 4, S2, and S3), respectively, indicating that Cu and Fe atoms are in the metallic state. For the Pd-$Fe_{0.5}/Fe_3O_4$ and Pd-$Cu_{0.5}/Fe_3O_4$, the unaltered binding energy (BE) of $Cu2p_{3/2}$, $Fe2p_{3/2}$, and $Pd3d_{5/2}$ relative to standard values implies that Pd does not form alloy with Cu or Fe (Figure S2). When iron is introduced in Pd-Cu/Fe_3O_4, a negative shift occurred for Cu $2p_{3/2}$ and a positive shift appeared for $Fe2p_{3/2}$ compared with their benchmark values, which indicates the electron transfer process. Meanwhile, the offset of Cu $2p_{3/2}$ BE in Pd-$FeCu/Fe_3O_4$ gradually increases along with the enhancement of the ratio of Fe to Cu, whereas the offset of Fe $2p_{3/2}$ displayed a gradual decrease. This is in agreement with the literature about fabrication of FeCu alloy (He et al., 2010; Ma et al., 2015).

The secondary amine selectivity and BE of Cu $2p_{3/2}$ are plotted against the Cu/Fe ratio for the PdFeCu-based catalysts (Figure 5), and the nature of the plot indicates that the electronic modulation of copper intensively affects the selectivity of reduction of nitrile. The alloying of Fe enhances the electron density of surface Cu; this hinders the activation of imine intermediates and consequently leads to the high selectivity of secondary amines.

The Substrate Exploration

In expectation, these pompon-like nanoparticles could smoothly catalyze the transfer hydrogenations of a broad scope of nitriles to selectively afford their corresponding primary or secondary amines along with perfect electronic modulation (Table 1). As investigated, the substrates bearing electron-donating groups, such as methyl benzonitrile and methoxy benzonitrile, produced the corresponding benzylamines with up to 97% selectivity (Table 1, entries 1–8), while the corresponding secondary amine products could be obtained with up to 98% selectivity (Table 1, entries 1–3, 5–8). Specifically, the slightly declined yield of bis(2-methylbenzyl)amine may be due to the steric hindrance (Table 1, entry 4). Likewise, electron-withdrawing functional groups, including fluoro, chloro, and trifluoromethyl, were all well tolerated to this methodology. They gave the desired benzylamine products with up to 90% selectivity (Table 1, entries 9–12) or generated the corresponding secondary amines with up to 95% selectivity (Table 1, entries 9–12). It is worth noting that no dehalogenated product was detectable in this catalytic system. Furthermore, aliphatic nitriles deserve particular mention in this regard, because the α-H can cause base-induced condensation as

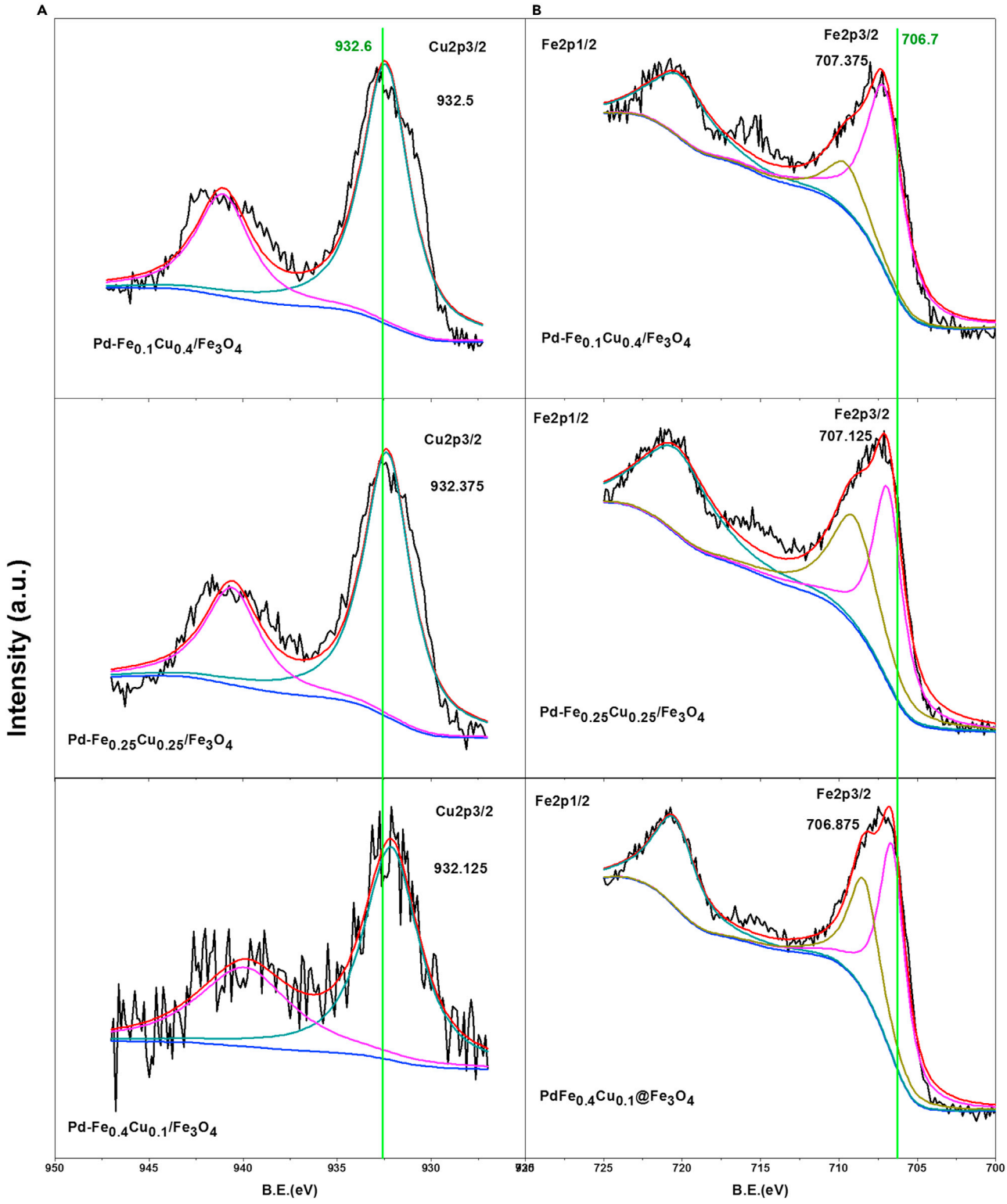

Figure 4. Characterization of Electron Modulation

X-ray photoelectron spectroscopy of Pd-FeCu/Fe_3O_4 in the (A) Cu 2p and (B) Fe 2p regions.

See also Figures S2 and S3.

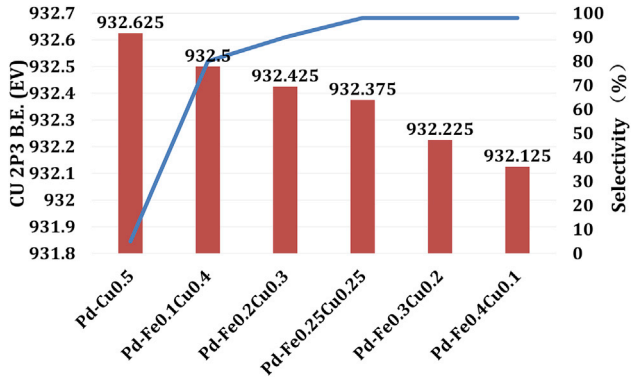

Figure 5. Cu $2p_{3/2}$ BEs and Secondary Amine Selectivities in Different Catalysts
See also Figure S3.

potential side reactions and aliphatic imines are usually unstable (Chakraborty and Milstein, 2017). However, in the present system, phenylacetonitrile underwent the transfer hydrogenation successfully, affording the corresponding primary and secondary amine products in 88% and 94% selectivities, respectively (Table 1, entry 13). Again, acetonitrile was also quantitatively converted into the corresponding products (Table 1, entry 14).

It should be mentioned that recyclability is an essential property for a heterogeneous catalyst. In this regard, we performed a reusability test for the Pd-$Fe_{0.25}Cu_{0.25}/Fe_3O_4$ catalysts in the synthesis of dibenzylamine at the optimized reaction conditions. The catalyst can be easily retrieved via magnetic separation at the end of a reaction. After lavation with ethanol and drying, a new batch was implemented. As shown in Figure 6, the catalyst exhibits almost no activity change in the first three runs, and the activity remained at 85% of the initial level after five runs. We attribute this robustness to the porous structure of the carrier (Figure S4) and magnetic attraction of Fe_3O_4 to FeCu alloy (Bao et al., 2018).

Based on these detailed experimental results, a plausible mechanism is depicted in Figure 7. Initially, the active hydrogen species are produced from the Pd-catalyzed decomposition of AB for further hydrogenation, and they are stored on ferric oxide, which has been reported to have hydrogen spillover capacity (Karim et al., 2017). The imine intermediate and primary amines were generated successively by hydrogen transfer. By alloying of iron, the activity of electron-rich copper decreased, which resulted in an extended life of the imine intermediates, which subsequently underwent nucleophilic attacked by the amine. The intermediate product was the unstable gem-diamine, whose deamination gave the secondary imine. Finally, the imine received active H species to provide the desired secondary amines. The role of copper is to activate the C-N multibond and make it easier to be broken, and the iron's function is to alloy with copper and thereby regulate the activation ability of copper. The trace amount of palladium is responsible for breaking down the NH_3BH_3 to provide active hydrogen species at a proper rate. The fissure-rich Fe_3O_4 nanospheres supply the workshop for the dispersion of active sites and storage of active hydrogen species. So each one of these components in our catalyst is indispensable, and the delicate proportion between them is also vital.

Conclusions

In summary, we have developed an efficient multi-metallic catalyst system for the controllable transfer hydrogenation of nitriles to generate primary and secondary amines with a perfect switch. Low-loading palladium, copper with cyano-activation, and iron with electronic modulation are indispensable, and the pompon-like magnetite nanosphere provides a workshop for the dispersion of active sites and magnetic recyclability. A variety of nitriles generated their corresponding primary and secondary amines with highly controllable selectivity applying NH_3BH_3 as the hydrogen donor. The high efficiency, controllable selectivity, good compatibility, and recyclability combined with mild reaction conditions makes this system a promising pathway for transfer hydrogenations of nitriles.

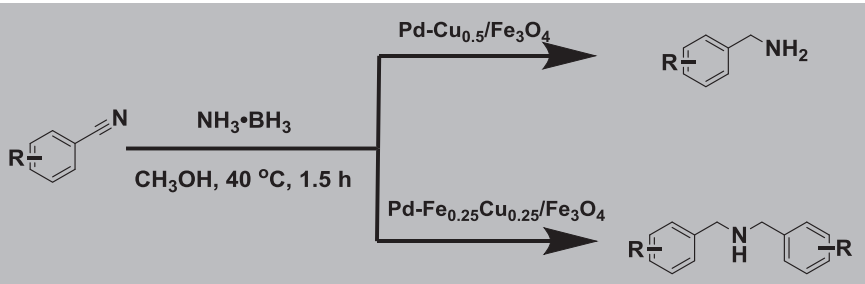

Entry	Substrate[a]	$Pd\text{-}Cu_{0.5}/Fe_3O_4$			$Pd\text{-}Fe_{0.25}Cu_{0.25}/Fe_3O_4$		
		Con. (%)	Product	Sel. (%)	Con. (%)	Product	Sel. (%)
1	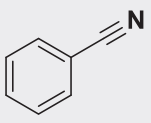	>99	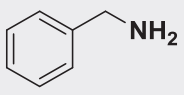	95	>99	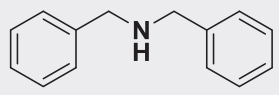	98
2	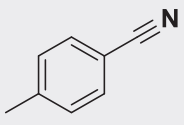	>99	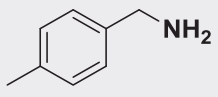	93	>99	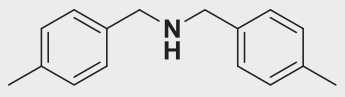	97
3	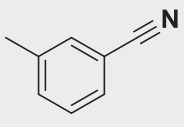	>99	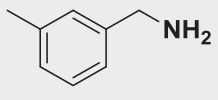	96	>99	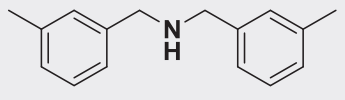	97
4	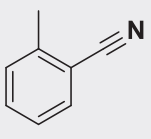	>99	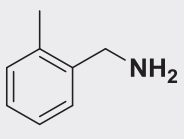	97	>99	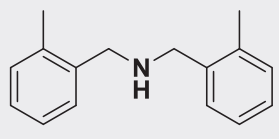	76
5	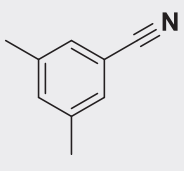	>99	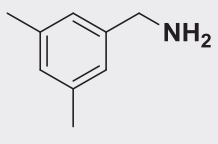	95	>99	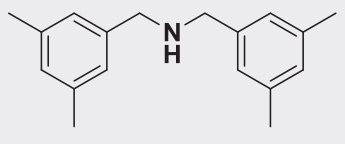	95

Table 1. Transfer Hydrogenation of Various Nitriles to Primary Amines and Secondary Amines

(Continued on next page)

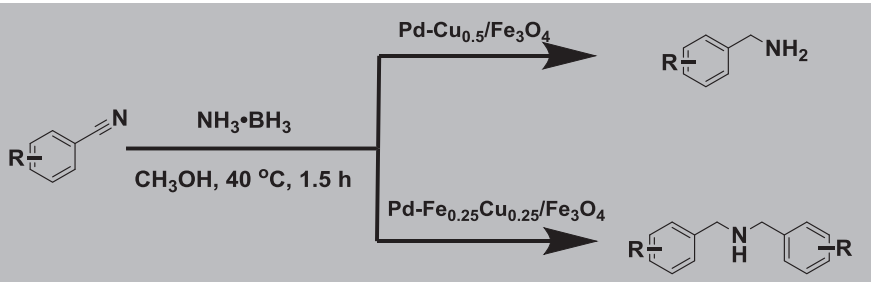

Entry	Substrate[a]	Pd-$Cu_{0.5}/Fe_3O_4$			Pd-$Fe_{0.25}Cu_{0.25}/Fe_3O_4$		
		Con. (%)	Product	Sel. (%)	Con. (%)	Product	Sel. (%)
6	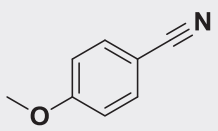	>99	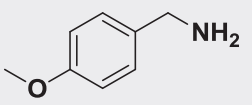	92	>99	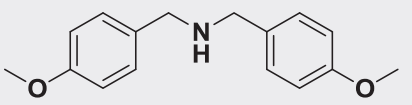	96
7	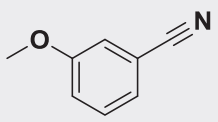	>99	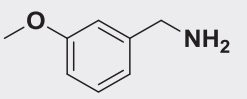	94	>99	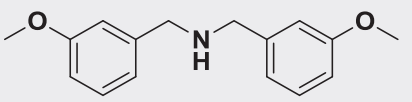	98
8	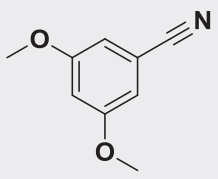	>99	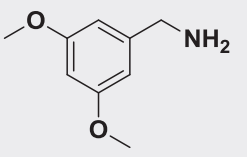	93	>99	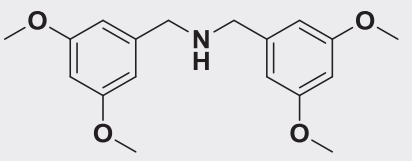	97
9	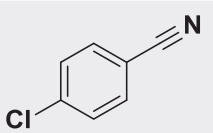	>99	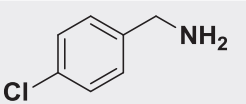	83	>99	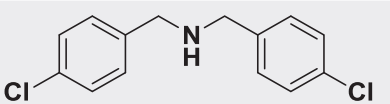	87
10	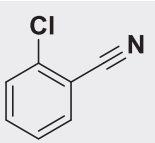	>99	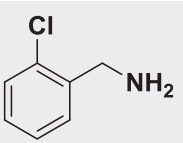	89	>99	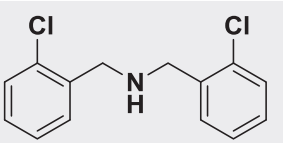	95

Table 1. ***Continued***

(Continued on next page)

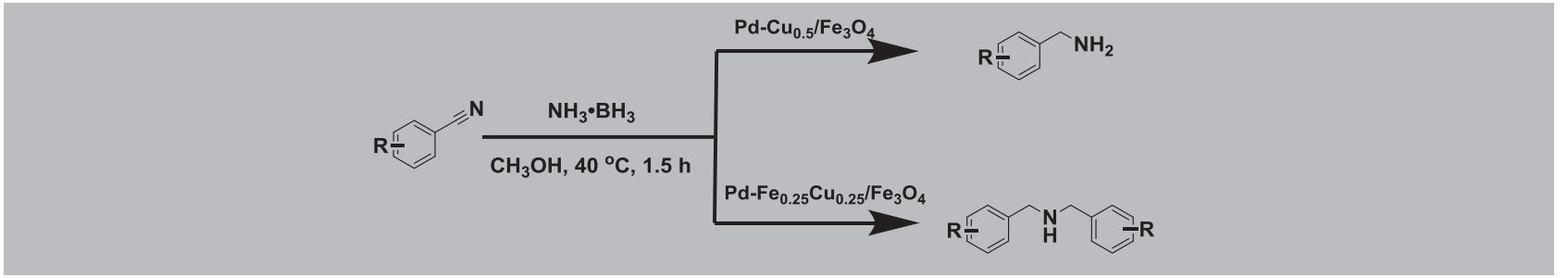

Entry	Substrate[a]	$Pd\text{-}Cu_{0.5}/Fe_3O_4$			$Pd\text{-}Fe_{0.25}Cu_{0.25}/Fe_3O_4$		
		Con. (%)	Product	Sel. (%)	Con. (%)	Product	Sel. (%)
11	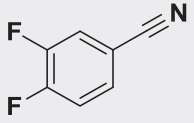	>99	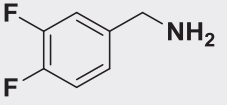	85	>99	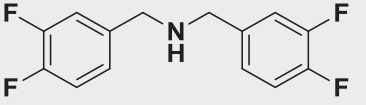	90
12	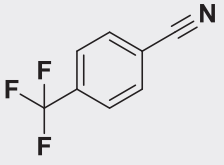	>99	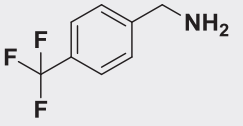	90	>99	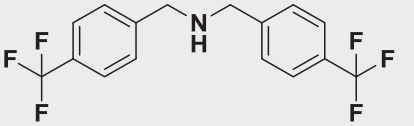	83
13	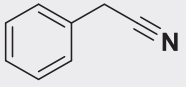	>99	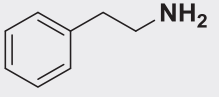	88	>99	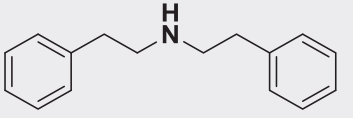	94
14	CH_3CN	>99	$CH_3CH_2NH_2$	97	>99	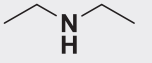	95

Table 1. Continued

GC, gas chromatography

[a]Reaction conditions: nitrile (1 mmol), AB (3 mmol), and catalyst (10 wt% of substrate) in 2 mL of CH_3OH were heated at 40°C for 90 min. GC yield (%) were shown using biphenyl as the internal standard.

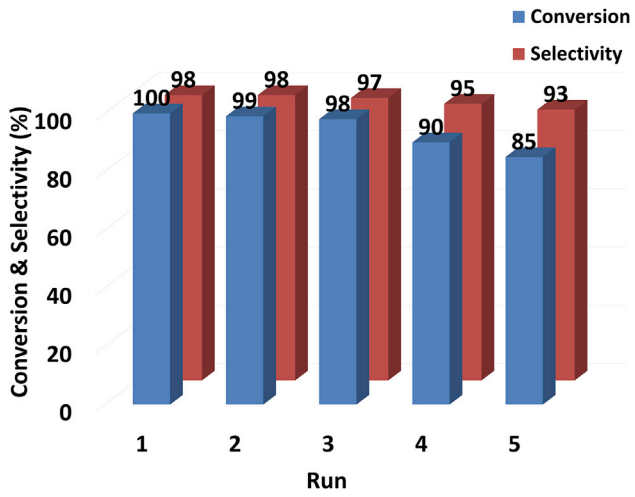

Figure 6. Stability of the Optimum Catalyst
See also Figure S4.

Limitations of Study

The higher reaction temperature will produce borate crystals above the bottle wall. The solvent is chromatographic methanol, otherwise the imine will hydrolyze. The regeneration of the catalyst has not been studied yet.

METHODS

All methods can be found in the accompanying Transparent Methods supplemental file.

SUPPLEMENTAL INFORMATION

Supplemental Information includes Transparent Methods, four figures, and one table and can be found with this article online at https://doi.org/10.1016/j.isci.2018.09.010.

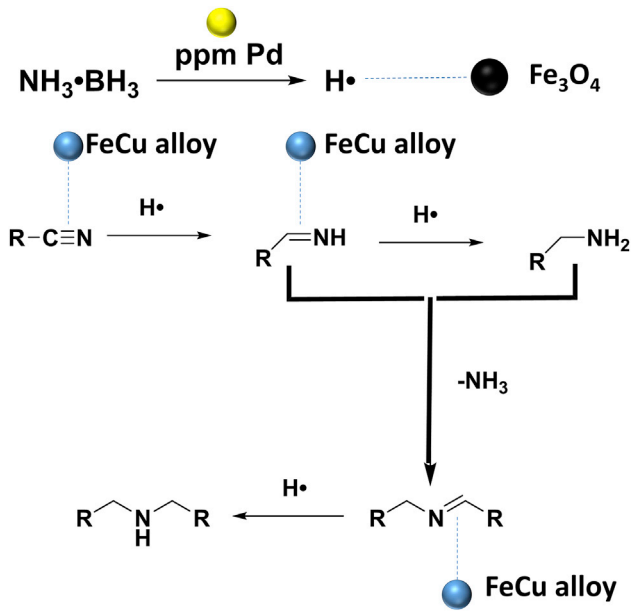

Figure 7. Plausible Mechanism for the Hydrogenation of Nitriles to Secondary Amines Catalyzed by Pd-$Fe_{0.25}Cu_{0.25}/Fe_3O_4$

ACKNOWLEDGMENTS

This work was financially supported by the National Science Fund for Excellent Young Scholars (51522504), the Ministry of Science and Technology (Nos.2017YFC0906902 and 2017ZX09301032), National Natural Science Foundation of China (No. 21621003) and Macau Science and Technology Development Fund (129/2017/A3 and 089/2013/A3).

AUTHOR CONTRIBUTIONS

L.L. conducted the experiments and finished the main manuscript. Y.A. performed the TEM and HRTEM characterization. Y.W. performed the XPS characterization. Y.L. and Q.L. provided financial support. J.L., J.Z., Z.F., H.B., R.J., Z.H., J.W., K.J., H.S. contributed to the analysis and discussion of data, reviewed the manuscript, and approved the final version of the manuscript.

DECLARATION OF INTERESTS

The authors declare no competing interests.

Received: August 5, 2018
Revised: September 1, 2018
Accepted: September 12, 2018
Published: October 26, 2018

REFERENCES

Adam, R., Alberico, E., Baumann, W., Drexler, H.-J., Jackstell, R., Junge, H., and Beller, M. (2016). NNP-type pincer imidazolylphosphine ruthenium complexes: efficient base-free hydrogenation of aromatic and aliphatic nitriles under mild conditions. Chem. Eur. J. *22*, 4991–5002.

Adam, R., Bheeter, C.B., Cabrero-Antonino, J.R., Junge, K., Jackstell, R., and Beller, M. (2017). Selective hydrogenation of nitriles to primary amines by using a cobalt phosphine catalyst. Chemsuschem *10*, 842–846.

Ai, Y.J., He, M.Q., Lv, Q.R., Liu, L., Sun, H.B., Ding, M.Y., and Liang, Q.L. (2018a). 3D porous carbon framework stabilized ultra-uniform nano gamma-Fe2O3: a useful catalyst system. Chem. Asian J. *13*, 89–98.

Ai, Y.J., Hu, Z.N., Shao, Z.X., Qi, L., Liu, L., Zhou, J.J., Sun, H.B., and Liang, Q.L. (2018b). Egg-like magnetically immobilized nanospheres: a long-lived catalyst model for the hydrogen transfer reaction in a continuous-flow reactor. Nano Res. *11*, 287–299.

Bagal, D.B., and Bhanage, B.M. (2015). Recent advances in transition metal-catalyzed hydrogenation of nitriles. Adv. Synth. Catal. *357*, 883–900.

Bai, S., Bu, L., Shao, Q., Zhu, X., and Huang, X. (2018). Multicomponent Pt-based zigzag nanowires as selectivity controllers for selective hydrogenation reactions. J. Am. Chem. Soc. *140*, 8384–8387.

Bao, H., Li, Y., Liu, L., Ai, Y., Zhou, J., Qi, L., Jiang, R., Hu, Z., Wang, J., Sun, H., and Liang, Q. (2018). Ultrafine FeCu alloy nanoparticles magnetically immobilized in amine-rich silica spheres for dehalogenation-proof hydrogenation of nitroarenes. Chem. Eur. J. https://doi.org/10.1002/chem.201801942.

Buchwald, S.L., Mauger, C., Mignani, G., and Scholz, U. (2006). Industrial-scale palladium-catalyzed coupling of aryl halides and amines - a personal account. Adv. Synth. Catal. *348*, 23–39.

Cao, Y., Niu, L., Wen, X., Feng, W., Huo, L., and Bai, G. (2016). Novel layered double hydroxide/oxide-coated nickel-based core-shell nanocomposites for benzonitrile selective hydrogenation: an interesting water switch. J. Catal. *339*, 9–13.

Chakraborty, S., and Berke, H. (2014). Homogeneous hydrogenation of nitriles catalyzed by molybdenum and tungsten amides. ACS Catal. *4*, 2191–2194.

Chakraborty, S., and Milstein, D. (2017). Selective hydrogenation of nitriles to secondary imines catalyzed by an iron pincer complex. ACS Catal. *7*, 3968–3972.

Chakraborty, S., Leitus, G., and Milstein, D. (2017). Iron-catalyzed mild and selective hydrogenative cross-coupling of nitriles and amines to form secondary aldimines. Angew. Chem. Int. Ed. *56*, 2074–2078.

Demirci, U.B., and Miele, P. (2009). Sodium borohydride versus ammonia borane, in hydrogen storage and direct fuel cell applications. Energ. Environ. Sci. *2*, 627–637.

Deng, H., Li, X.L., Peng, Q., Wang, X., Chen, J.P., and Li, Y.D. (2005). Monodisperse magnetic single-crystal ferrite microspheres. Angew. Chem. Int. Ed. *44*, 2782–2785.

Diyarbakir, S., Can, H., and Metin, O. (2015). Reduced graphene oxide-supported CuPd alloy nanoparticles as efficient catalysts for the Sonogashira cross-coupling reactions. ACS Appl. Mater. Interfaces *7*, 3199–3206.

Elangovan, S., Topf, C., Fischer, S., Jiao, H., Spannenberg, A., Baumann, W., Ludwig, R., Junge, K., and Beller, M. (2016). Selective catalytic hydrogenations of nitriles, ketones, and aldehydes by well-defined manganese pincer complexes. J. Am. Chem. Soc. *138*, 8809–8814.

Gawande, M.B., Rathi, A.K., Branco, P.S., Nogueira, I.D., Velhinho, A., Shrikhande, J.J., Indulkar, U.U., Jayaram, R.V., Ghumman, C.A.A., Bundaleski, N., and Teodoro, O.M.N.D. (2012). Regio- and chemoselective reduction of nitroarenes and carbonyl compounds over recyclable magnetic ferrite-nickel nanoparticles (Fe3O4-Ni) by using glycerol as a hydrogen source. Chem. Eur. J. *18*, 12628–12632.

Gladiali, S., and Alberico, E. (2006). Asymmetric transfer hydrogenation: chiral ligands and applications. Chem. Soc. Rev. *35*, 226–236.

Goksu, H., Ho, S.F., Metin, O., Korkmaz, K., Garcia, A.M., Gultekin, M.S., and Sun, S.H. (2014). Tandem dehydrogenation of ammonia borane and hydrogenation of nitro/nitrile compounds catalyzed by graphene-supported NiPd alloy nanoparticles. ACS Catal. *4*, 1777–1782.

Gross, T., Seayad, A.M., Ahmad, M., and Beller, M. (2002). Synthesis of primary amines: first homogeneously catalyzed reductive amination with ammonia. Org. Lett. *4*, 2055–2058.

Gunanathan, C., and Milstein, D. (2008). Selective synthesis of primary amines directly from alcohols and ammonia. Angew. Chem. Int. Ed. *47*, 8661–8664.

Guo, M., Li, H., Ren, Y., Ren, X., Yang, Q., and Li, C. (2018). Improving catalytic hydrogenation performance of Pd nanoparticles by electronic modulation using phosphine ligands. ACS Catal. https://doi.org/10.1021/acscatal.8b00872.

Gutowska, A., Li, L.Y., Shin, Y.S., Wang, C.M.M., Li, X.H.S., Linehan, J.C., Smith, R.S., Kay, B.D., Schmid, B., Shaw, W., et al. (2005). Nanoscaffold mediates hydrogen release and the reactivity of ammonia borane. Angew. Chem. Int. Ed. *44*, 3578–3582.

Hartwig, J.F. (2006). Discovery and understanding of transition-metal-catalyzed aromatic substitution reactions. Synlett *9*, 1283–1294.

Hartwig, J.F. (2008). Carbon-heteroatom bond formation catalysed by organometallic complexes. Nature *455*, 314–322.

He, M., Chernov, A.I., Fedotov, P.V., Obraztsova, E.D., Sainio, J., Rikkinen, E., Jiang, H., Zhu, Z., Tian, Y., Kauppinen, E.I., et al. (2010). Predominant (6,5) single-walled carbon nanotube growth on a copper-promoted iron catalyst. J. Am. Chem. Soc. *132*, 13994–13996.

Imm, S., Baehn, S., Neubert, L., Neumann, H., and Beller, M. (2010). An efficient and general synthesis of primary amines by ruthenium-catalyzed amination of secondary alcohols with ammonia. Angew. Chem. Int. Ed. *49*, 8126–8129.

Ji, P., Manna, K., Lin, Z., Feng, X., Urban, A., Song, Y., and Lin, W. (2017). Single-site cobalt catalysts at new Z(r12)(mu(3)-O)(8)(mu(3)-OH)(8)(mu(2)-OH)(6) metal-organic framework nodes for highly active hydrogenation of nitroarenes, nitriles, and isocyanides. J. Am. Chem. Soc. *139*, 7004–7011.

Karim, W., Spreafico, C., Kleibert, A., Gobrecht, J., VandeVondele, J., Ekinci, Y., and van Bokhoven, J.A. (2017). Catalyst support effects on hydrogen spillover. Nature *541*, 68.

Koepke, J.C., Wood, J.D., Chen, Y.F., Schmucker, S.W., Liu, X.M., Chang, N.N., Nienhaus, L., Do, J.W., Carrion, E.A., Hewaparakrama, J., et al. (2016). Role of pressure in the growth of hexagonal boron nitride thin films from ammonia-borane. Chem. Mater. *28*, 4169–4179.

Kumarraja, M., and Pitchumani, K. (2004). Simple and efficient reduction of nitroarenes by hydrazine in faujasite zeolites. Appl. Catal. A *265*, 135–139.

Long, J., Shen, K., Chen, L., and Li, Y. (2016). Multimetal-MOF-derived transition metal alloy NPs embedded in an N-doped carbon matrix: highly active catalysts for hydrogenation reactions. J. Mater. Chem. A *4*, 10254–10262.

Long, J., Shen, K., and Li, Y. (2017). Bifunctional N-doped Co@C catalysts for base-free transfer hydrogenations of nitriles: controllable selectivity to primary amines vs imines. ACS Catal. *7*, 275–284.

Ma, C.L., Chen, Y.L., and Chen, J.G. (2015). Surfactant-assisted preparation of FeCu catalyst for Fischer-Tropsch synthesis. J. Brazil. Chem. Soc. *26*, 1520–1526.

Metin, O., Mazumder, V., Ozkar, S., and Sun, S.S. (2010). Monodisperse nickel nanoparticles; and their catalysis in hydrolytic dehydrogenation of ammonia borane. J. Am. Chem. Soc. *132*, 1468.

Metin, O., Mendoza-Garcia, A., Dalmizrak, D., Gultekin, M.S., and Sun, S.H. (2016). FePd alloy nanoparticles assembled on reduced graphene oxide as a catalyst for selective transfer hydrogenation of nitroarenes to anilines using ammonia borane as a hydrogen source. Catal. Sci. Technol. *6*, 6137–6143.

Mohapatra, S.K., Sonavane, S.U., Jayaram, R.V., and Selvam, P. (2002). Heterogeneous catalytic transfer hydrogenation of aromatic nitro and carbonyl compounds over cobalt(II) substituted hexagonal mesoporous aluminophosphate molecular sieves. Tetrahedron Lett. *43*, 8527–8529.

Mueller, T.E., Hultzsch, K.C., Yus, M., Foubelo, F., and Tada, M. (2008). Hydroamination: direct addition of amines to alkenes and alkynes. Chem. Rev. *108*, 3795–3892.

Mukherjee, A., Srimani, D., Ben-David, Y., and Milstein, D. (2017). Low-pressure hydrogenation of nitriles to primary amines catalyzed by ruthenium pincer complexes. scope and mechanism. Chemcatchem *9*, 559–563.

Muller, T.E., and Beller, M. (1998). Metal-initiated amination of alkenes and alkynes. Chem. Rev. *98*, 675–703.

Oldenhuis, N.J., Dong, V.M., and Guan, Z. (2014). From racemic alcohols to enantiopure amines: Ru-catalyzed diastereoselective amination. J. Am. Chem. Soc. *136*, 12548–12551.

Peng, B., and Chen, J. (2008). Ammonia borane as an efficient and lightweight hydrogen storage medium. Energ. Environ. Sci. *1*, 479–483.

Pingen, D., Muller, C., and Vogt, D. (2010). Direct amination of secondary alcohols using ammonia. Angew. Chem. Int. Ed. *49*, 8130–8133.

Pohlki, F., and Doye, S. (2003). The catalytic hydroamination of alkynes. Chem. Soc. Rev. *32*, 104–114.

Prasad, K., Jiang, X.L., Slade, J.S., Clemens, J., Repic, O., and Blacklock, T.J. (2005). New trends in palladium-catalyzed transfer hydrogenations using formic acid. Adv. Synth. Catal. *347*, 1769–1773.

Rossin, A., and Peruzzini, M. (2016). Ammonia-borane and amine-borane dehydrogenation mediated by complex metal hydrides. Chem. Rev. *116*, 8848–8872.

Schafer, C., Ellstrom, C.J., Cho, H., and Torok, B. (2017). Pd/C-Al-water facilitated selective reduction of a broad variety of functional groups. Green Chem. *19*, 1230–1234.

Severin, R., and Doye, S. (2007). The catalytic hydroamination of alkynes. Chem. Soc. Rev. *36*, 1407–1420.

Shao, Z., Fu, S., Wei, M., Zhou, S., and Liu, Q. (2016). Mild and selective cobalt-catalyzed chemodivergent transfer hydrogenation of nitriles. Angew. Chem. Int. Ed. *55*, 14653–14657.

Srimani, D., Feller, M., Ben-David, Y., and Milstein, D. (2012). Catalytic coupling of nitriles with amines to selectively form imines under mild hydrogen pressure. Chem. Commun. *48*, 11853–11855.

Storer, R.I., Carrera, D.E., Ni, Y., and MacMillan, D.W.C. (2006). Enantioselective organocatalytic reductive amination. J. Am. Chem. Soc. *128*, 84–86.

Sun, H.B., Ai, Y.J., Li, D., Tang, Z.K., Shao, Z.X., and Liang, Q.L. (2017). Bismuth iron oxide nanocomposite supported on graphene oxides as the high efficient, stable and reusable catalysts for the reduction of nitroarenes under continuous flow conditions. Chem. Eng. J. *314*, 328–335.

Tang, W.J., and Zhang, X.M. (2003). New chiral phosphorus ligands for enantioselective hydrogenation. Chem. Rev. *103*, 3029–3069.

Tokmic, K., Jackson, B.J., Salazar, A., Woods, T.J., and Fout, A.R. (2017). Cobalt-catalyzed and Lewis acid-assisted nitrile hydrogenation to primary amines: a combined effort. J. Am. Chem. Soc. *139*, 13554–13561.

Vilches-Herrera, M., Werkmeister, S., Junge, K., Boerner, A., and Beller, M. (2014). Selective catalytic transfer hydrogenation of nitriles to primary amines using Pd/C. Catal. Sci. Technol. *4*, 629–632.

Werkmeister, S., Junge, K., and Beller, M. (2014). Catalytic hydrogenation of carboxylic acid esters, amides, and nitriles with homogeneous catalysts. Org. Process. Res. Dev. *18*, 289–302.

Woeckel, S., Plessow, P., Schelwies, M., Brinks, M.K., Rominger, F., Hofmann, P., and Limbach, M. (2014). Alcohol amination with aminoacidato Cp*Ir(III)-complexes as catalysts: dissociation of the chelating ligand during initiation. ACS Catal. *4*, 152–161.

Ye, X., Plessow, P.N., Brinks, M.K., Schelwies, M., Schaub, T., Rominger, F., Paciello, R., Limbach, M., and Hofmann, P. (2014). Alcohol amination with ammonia catalyzed by an acridine-based ruthenium pincer complex: a mechanistic study. J. Am. Chem. Soc. *136*, 5923–5929.

Yoshimura, M., Komatsu, A., Niimura, M., Takagi, Y., Takahashi, T., Ueda, S., Ichikawa, T., Kobayashi, Y., Okami, H., Hattori, T., et al. (2018). Selective synthesis of primary amines from nitriles under hydrogenation conditions. Adv. Synth. Catal. *360*, 1726–1732.

Yu, C., Fu, J.J., Muzzio, M., Shen, T.L., Su, D., Zhu, J.J., and Sun, S.H. (2017). CuNi nanoparticles assembled on graphene for catalytic methanolysis of ammonia borane and hydrogenation of nitro/nitrile compounds. Chem. Mater. *29*, 1413–1418.

Zen, Y.F., Fu, Z.C., Liang, F., Xu, Y., Yang, D.D., Yang, Z., Gan, X., Lin, Z.S., Chen, Y., and Fu, W.F. (2017). Robust hydrogenation of nitrile and nitro groups to primary amines using Ni2P as a catalyst and ammonia borane under ambient conditions. Asian J. Org. Chem. *6*, 1589–1593.

Zhang, L., Su, H.Y., Sun, M., Wang, Y.C., Wu, W.L., Yu, T.Y., and Zeng, J. (2015). Concave Cu-Pd bimetallic nanocrystals: ligand-based Co-reduction and mechanistic study. Nano Res. *8*, 2415–2430.

Zhou, J.J., Li, Y.N., Sun, H.B., Tang, Z.K., Qi, L., Liu, L., Ai, Y.J., Li, S., Shao, Z.X., and Liang, Q.L. (2017). Porous silica-encapsulated and magnetically recoverable Rh NPs: a highly efficient, stable and green catalyst for catalytic transfer hydrogenation with "slow-release" of stoichiometric hydrazine in water. Green Chem. *19*, 3400–3407.

ISCI, Volume *8*

Supplemental Information

Pd-CuFe Catalyst for Transfer Hydrogenation of Nitriles: Controllable Selectivity to Primary Amines and Secondary Amines

Lei Liu, Yuhong Liu, Yongjian Ai, Jifan Li, Junjie Zhou, Zhibo Fan, Hongjie Bao, Ruihang Jiang, Zenan Hu, Jingting Wang, Ke Jing, Yue Wang, Qionglin Liang, and Hongbin Sun

Contents

Transparent Methods

Preparation of Fe_3O_4 microsphere : 1.35 g $FeCl_3 \cdot 6H_2O$ was dissolved in 40 ml ethylene glycol to form a clear solution, subsequently NaAc (3.6 g) and PEG-200 (1.0 g) were added. The mixture was stirred vigorously for 30 min and then sealed in a Teflon-lined stainless-steel autoclave (50 mL capacity). The autoclave was heated to 200 ^oC and maintained for 8 h, and allowed to cool to room temperature. The black products were washed several times with ethanol and dried at 60 ^oC for 6 h.

Fabrication of Pd-$Fe_{0.25}Cu_{0.25}/Fe_3O_4$: 0.5 mg $PdCl_2$ were dissolved in 10 ml 0.1 mol/L KCl solution, and then transferred to a round-bottom flask (250 mL) contains 0.25 mmol $Fe(NO_3)_3$, 0.25 mmol $Cu(NO_3)_2$ and 100 mg Fe_3O_4 activated by 60 mL 0.1 mol/L HCl for 30 min. Subsequently, 40 mL methanol and 40 mL H_2O were added. The mixture was stirred vigorously for 1 hour under Ar atmosphere. In the end, 0.1 g $NaBH_4$ were dissolved in 10 mL methanol and then transferred to above reactor and maintained overnight. The final material were separated by a magnet and washed several times with ethanol, then dried at 60 ^oC for 6 h. Other catalysts were prepared by similar procedure.

Typical procedure for the synthesis of benzylamine.

1 mmol benzonitrile, 3 mmol AB, 10 mg Pd-$Cu_{0.5}/Fe_3O_4$ and 2 mL methanol were added to a sealed tube (15 mL) and heated at 40 ^oC for 1.5 hour. After quenching, the mixture were analyzed by GC with the biphenyl as internal standard. The reaction liquid were extracted with H_2O (10 mL) and CH_2Cl_2 (30 mL). The organic phase was dried with hydrous Na_2SO_4 and evaporated in vacuum. The residue was purified by flash column chromatography on silica gel (SiO_2, petroleum ether/EtOAc) to afford the benzylamine.

Typical procedure for the synthesis of dibenzylamine.

1 mmol benzonitrile, 3 mmol AB, 10 mg Pd-$Fe_{0.25}Cu_{0.25}/Fe_3O_4$ and 2 mL methanol were added to a sealed tube (15 mL) and heated at 40 ^oC for 1.5 hour. After quenching, the mixture were analyzed by GC with the biphenyl as internal standard. The reaction liquid were extracted with H_2O (10 mL) and CH_2Cl_2 (30 mL). The organic phase was dried with hydrous Na_2SO_4 and evaporated in vacuum. The residue was purified by flash column chromatography on silica gel (SiO_2, petroleum ether/EtOAc) to afford the dibenzylamine.

Table S1. Conditions optimization experiments, related to Fig.1.

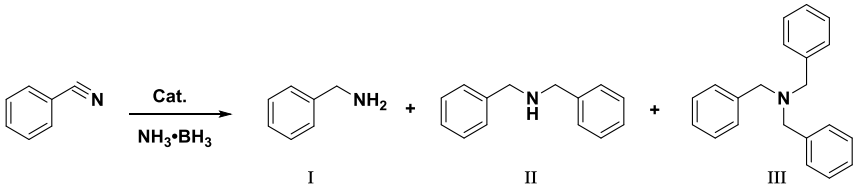

Entry	Catalyst	Conversion (%)	Selectivity (%)		
			I	II	III
1	0.5%Pd/Fe_3O_4	trace	-	-	-
2	1%Pd/Fe_3O_4	trace	-	-	-
3	3%Pd/Fe_3O_4	trace	-	-	-
4	5%Pd/Fe_3O_4	19	65	22	13
5	7%Pd/Fe_3O_4	21	67	23	10
6[b]	Pd-Ni/Fe_3O_4	45	80	15	5
7[b]	Pd-Co/Fe_3O_4	39	75	19	6
8[b]	Pd-Fe/Fe_3O_4	20	86	14	-
9[b]	Pd-Cu/Fe_3O_4	>99	95	5	-
10[c]	Pd-Cu/Fe_3O_4	>99	95	5	-
11[c]	Pd-$Fe_{0.1}Cu_{0.4}$/Fe_3O_4	>99	20	80	-
12[c]	Pd-$Fe_{0.2}Cu_{0.3}$/Fe_3O_4	>99	10	90	-
13[c]	Pd-$Fe_{0.25}Cu_{0.25}$/Fe_3O_4	>99	2	98	-
14[c]	Pd-$Fe_{0.3}Cu_{0.2}$/Fe_3O_4	>99	2	98	-
15[c]	Pd-$Fe_{0.4}Cu_{0.1}$/Fe_3O_4	>99	2	98	-
16[c]	Pd-$Co_{0.25}Cu_{0.25}$/Fe_3O_4	>99	15	85	-
17[c]	Pd-$Ni_{0.25}Cu_{0.25}$/Fe_3O_4	>99	14	86	-
18[d]	Pd-$Fe_{0.25}Cu_{0.25}$/Fe_3O_4	90	5	95	-
19[e]	Pd-$Fe_{0.25}Cu_{0.25}$/Fe_3O_4	60	6	94	-
20	$Fe_{0.25}Cu_{0.25}$/Fe_3O_4	none	-	-	-
21[f]	Pd-$Fe_{0.25}Cu_{0.25}$/Fe_3O_4	>99	2	98	-
22	Pd-$Cu_{0.5}$/Fe_3O_4+Fe/Fe_3O_4	>99	96	4	-
23[g]	Pd-$Cu_{0.5}$/Fe_3O_4	58	98	2	-
24[h]	Pd-$Cu_{0.5}$/Fe_3O_4	none	-	-	-
25[i]	Pd-$Cu_{0.5}$/Fe_3O_4	26	-	-	-

[a]Reactions conditions unless specified otherwise: benzonitrile (1 mmol), NH_3BH_3 (3 mmol), catalyst (10 wt %), methanol (2 mL), 40 °C, 1.5 h. [b]5 mg $PdCl_2$+0.5 mmol base metal/100 mg Fe_3O_4. [C]0.5 mg $PdCl_2$+0.5 mmol base metal/100 mg Fe_3O_4 (The subscript represents the mmol of that element in 100 mg Fe_3O_4.). [d]The solvent is anhydrous ethanol. [e]The solvent is isopropanol. [f]0.2 mg $PdCl_2$+0.5 mmol base metal/100 mg Fe_3O_4, 2 h. [g]The donor is $NaBH_4$. [h]The donor is isopropanol. [i]The donor is hydrazine. GC yield (%) were shown using biphenyl as the internal standard.

Generally, iron oxide is a fine carrier in the hydrogenation, so we decided to employ the Fe_3O_4 as the basis for the catalyst. The conversion of benzonitrile and the selectivity of products over various catalysts are shown in Table S1. Based on literatures on palladium-catalyzed reduction of nitriles, we firstly screened a series of metal loadings (Table S1, entries 1-5). It turns out that the conversion of benzonitrile is not satisfactory in the case of low loadings. And the support is not able to carry more active sites otherwise the palladium nanoparticles aggregated severely. Compared with monometallic NPs, the bimetallic and trimetallic integration or alloy NPs of these transition metals emerged distinct and superior catalytic activity in many reaction systems due to the strong metal–metal interactions and altered electronic character. Therefore, we added several transition metals that are usually utilized in hydrogenation with palladium to inspect their catalytic ability (Table S1, entries 6-9). It is obvious that only the copper element can greatly enhance the catalytic effect of the low-loading palladium metal catalyst and complete the transformation of benzonitrile to primary amines. Subsequently, we still got an ideal yield when we declined the amount of expensive palladium to 0.5% and kept the copper content unchanged (Table S1, entry 10). Considering the experimental data, we believe that the copper activated the cyano group and made the triple bond easier to break through. By virtue of the reduction process of nitriles (Scheme 1), it can be found that the life of intermediate imine largely determines the selectivity of products. When it is short lived the product is primary amine, otherwise else multi substituted amine will be acquired. Therefore we designed new catalyst applying the electronic modulation to lessen the activation of copper so as to obtain other amines (Table S1, entries 11-17). It is simple to observe from the experimental results that secondary amines were selectively obtained when the more active metal (Fe, Co, Ni) was alloyed with copper. Considering the severe loss of cobalt in the process of reaction and vast formation of NiB in the preparation procedure of nickel catalyst, the ideal introduced element is iron. Afterwards, we fixed the total amount of transition metals to explore the effect of the ratio of elements on selectivity, and the ultimate catalyst was confirmed as Pd-$Fe_{0.25}Cu_{0.25}/Fe_3O_4$. The actual composition determined by ICP-MS is 0.24% Pd and 11.86% Cu, and that means each reaction just need 228 ppm Pd. The TOF reached 2929 h^{-1} for Pd and 35.42 h^{-1} for Fe or Cu. The catalyst that contains no palladium element was inactive for hydrogenating the nitriles (Table S1, entry 20). The reaction rate slowed down with further reducing amount of palladium content (0.15% Pd calculated by ICP-MS), however, each reaction just needs 139 ppm Pd and the TOF reached up to 3597 h^{-1} in this moment (Table S1, entry 21). That the mixture of Pd-$Cu_{0.5}/Fe_3O_4$ and Fe/Fe_3O_4 catalyzed the transformation to primary amine confirmed the alloying of Fe to Cu tuned the selectivity (Table S1, entry 22). Other hydrogen donors were unsatisfactory with Pd-$Cu_{0.5}/Fe_3O_4$, especially for hydrazine, the product was azine (Table S1, entries 23-25). To elucidate the real active catalyst species, a hot filtration test was performed. Once 30% of the benzonitrile was transformed (10min, detected by GC), the Pd-$Fe_{0.25}Cu_{0.25}/Fe_3O_4$ catalysts were magnetically separated and the reaction was then continued in the tube for an additional 1 h at 40 °C. There was no noticeable increase of conversion revealed the amount of Pd(II), Cu(II), Fe(III) ions leaching out was negligible and the catalyst was indeed heterogeneous in nature.

The crystal lattice of CuFe alloy was discovered on a scattered particle that we had strived to search, as no active sites was observed on the regular catalyst nanoparticles because of the interference of ferric oxide (Fig. S1). From the figure S1, we could only confirm the existence of

Fe_3O_4, because the find of (111) of ferric oxide.

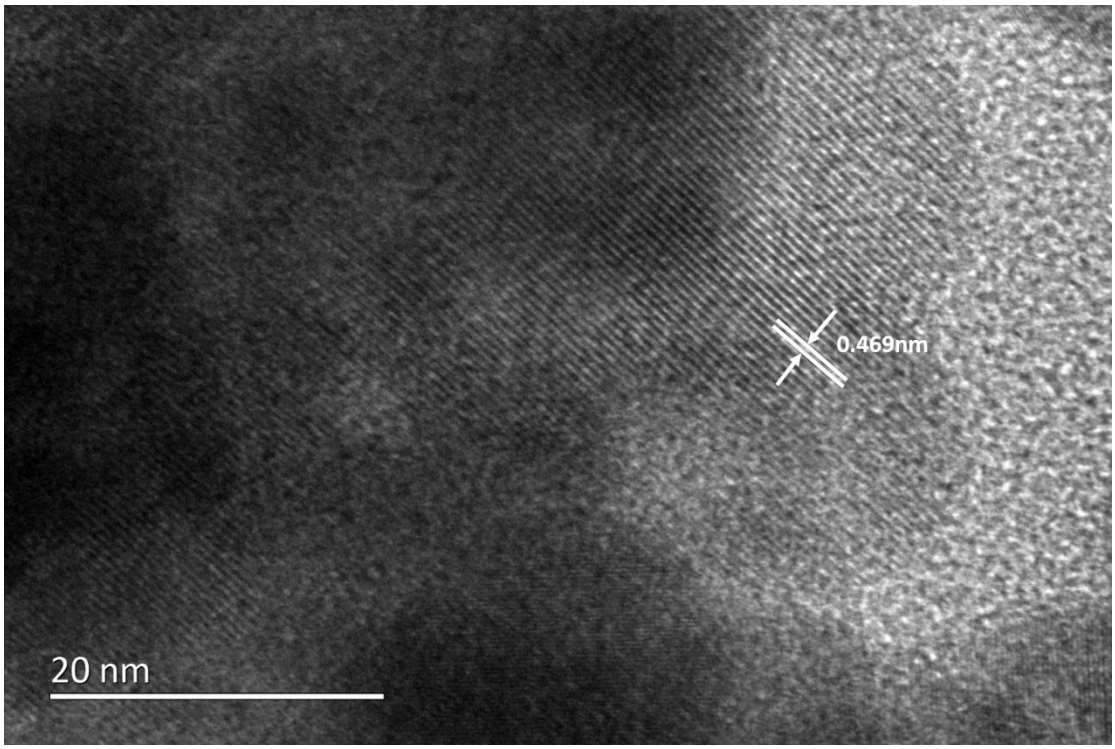

Figure S1. The HRTEM of regular catalyst nanoparticles, related to Fig.2.

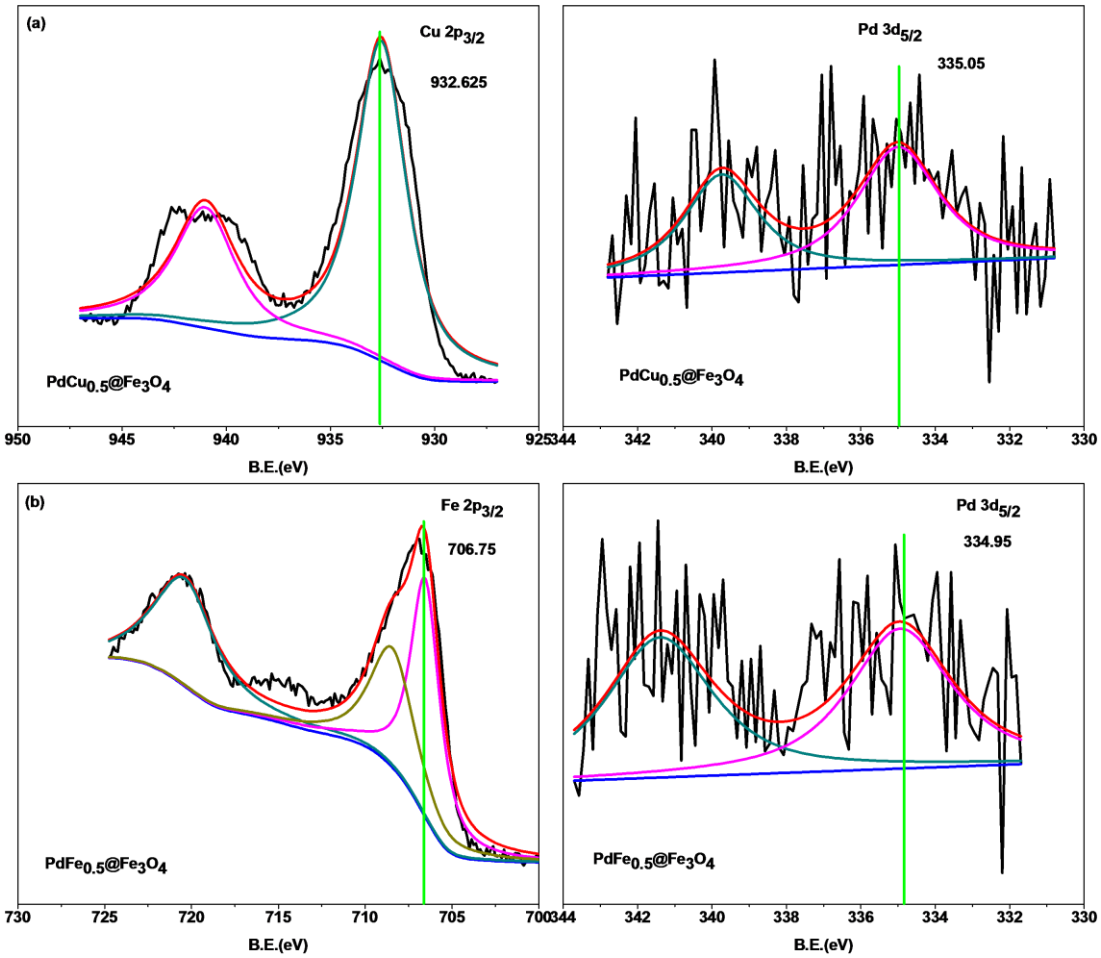

Figure S2. The spectrum of Pd-$Cu_{0.5}/Fe_3O_4$ and Pd-$Fe_{0.5}/Fe_3O_4$, related to Fig.4.

The almost identical peak position of each metal compared with standard values indirectly indicates that palladium alloy is not formed. And the large noise of palladium spectrum manifests the low level of palladium (Figure S2).

The shift tendency of $Cu2p_{3/2}$ and $Fe2p_{3/2}$ are distinguishable. The BE of $Cu2p_{3/2}$, namely 932.625 eV, 932.5 eV, 932.425 eV, 932.375 eV, 932.225 eV, 932.125 eV, correspond to Pd-$Cu_{0.5}/Fe_3O_4$, Pd-$Fe_{0.1}Cu_{0.4}/Fe_3O_4$, Pd-$Fe_{0.2}Cu_{0.3}/Fe_3O_4$, Pd-$Fe_{0.25}Cu_{0.25}/Fe_3O_4$, Pd-$Fe_{0.3}Cu_{0.2}/Fe_3O_4$ and Pd-$Fe_{0.4}Cu_{0.1}/Fe_3O_4$ respectively. The BE of $Fe2p_{3/2}$, namely 707.375 eV, 707.25 eV, 707.125 eV, 707 eV, 706.875 eV, 706.7 eV, correspond to Pd-$Fe_{0.1}Cu_{0.4}/Fe_3O_4$, Pd-$Fe_{0.2}Cu_{0.3}/Fe_3O_4$, Pd-$Fe_{0.25}Cu_{0.25}/Fe_3O_4$, Pd-$Fe_{0.3}Cu_{0.2}/Fe_3O_4$, Pd-$Fe_{0.4}Cu_{0.1}/Fe_3O_4$ and Pd-$Fe_{0.5}/Fe_3O_4$ respectively (Figure S3).

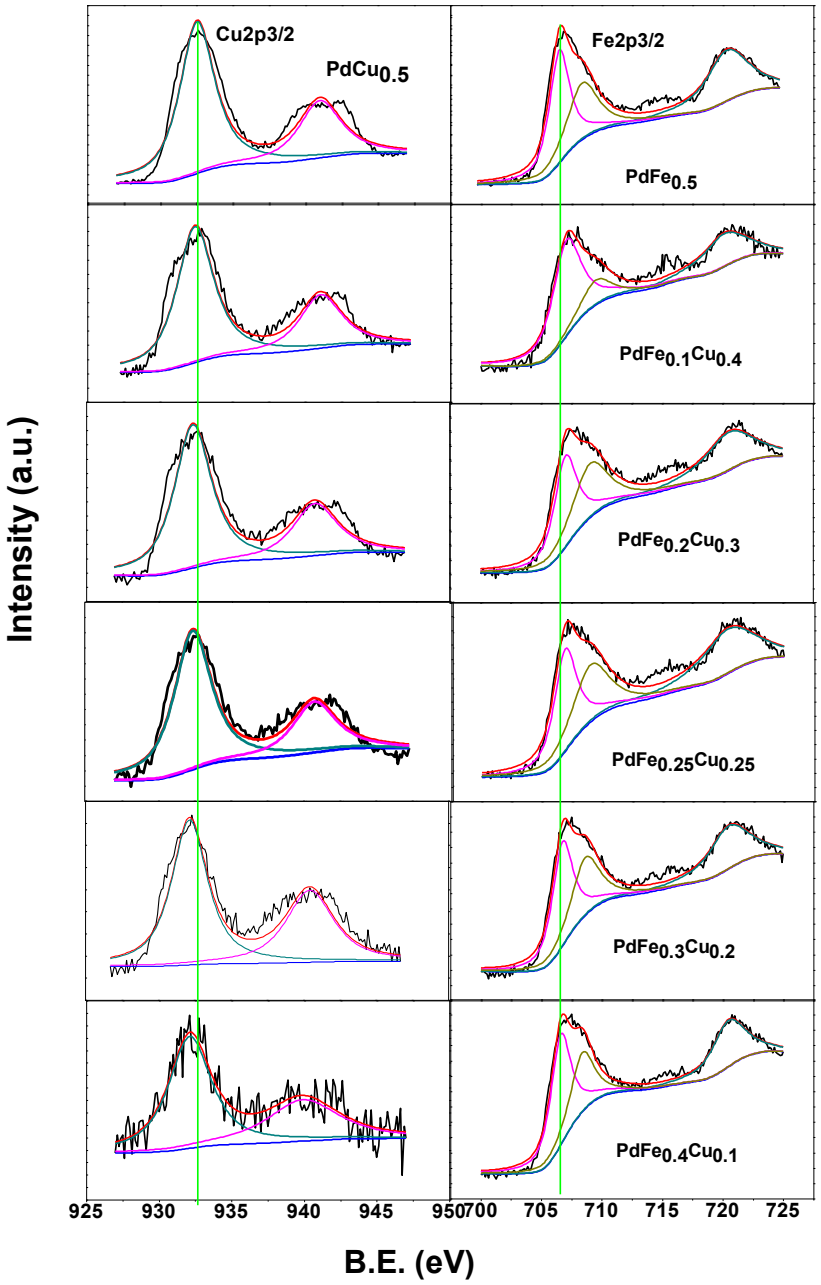

Figure S3. All XPS spectrum of the Pd-FeCu/Fe_3O_4 in the Cu 2p and Fe 2p regions, related to Fig.5.

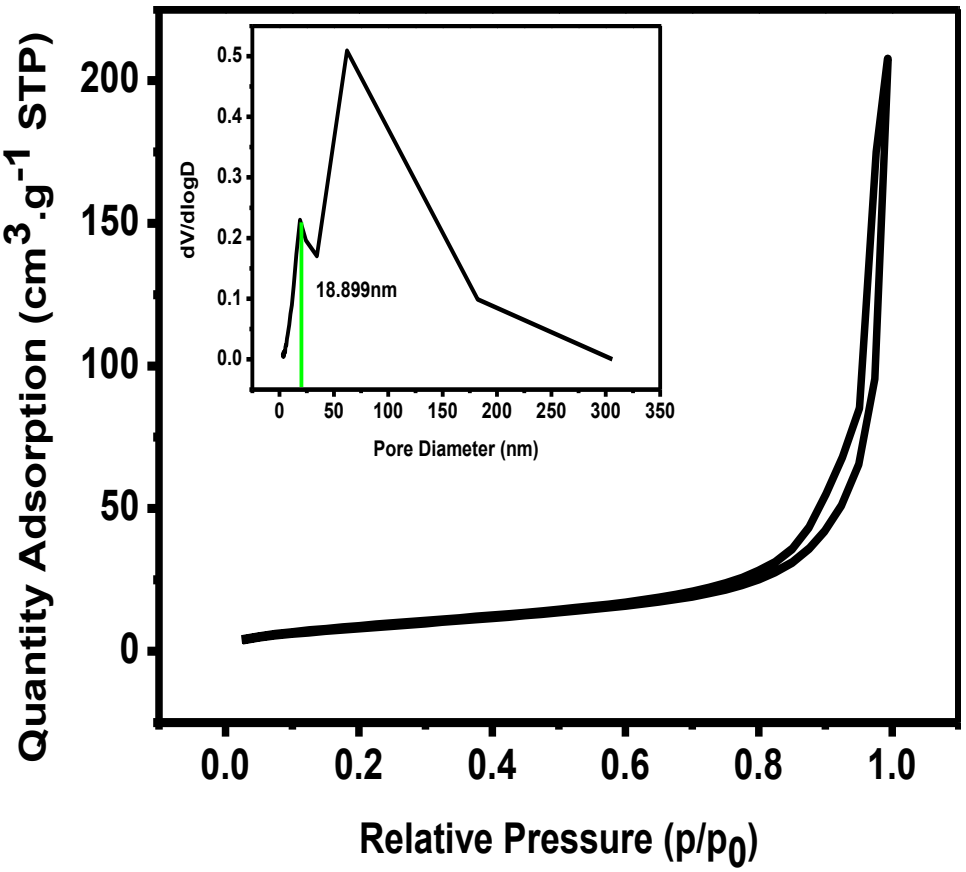

Figure S4. N_2-adsorption-desorption isotherm and pore size distribution of dandelion-like Fe_3O_4, related to Fig.6.

It can be concluded from nitrogen adsorption-desorption data (Fig. S4) that dandelion-like ferric oxide has rich porous structure. The surface area of the material is 39.924 m^2/g and pore diameter is 18.899 nm, which is beneficial for active site dispersion and retention.

Characterization data of products

Primary amines

Benzylamine **(1a)**(Adam et al., 2017)

^{1}H NMR (600 MHz, CHLOROFORM-D) δ 7.30 – 7.25 (m, 5H), 3.83 (s, 2H), 2.03 (s, active H).

^{13}C NMR (151 MHz, CHLOROFORM-D) δ 129.0, 128.8, 128.63, 127.79, 45.40.

GC-MS: m/z(%) 51(11), 79(49), 106(100)

p-tolylmethanamine **(2a)**(Mukherjee et al., 2017)

^{1}H NMR (600 MHz, CHLOROFORM-D) δ 7.20 (d, *J* = 7.9 Hz, 2H), 7.14 (d, *J* = 7.8 Hz, 2H), 3.82 (s, 2H), 2.34 (s, 3H), 1.74 (s, active H).

^{13}C NMR (151 MHz, CHLOROFORM-D) δ 140.03, 136.46, 129.23, 127.09, 46.16, 21.06.

GC-MS: m/z(%) 65(30), 77(45), 104(100), 120(65)

m-tolylmethanamine **(3a)**(Mukherjee et al., 2017)

^{1}H NMR (600 MHz, CHLOROFORM-D) δ 7.23 (t, *J* = 7.4 Hz, 1H), 7.14 – 7.09 (m, 2H), 7.07 (d, *J* = 6.8 Hz, 1H), 3.83 (s, 2H), 2.35 (s, 3H), 1.98 (s, 2H).

^{13}C NMR (151 MHz, CHLOROFORM-D) δ 138.24, 131.57, 128.50, 127.98, 127.66, 124.20, 46.31, 21.39.

GC-MS: m/z(%) 65(30), 77(45), 104(100), 120(65)

o-tolylmethanamine **(4a)**(Shao et al., 2016)

^{1}H NMR (600 MHz, CHLOROFORM-D) δ 7.31 (d, *J* = 7.2 Hz, 1H), 7.22 (d, *J* = 7.5 Hz, 1H), 7.19 (s, 1H), 7.17 (d, *J* = 2.1 Hz, 1H), 3.87 (s, 2H), 2.34 (s, 3H), 1.89 (s, 2H).

^{13}C NMR (151 MHz, CHLOROFORM-D) δ 140.50, 135.55, 130.32, 127.15, 126.96, 126.22, 43.91, 18.83.

GC-MS: m/z(%) 65(30), 77(45), 104(100), 120(65)

(3,5-dimethylphenyl)methanamine **(5a)**

^{1}H NMR (600 MHz, CHLOROFORM-D) δ 6.90 (s, 2H), 6.87 (s, 1H), 3.75 (s, 2H), 2.30 (s, 6H), 1.97 (s, 2H).

^{13}C NMR (151 MHz, CHLOROFORM-D) δ 143.04, 138.08, 128.43, 124.93, 46.31, 21.25.

GC-MS: m/z(%) 65(20), 77(35), 91(65), 118(100), HRMS Calcd. (ESI) m/z for $C_9H_{13}N$: $[M+H]^+$ 136.1121, found 136.1117

(4-methoxyphenyl)methanamine **(6a)**(Adam et al., 2017)

^{1}H NMR (600 MHz, CHLOROFORM-D) δ 7.21 (d, *J* = 8.6 Hz, 2H), 6.86 (d, *J* = 8.6 Hz, 2H), 3.78 (s, 3H), 3.78 (s, 2H), 1.83 (s, 2H).

^{13}C NMR (151 MHz, CHLOROFORM-D) δ 158.52, 135.37, 128.29, 113.92, 55.27, 45.81.

GC-MS: m/z(%) 65(30), 77(55), 106(70), 136(100), 137(65)

(3-methoxyphenyl)methanamine **(7a)**(Zen et al., 2017)

^{1}H NMR (600 MHz, CHLOROFORM-D) δ 7.23 (t, *J* = 7.8 Hz, 1H), 6.90 – 6.84 (m, 2H), 6.77 (d, *J* = 10.3 Hz, 1H), 3.81 (s, 2H), 3.79 (s, 3H), 1.76 (s, 2H).

^{13}C NMR (151 MHz, CHLOROFORM-D) δ 159.83, 144.89, 129.53, 119.32, 112.60, 112.22, 55.16, 46.40.

GC-MS: m/z(%) 65(30), 77(55), 106(70), 136(100), 137(65)

(3,5-dimethoxyphenyl)methanamine **(8a)**

^{1}H NMR (600 MHz, CHLOROFORM-D) δ 6.45 (s, 2H), 6.32 (s, 1H), 3.76 (s, 2H), 3.75 (s, 6H), 1.94 (s, 2H).

^{13}C NMR (151 MHz, CHLOROFORM-D) δ 161.01, 145.73, 104.94, 98.76, 55.26, 46.53.

HRMS Calcd. (ESI) m/z for $C_9H_{13}NO_2$: $[M+H]^+$ 168.1019, found 168.1015

(4-chlorophenyl)methanamine **(9a)**(Adam et al., 2016)

^{1}H NMR (600 MHz, CHLOROFORM-D) δ 7.30 (d, *J* = 9.2 Hz, 2H), 7.25 (d, *J* = 8.4 Hz, 2H), 3.84 (s, 2H), 1.73 (s, active H).

^{13}C NMR (151 MHz, CHLOROFORM-D) δ 141.56, 132.59, 128.70, 128.56, 45.82.

GC-MS: m/z(%) 51(25), 77(45), 106(100), 125(10), 140(35)

(2-chlorophenyl)methanamine **(10a)**(Adam et al., 2017)

^{1}H NMR (600 MHz, CHLOROFORM-D) δ 7.38 (d, *J* = 7.7 Hz, 1H), 7.35 (d, *J* = 7.6 Hz, 1H), 7.24 (d, *J* = 7.3 Hz, 1H), 7.20 (t, *J* = 7.6 Hz, 1H), 3.94 (s, 2H), 2.29 (s, 2H).

^{13}C NMR (151 MHz, CHLOROFORM-D) δ 139.86, 133.40, 129.58, 129.15, 128.39, 127.13, 44.33.

GC-MS: m/z(%) 51(25), 77(45), 106(100), 125(10), 140(35)

(3,4-difluorophenyl)methanamine **(11a)**

^{1}H NMR (600 MHz, CHLOROFORM-D) δ 7.14 (d, *J* = 9.4 Hz, 1H), 7.10 (d, *J* = 10.2 Hz, 1H), 7.03 (s, 1H), 3.84 (s, 2H), 1.71 (s, active H).

^{13}C NMR (151 MHz, CHLOROFORM-D) δ 150.37 (dd, J=250 Hz, 12 Hz), 149.27 (dd, J=249 Hz, 12 Hz), 140.10 (dd, *J* = 6 Hz, 4 Hz), 122.83 (dd, J=7 Hz, 4Hz), 117.33 (d, J= 18 Hz), 116.19 (d, J=17 Hz), 45.44.

GC-MS: m/z(%) 63(40), 75(20), 95(15), 123(100), 142(65), HRMS Calcd. (ESI) m/z for $C_7H_7F_2N$: $[M+H]^+$ 144.0619, found 144.0615

(4-(trifluoromethyl)phenyl)methanamine **(12a)**(Adam et al., 2017)

^{1}H NMR (600 MHz, CHLOROFORM-D) δ 7.59 (d, *J* = 8.0 Hz, 2H), 7.44 (d, *J* = 8.0 Hz, 2H), 3.94 (s, 2H), 1.76 (s, 2H).

^{13}C NMR (151 MHz, CHLOROFORM-D) δ 146.93, 128.49 (q, J=35.1 Hz), 127.36, 125.49 (tt, *J* = 44.9, 22.4 Hz), 124.98 (q, 3.0Hz), 45.96.

GC-MS: m/z(%) 51(30), 77(30), 106(100), 127(65), 156(20), 174(90)

Phenethylamine **(13a)**(Adam et al., 2017)

^{1}H NMR (600 MHz, CHLOROFORM-D) δ 7.31 (d, *J* = 7.8 Hz, 2H), 7.26 (s, 2H), 7.20 (s, 1H), 3.52 (dd, *J* = 13.0, 6.8 Hz, 2H), 2.82 (d, *J* = 6.9 Hz, 2H), 2.28 (s, 2H).

^{13}C NMR (151 MHz, CHLOROFORM-D) δ 138.87, 128.71 (d, *J* = 13.0 Hz), 126.54, 40.64, 35.63.

GC-MS: m/z(%) 65(70), 77(20), 91(100), 121(20)

Secondary amines

Dibenzylamine **(1b)**(Shao et al., 2016)

^{1}H NMR (600 MHz, CHLOROFORM-D) δ 7.29 (d, *J* = 14.8 Hz, 8H), 7.21 (s, 2H), 3.76 (s, 4H), 1.92 (s, 1H).

^{13}C NMR (151 MHz, CHLOROFORM-D) δ 140.25, 128.43, 128.21, 127.00, 53.15.

GC-MS: m/z(%) 65(20), 77(8), 91(100), 120(8)

bis(4-methylbenzyl)amine **(2b)**(Shao et al., 2016)

^{1}H NMR (600 MHz, CHLOROFORM-D) δ 7.20 (d, *J* = 7.9 Hz, 4H), 7.12 (t, *J* = 7.2 Hz, 4H), 3.73 (s, 4H), 2.32 (s, 6H), 2.11 (s, 1H).

^{13}C NMR (151 MHz, CHLOROFORM-D) δ 137.20, 136.66, 129.23, 128.32, 52.86, 21.25.

GC-MS: m/z(%) 65(10), 77(30), 105(100), 120(65), 225(10)

bis(3-methylbenzyl)amine **(3b)**(Lu et al., 2014)

^{1}H NMR (600 MHz, CHLOROFORM-D) δ 7.22 (dd, *J* = 15.4, 7.9 Hz, 2H), 7.15 (s, 2H), 7.12 (d, *J* = 7.6 Hz, 2H), 7.06 (d, *J* = 7.4 Hz, 2H), 3.77 (s, 4H), 2.34 (s, 6H), 2.22 (s, 1H).

^{13}C NMR (151 MHz, CHLOROFORM-D) δ 139.66, 138.04, 129.04, 128.31, 127.81, 125.31, 53.03,

21.39.

GC-MS: m/z(%) 65(10), 77(30), 105(100), 120(65), 225(10)

bis(2-methylbenzyl)amine **(4b)**(Lu et al., 2014)

^{1}H NMR (600 MHz, CHLOROFORM-D) δ 7.27 (d, *J* = 7.2 Hz, 2H), 7.23 – 7.12 (m, 6H), 3.82 (s, 4H), 2.31 (s, 6H).

^{13}C NMR (151 MHz, CHLOROFORM-D) δ 140.85, 135.45, 130.24, 127.00, 126.82, 126.16, 43.92, 18.77.

GC-MS: m/z(%) 65(10), 77(30), 105(100), 120(65), 225(10)

bis(3,5-dimethylbenzyl)amine **(5b)**

^{1}H NMR (600 MHz, CHLOROFORM-D) δ 6.94 (s, 4H), 6.88 (s, 2H), 3.72 (s, 4H), 2.30 (s, 12H), 2.03 (s, 1H).

^{13}C NMR (151 MHz, CHLOROFORM-D) δ 139.96, 137.87, 128.57, 126.03, 53.21, 21.25.

HRMS Calcd. (ESI) m/z for $C_{18}H_{23}N$: $[M+H]^+$ 254.1903, found 254.1905

bis(4-methoxybenzyl)amine **(6b)**(Shao et al., 2016)

^{1}H NMR (600 MHz, CHLOROFORM-D) δ 7.24 (d, *J* = 8.6 Hz, 4H), 6.85 (d, *J* = 8.6 Hz, 4H), 3.77 (s, 6H), 3.71 (s, 4H).

^{13}C NMR (151 MHz, CHLOROFORM-D) δ 158.62, 132.42, 129.31, 113.74, 55.15, 52.41.

MS (ESI) m/z for $C_{16}H_{19}NO_2$: 258 ($[M+H]^+$)

bis(3-methoxybenzyl)amine **(7b)**(Shao et al., 2016)

^{1}H NMR (600 MHz, CHLOROFORM-D) δ 7.22 (t, *J* = 8.0 Hz, 2H), 6.90 (s, 4H), 6.79 (d, *J* = 10.2 Hz, 2H), 3.78 (s, 6H), 3.76 (s, 4H), 2.16 (s, 1H).

^{13}C NMR (151 MHz, CHLOROFORM-D) δ 159.75, 141.69, 129.37, 120.47, 113.62, 112.53, 55.15, 52.94.

MS (ESI) m/z for $C_{16}H_{19}NO_2$: 258 ($[M+H]^+$)

bis(3,5-dimethoxybenzyl)amine **(8b)**

^{1}H NMR (600 MHz, CHLOROFORM-D) δ 6.50 (s, 4H), 6.34 (s, 2H), 3.74 (s, 12H), 3.71 (s, 4H), 2.10 (s, 1H).

^{13}C NMR (151 MHz, CHLOROFORM-D) δ 160.99, 142.83, 106.06, 99.12, 55.32, 53.23.

HRMS Calcd. (ESI) m/z for $C_{18}H_{23}NO_4$: $[M+H]^+$ 318.1700, found 318.1705

bis(4-chlorobenzyl)amine **(9b)**(Shao et al., 2016)

^{1}H NMR (600 MHz, CHLOROFORM-D) δ 7.27 (d, *J* = 8.4 Hz, 4H), 7.24 (d, *J* = 8.4 Hz, 4H), 3.72 (s, 4H), 1.90 (s, 1H).

^{13}C NMR (151 MHz, CHLOROFORM-D) δ 138.57, 132.85, 129.59, 128.65, 52.39.

MS (ESI) m/z for $C_{14}H_{13}Cl_2N$: 266 ($[M+H]^+$)

bis(2-chlorobenzyl)amine **(10b)**(Shao et al., 2016)

^{1}H NMR (600 MHz, CHLOROFORM-D) δ 7.44 (d, *J* = 6.0 Hz, 2H), 7.35 (d, *J* = 7.8 Hz, 2H), 7.26 – 7.23 (m, 2H), 7.20 (t, *J* = 6.8 Hz, 2H), 3.91 (s, 4H), 2.23 (s, 1H).

^{13}C NMR (151 MHz, CHLOROFORM-D) δ 137.23, 133.81, 130.19, 129.50, 128.41, 126.84, 50.63.

MS (ESI) m/z for $C_{14}H_{13}Cl_2N$: 266 ($[M+H]^+$)

bis(3,4-difluorobenzyl)amine **(11b)**

^{1}H NMR (600 MHz, CHLOROFORM-D) δ 7.21 – 7.15 (m, 2H), 7.09 (d, *J* = 10.1 Hz, 2H), 7.04 (d, *J* = 3.8 Hz, 2H), 3.74 (s, 4H), 1.83 (s, 1H).

^{13}C NMR (151 MHz, CHLOROFORM-D) δ 150.76 (dd, J=259 Hz, 12 Hz), 149.12 (dd, J=254 Hz, 13 Hz), 137.13 (dd, J=7 Hz, 4 Hz), 123.88 (dd, J=6 Hz, 4Hz), 117.08 (d, J=18 Hz), 116.87 (d, J=17 Hz), 52.00.

HRMS Calcd. (ESI) m/z for $C_{14}H_{11}F_4N$: $[M+H]^+$ 270.0900, found 270.0904

bis(4-(trifluoromethyl)benzyl)amine **(12b)**(Shao et al., 2016)

^1H NMR (600 MHz, CHLOROFORM-D) δ 7.59 (d, *J* = 8.2 Hz, 4H), 7.47 (d, *J* = 8.0 Hz, 4H), 3.86 (s, 4H), 1.95 (s, 1H).

^{13}C NMR (151 MHz, CHLOROFORM-D) δ 144.02, 129.48(q, 31.7Hz), 128.37, 126.84, 125.42 (q, *J* = 3.7 Hz), 52.59.

MS (ESI) m/z for $C_{16}H_{13}F_6N$: 334 ($[M+H]^+$)

Diphenethylamine **(13b)**(Shao et al., 2016)

^1H NMR (600 MHz, CHLOROFORM-D) δ 7.25 (t, *J* = 7.5 Hz, 4H), 7.18 (d, *J* = 7.4 Hz, 2H), 7.16 (dd, *J* = 6.3, 5.3 Hz, 4H), 2.93 (s, 4H), 2.77 (t, *J* = 7.1 Hz, 4H), 1.54 (s, 1H).

^{13}C NMR (151 MHz, CHLOROFORM-D) δ 140.07, 128.80, 128.58, 126.26, 51.00, 36.52.

GC-MS: m/z(%) 65(15), 77(25), 105(100), 134(95)

Copies of 1H and 13C NMR spectrums

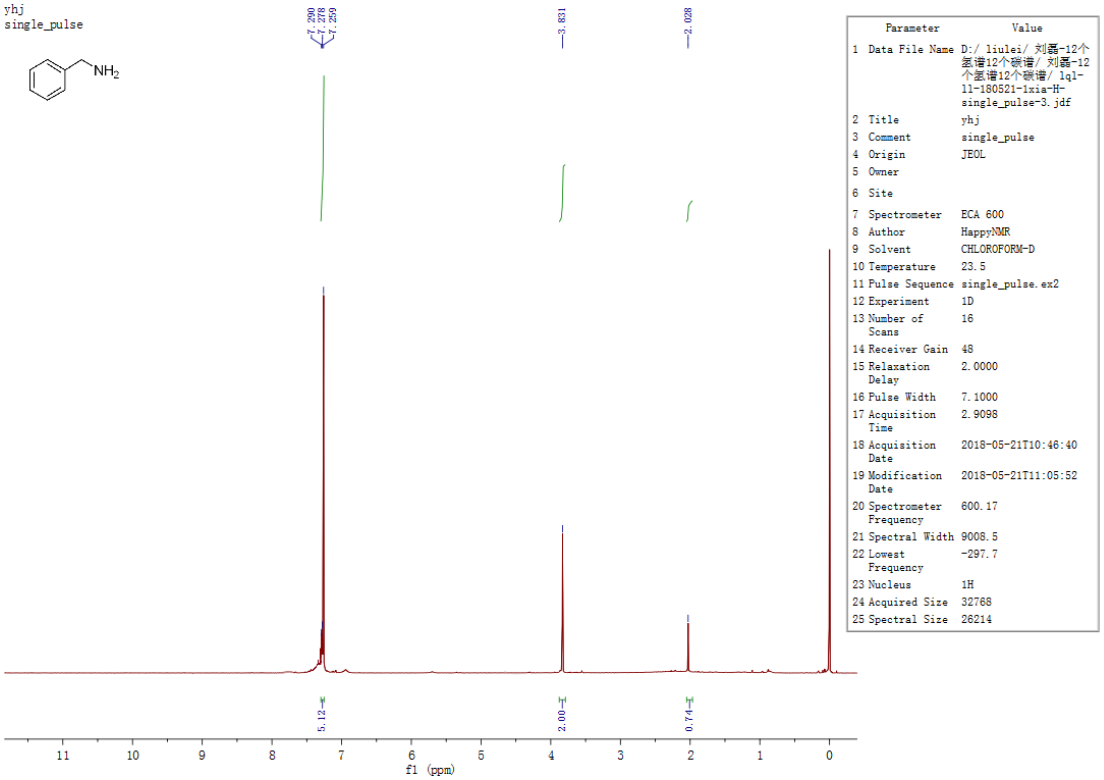

	Parameter	Value
1	Data File Name	D:/ liulei/ 刘磊-12个氢谱12个碳谱/ 刘磊-12个氢谱12个碳谱/ lql-11-180521-1xia-H-single_pulse-3.jdf
2	Title	yhj
3	Comment	single_pulse
4	Origin	JEOL
5	Owner	
6	Site	
7	Spectrometer	ECA 600
8	Author	HappyNMR
9	Solvent	CHLOROFORM-D
10	Temperature	23.5
11	Pulse Sequence	single_pulse.ex2
12	Experiment	1D
13	Number of Scans	16
14	Receiver Gain	48
15	Relaxation Delay	2.0000
16	Pulse Width	7.1000
17	Acquisition Time	2.9098
18	Acquisition Date	2018-05-21T10:46:40
19	Modification Date	2018-05-21T11:05:52
20	Spectrometer Frequency	600.17
21	Spectral Width	9008.5
22	Lowest Frequency	-297.7
23	Nucleus	1H
24	Acquired Size	32768
25	Spectral Size	26214

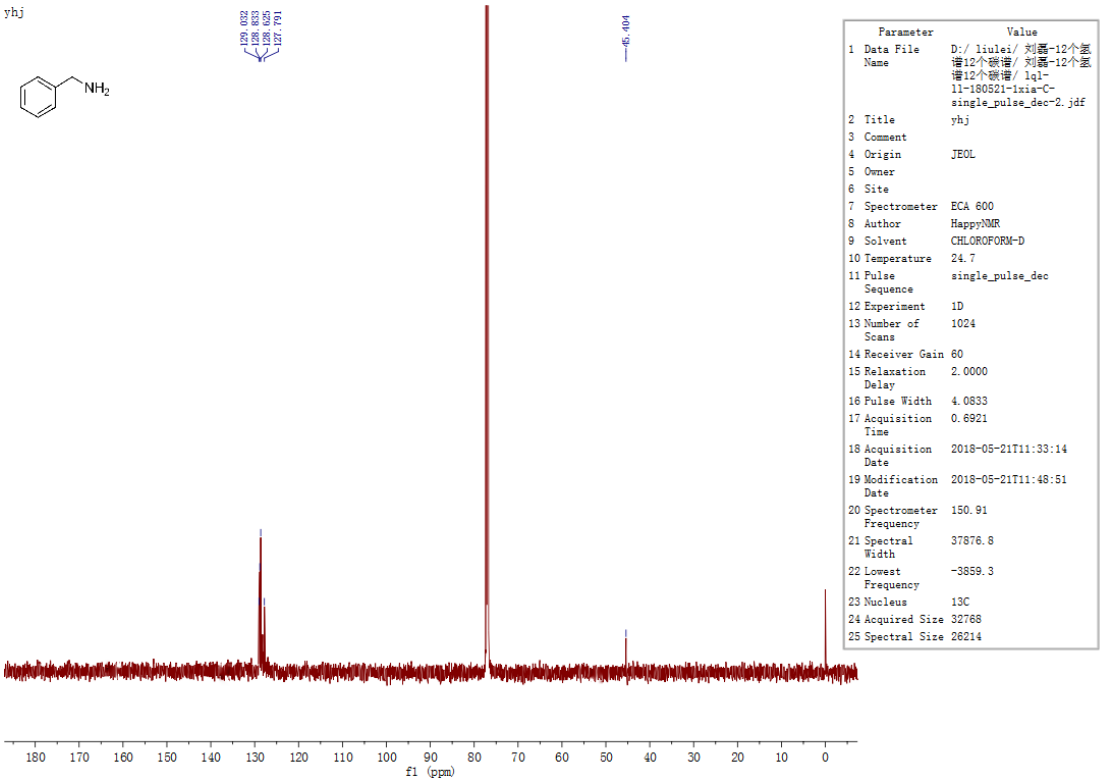

	Parameter	Value
1	Data File Name	D:/ liulei/ 刘磊-12个氢谱12个碳谱/ 刘磊-12个氢谱12个碳谱/ lql-11-180521-1xia-C-single_pulse_dec-2.jdf
2	Title	yhj
3	Comment	
4	Origin	JEOL
5	Owner	
6	Site	
7	Spectrometer	ECA 600
8	Author	HappyNMR
9	Solvent	CHLOROFORM-D
10	Temperature	24.7
11	Pulse Sequence	single_pulse_dec
12	Experiment	1D
13	Number of Scans	1024
14	Receiver Gain	60
15	Relaxation Delay	2.0000
16	Pulse Width	4.0833
17	Acquisition Time	0.6921
18	Acquisition Date	2018-05-21T11:33:14
19	Modification Date	2018-05-21T11:48:51
20	Spectrometer Frequency	150.91
21	Spectral Width	37876.8
22	Lowest Frequency	-3859.3
23	Nucleus	13C
24	Acquired Size	32768
25	Spectral Size	26214

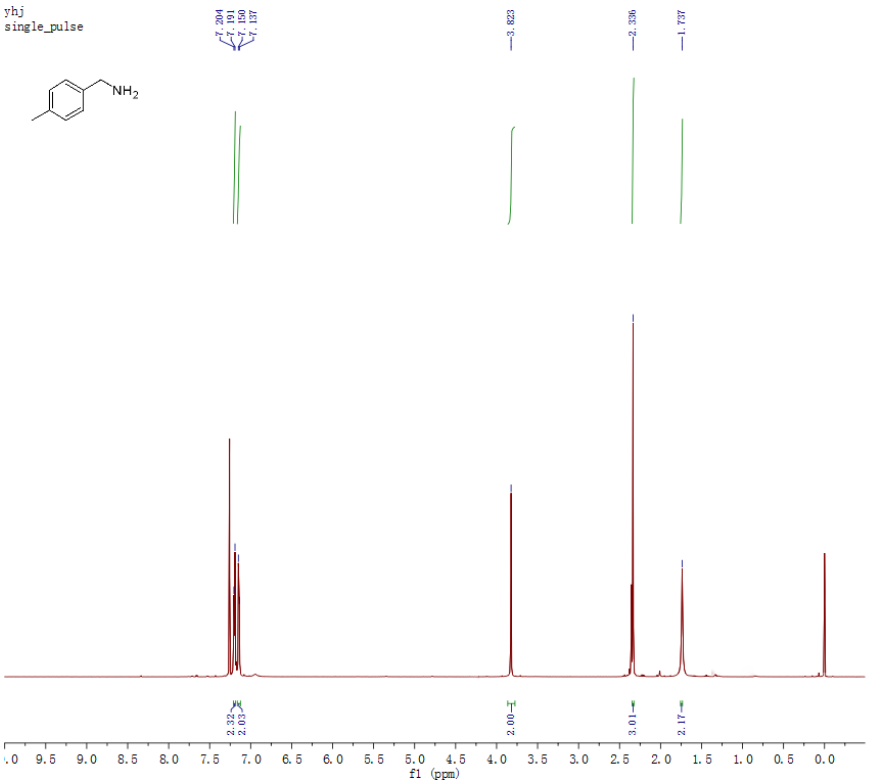

	Parameter	Value
1	Data File Name	D:/ liulei/ Fw_thunmr-180423/ lql-ayj-180420-2xia-H-single_pulse-3.jdf
2	Title	yhj
3	Comment	single_pulse
4	Origin	JEOL
5	Owner	
6	Site	
7	Spectrometer	ECA 600
8	Author	HappyNMR
9	Solvent	CHLOROFORM-D
10	Temperature	25.8
11	Pulse Sequence	single_pulse.ex2
12	Experiment	1D
13	Number of Scans	16
14	Receiver Gain	46
15	Relaxation Delay	2.0000
16	Pulse Width	7.1000
17	Acquisition Time	2.9098
18	Acquisition Date	2018-04-20T16:18:39
19	Modification Date	2018-04-20T16:35:40
20	Spectrometer Frequency	600.17
21	Spectral Width	9008.5
22	Lowest Frequency	-298.3
23	Nucleus	1H
24	Acquired Size	32768
25	Spectral Size	26214

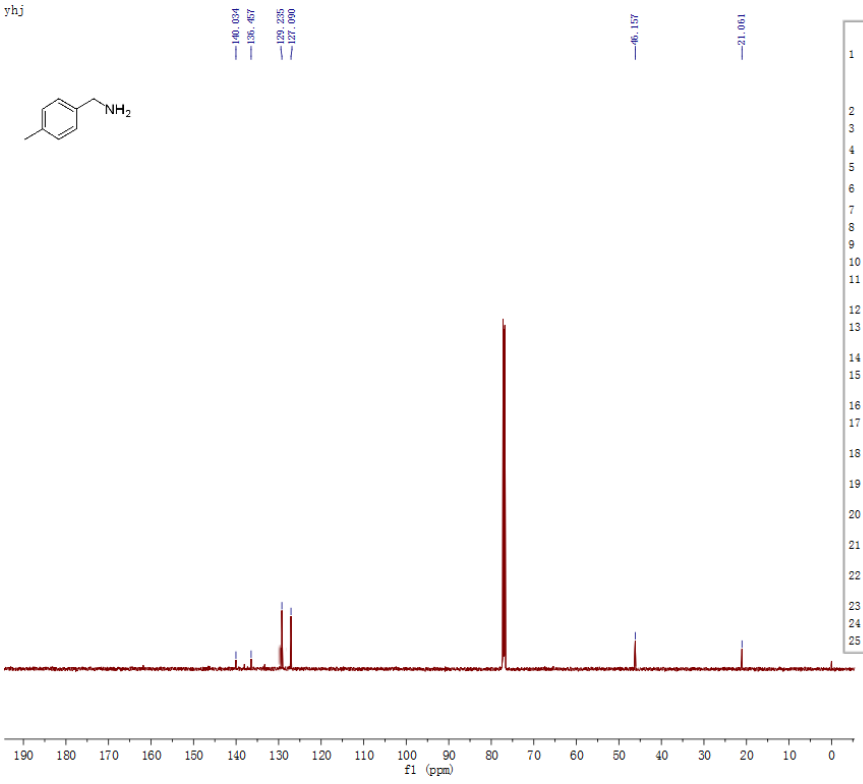

	Parameter	Value
1	Data File Name	D:/ liulei/ Fw_thunmr-180423/ lql-ayj-180420-2xia-C-single_pulse_dec-3.jdf
2	Title	yhj
3	Comment	
4	Origin	JEOL
5	Owner	
6	Site	
7	Spectrometer	ECA 600
8	Author	HappyNMR
9	Solvent	CHLOROFORM-D
10	Temperature	24.5
11	Pulse Sequence	single_pulse_dec
12	Experiment	1D
13	Number of Scans	1024
14	Receiver Gain	58
15	Relaxation Delay	2.0000
16	Pulse Width	4.0833
17	Acquisition Time	0.6921
18	Acquisition Date	2018-04-23T08:58:52
19	Modification Date	2018-04-23T09:15:31
20	Spectrometer Frequency	150.91
21	Spectral Width	37876.8
22	Lowest Frequency	-3859.3
23	Nucleus	13C
24	Acquired Size	32768
25	Spectral Size	26214

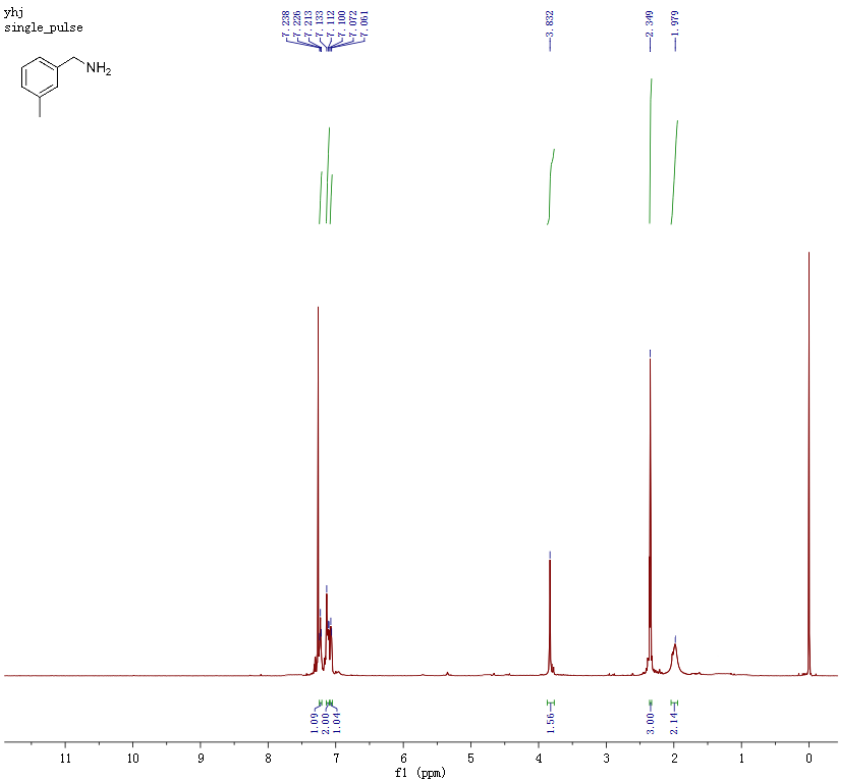

	Parameter	Value
1	Data File Name	D:/ liulei/ 刘磊-12个氢谱12个碳谱/ 刘磊-12个氢谱12个碳谱/ lql-ll-180521-3xia-H-single_pulse-3.jdf
2	Title	yhj
3	Comment	single_pulse
4	Origin	JEOL
5	Owner	
6	Site	
7	Spectrometer	ECA 600
8	Author	HappyNMR
9	Solvent	CHLOROFORM-D
10	Temperature	23.4
11	Pulse Sequence	single_pulse.ex2
12	Experiment	1D
13	Number of Scans	16
14	Receiver Gain	44
15	Relaxation Delay	2.0000
16	Pulse Width	7.1000
17	Acquisition Time	2.9098
18	Acquisition Date	2018-05-21T12:02:53
19	Modification Date	2018-05-21T12:19:04
20	Spectrometer Frequency	600.17
21	Spectral Width	9008.5
22	Lowest Frequency	-298.3
23	Nucleus	1H
24	Acquired Size	32768
25	Spectral Size	26214

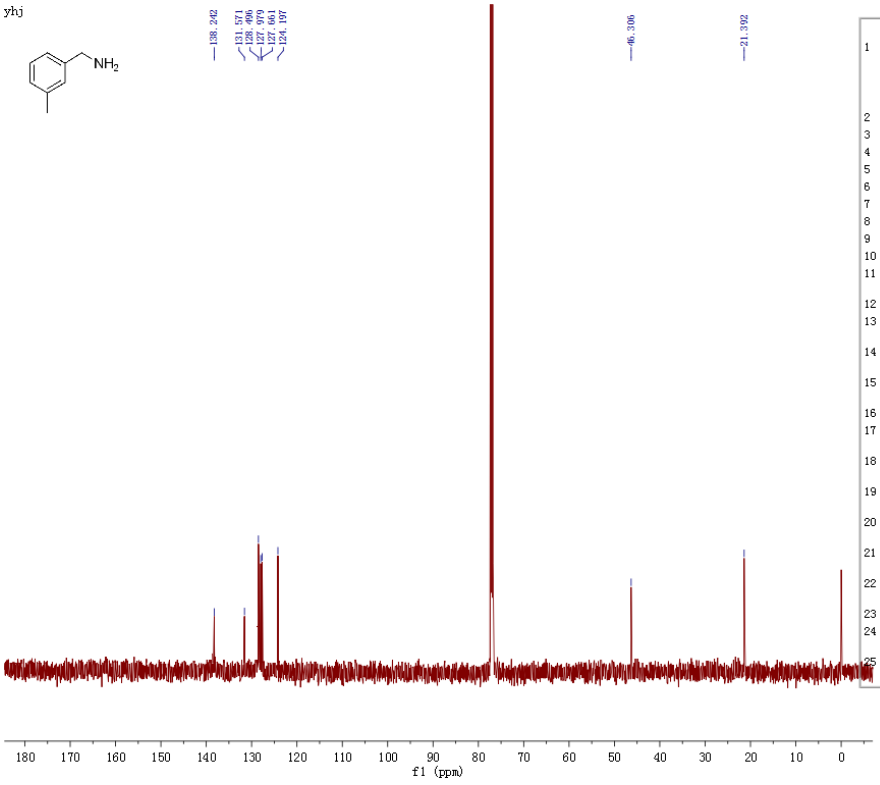

	Parameter	Value
1	Data File Name	D:/ liulei/ 刘磊-12个氢谱12个碳谱/ 刘磊-12个氢谱12个碳谱/ lql-ll-180521-3xia-C-single_pulse_dec-2.jdf
2	Title	yhj
3	Comment	
4	Origin	JEOL
5	Owner	
6	Site	
7	Spectrometer	ECA 600
8	Author	HappyNMR
9	Solvent	CHLOROFORM-D
10	Temperature	24.7
11	Pulse Sequence	single_pulse_dec
12	Experiment	1D
13	Number of Scans	1024
14	Receiver Gain	58
15	Relaxation Delay	2.0000
16	Pulse Width	4.0633
17	Acquisition Time	0.6921
18	Acquisition Date	2018-05-21T12:49:26
19	Modification Date	2018-05-21T13:05:04
20	Spectrometer Frequency	150.91
21	Spectral Width	37876.8
22	Lowest Frequency	-3859.4
23	Nucleus	13C
24	Acquired Size	32768
25	Spectral Size	26214

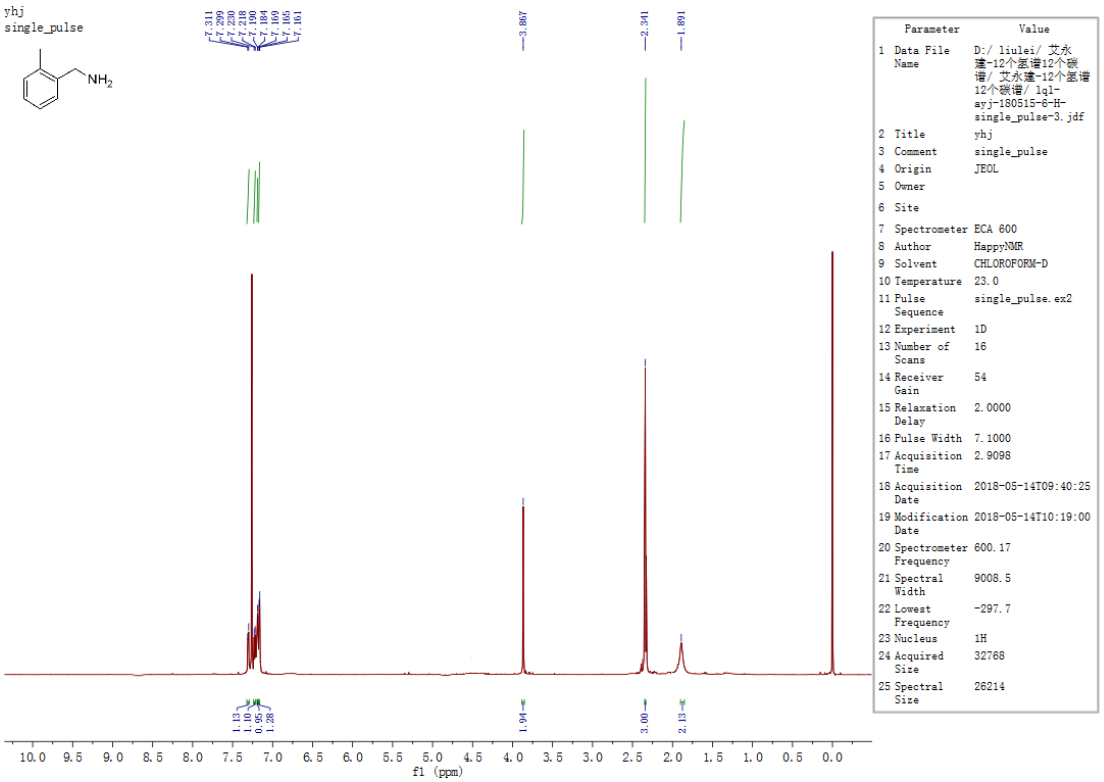

	Parameter	Value
1	Data File Name	D:/ liulei/ 艾永建-12个氢谱12个碳谱/ 艾永建-12个氢谱12个碳谱/ lql-ayj-180515-6-H-single_pulse-3.jdf
2	Title	yhj
3	Comment	single_pulse
4	Origin	JEOL
5	Owner	
6	Site	
7	Spectrometer	ECA 600
8	Author	HappyNMR
9	Solvent	CHLOROFORM-D
10	Temperature	23.0
11	Pulse Sequence	single_pulse.ex2
12	Experiment	1D
13	Number of Scans	16
14	Receiver Gain	54
15	Relaxation Delay	2.0000
16	Pulse Width	7.1000
17	Acquisition Time	2.9098
18	Acquisition Date	2018-05-14T09:40:25
19	Modification Date	2018-05-14T10:19:00
20	Spectrometer Frequency	600.17
21	Spectral Width	9008.5
22	Lowest Frequency	-297.7
23	Nucleus	1H
24	Acquired Size	32768
25	Spectral Size	26214

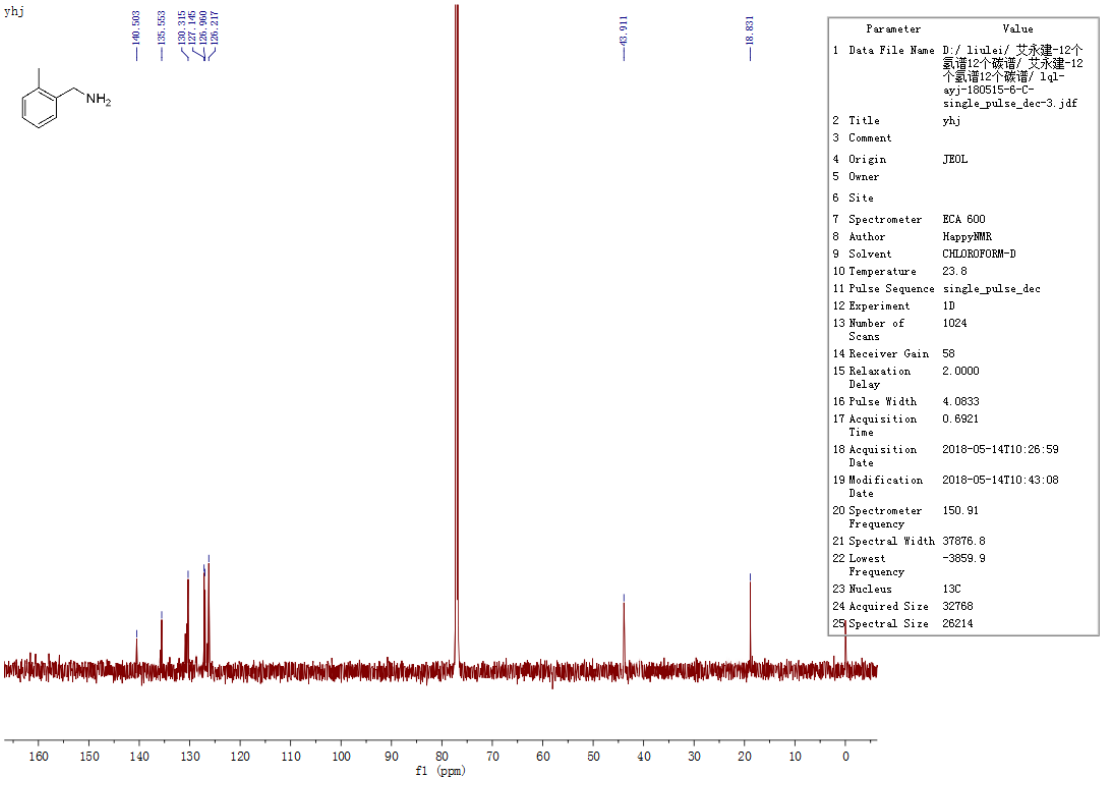

	Parameter	Value
1	Data File Name	D:/ liulei/ 艾永建-12个氢谱12个碳谱/ 艾永建-12个氢谱12个碳谱/ lql-ayj-180515-6-C-single_pulse_dec-3.jdf
2	Title	yhj
3	Comment	
4	Origin	JEOL
5	Owner	
6	Site	
7	Spectrometer	ECA 600
8	Author	HappyNMR
9	Solvent	CHLOROFORM-D
10	Temperature	23.8
11	Pulse Sequence	single_pulse_dec
12	Experiment	1D
13	Number of Scans	1024
14	Receiver Gain	58
15	Relaxation Delay	2.0000
16	Pulse Width	4.0833
17	Acquisition Time	0.6921
18	Acquisition Date	2018-05-14T10:26:59
19	Modification Date	2018-05-14T10:43:08
20	Spectrometer Frequency	150.91
21	Spectral Width	37876.8
22	Lowest Frequency	-3859.9
23	Nucleus	13C
24	Acquired Size	32768
25	Spectral Size	26214

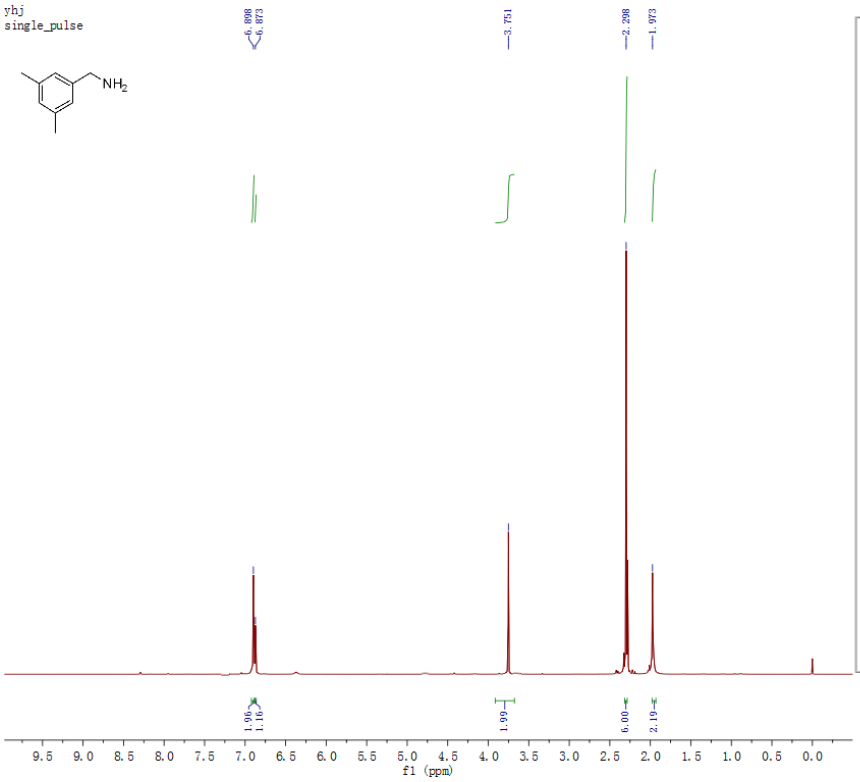

	Parameter	Value
1	Data File Name	D:/ liulei/ 艾永建-12个氢谱12个碳谱/ 艾永建-12个氢谱12个碳谱/ lql-ayj-180515-8xia-H-single_pulse-3.jdf
2	Title	yhj
3	Comment	single_pulse
4	Origin	JEOL
5	Owner	
6	Site	
7	Spectrometer	ECA 600
8	Author	HappyNMR
9	Solvent	CHLOROFORM-D
10	Temperature	23.8
11	Pulse Sequence	single_pulse.ex2
12	Experiment	1D
13	Number of Scans	16
14	Receiver Gain	26
15	Relaxation Delay	2.0000
16	Pulse Width	7.1000
17	Acquisition Time	2.9098
18	Acquisition Date	2018-05-18T15:17:13
19	Modification Date	2018-05-18T15:34:36
20	Spectrometer Frequency	600.17
21	Spectral Width	9008.5
22	Lowest Frequency	-307.3
23	Nucleus	1H
24	Acquired Size	32768
25	Spectral Size	26214

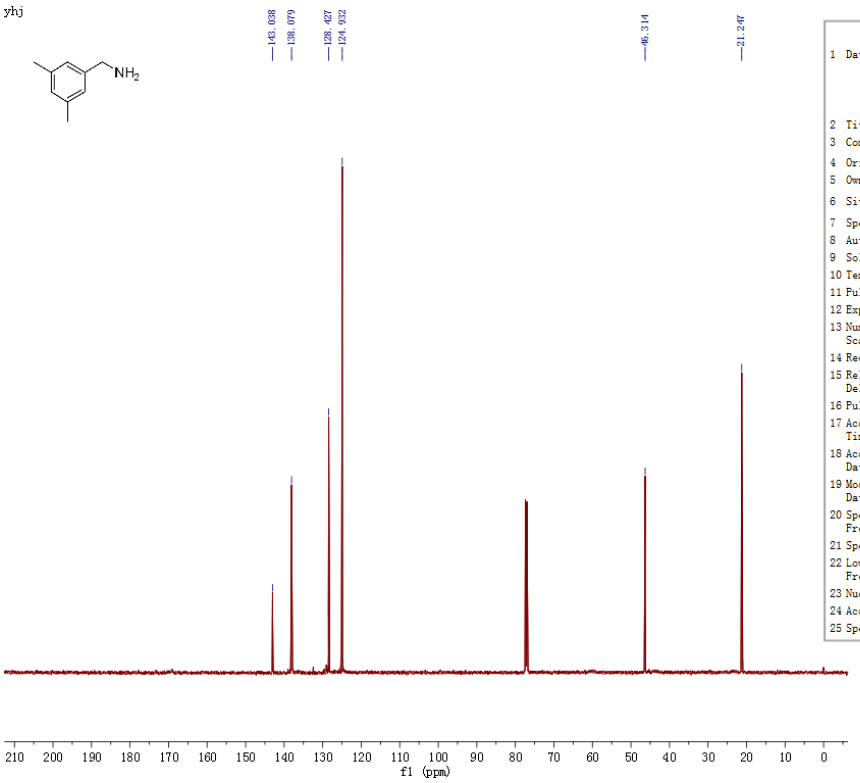

	Parameter	Value
1	Data File Name	D:/ liulei/ 艾永建-12个氢谱12个碳谱/ 艾永建-12个氢谱12个碳谱/ lql-ayj-180515-8xia-C-single_pulse_dec-3.jdf
2	Title	yhj
3	Comment	
4	Origin	JEOL
5	Owner	
6	Site	
7	Spectrometer	ECA 600
8	Author	HappyNMR
9	Solvent	CHLOROFORM-D
10	Temperature	25.0
11	Pulse Sequence	single_pulse_dec
12	Experiment	1D
13	Number of Scans	247
14	Receiver Gain	58
15	Relaxation Delay	2.0000
16	Pulse Width	4.0833
17	Acquisition Time	0.6921
18	Acquisition Date	2018-05-18T15:30:25
19	Modification Date	2018-05-18T15:47:15
20	Spectrometer Frequency	150.91
21	Spectral Width	37876.8
22	Lowest Frequency	-3861.5
23	Nucleus	13C
24	Acquired Size	32768
25	Spectral Size	26214

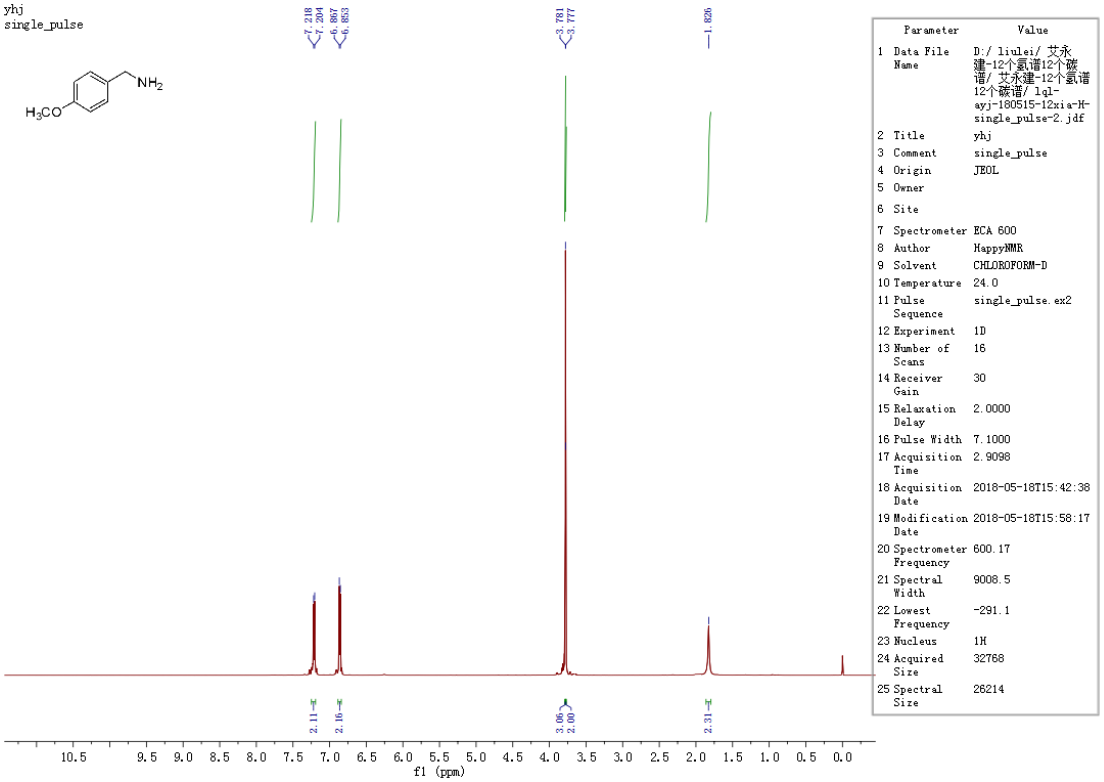

	Parameter	Value
1	Data File Name	D:/ liulei/ 艾永建-12个氢谱12个碳谱/ 艾永建-12个氢谱12个碳谱/ lql-ayj-180515-12xia-H-single_pulse-2.jdf
2	Title	yhj
3	Comment	single_pulse
4	Origin	JEOL
5	Owner	
6	Site	
7	Spectrometer	ECA 600
8	Author	HappyNMR
9	Solvent	CHLOROFORM-D
10	Temperature	24.0
11	Pulse Sequence	single_pulse.ex2
12	Experiment	1D
13	Number of Scans	16
14	Receiver Gain	30
15	Relaxation Delay	2.0000
16	Pulse Width	7.1000
17	Acquisition Time	2.9098
18	Acquisition Date	2018-05-18T15:42:38
19	Modification Date	2018-05-18T15:58:17
20	Spectrometer Frequency	600.17
21	Spectral Width	9008.5
22	Lowest Frequency	-291.1
23	Nucleus	1H
24	Acquired Size	32768
25	Spectral Size	26214

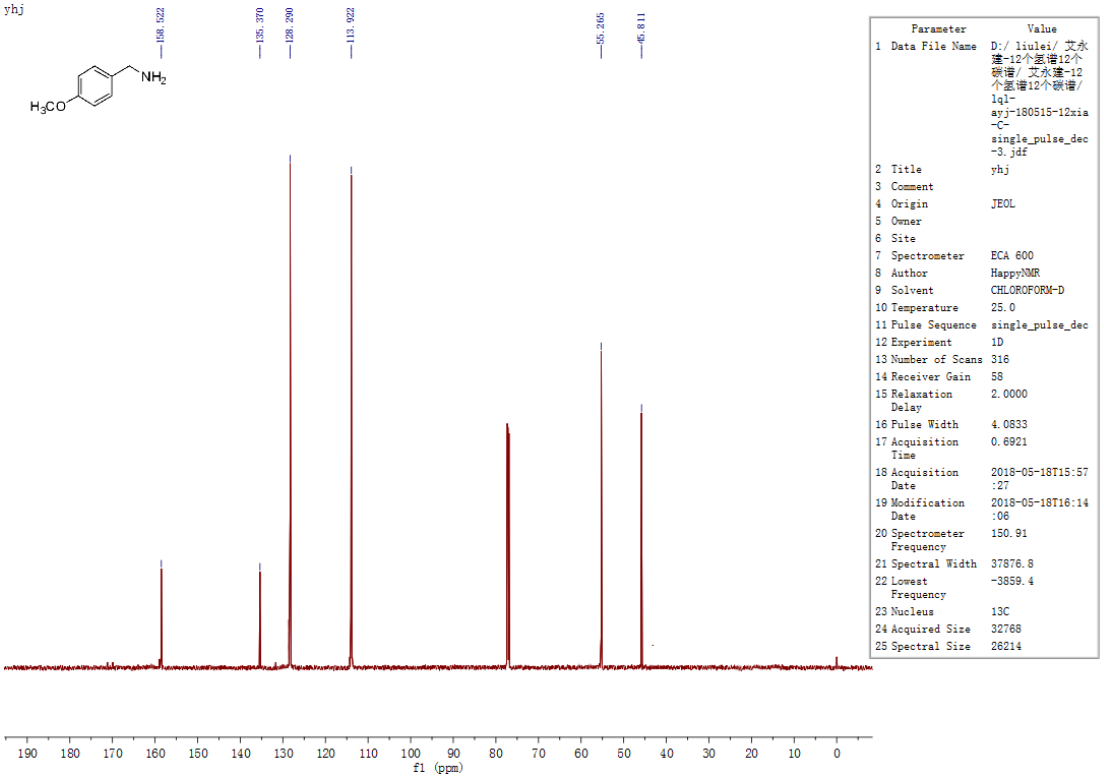

	Parameter	Value
1	Data File Name	D:/ liulei/ 艾永建-12个氢谱12个碳谱/ 艾永建-12个氢谱12个碳谱/ lql-ayj-180515-12xia-C-single_pulse_dec-3.jdf
2	Title	yhj
3	Comment	
4	Origin	JEOL
5	Owner	
6	Site	
7	Spectrometer	ECA 600
8	Author	HappyNMR
9	Solvent	CHLOROFORM-D
10	Temperature	25.0
11	Pulse Sequence	single_pulse_dec
12	Experiment	1D
13	Number of Scans	316
14	Receiver Gain	58
15	Relaxation Delay	2.0000
16	Pulse Width	4.0833
17	Acquisition Time	0.6921
18	Acquisition Date	2018-05-18T15:57:27
19	Modification Date	2018-05-18T16:14:06
20	Spectrometer Frequency	150.91
21	Spectral Width	37876.8
22	Lowest Frequency	-3859.4
23	Nucleus	13C
24	Acquired Size	32768
25	Spectral Size	26214

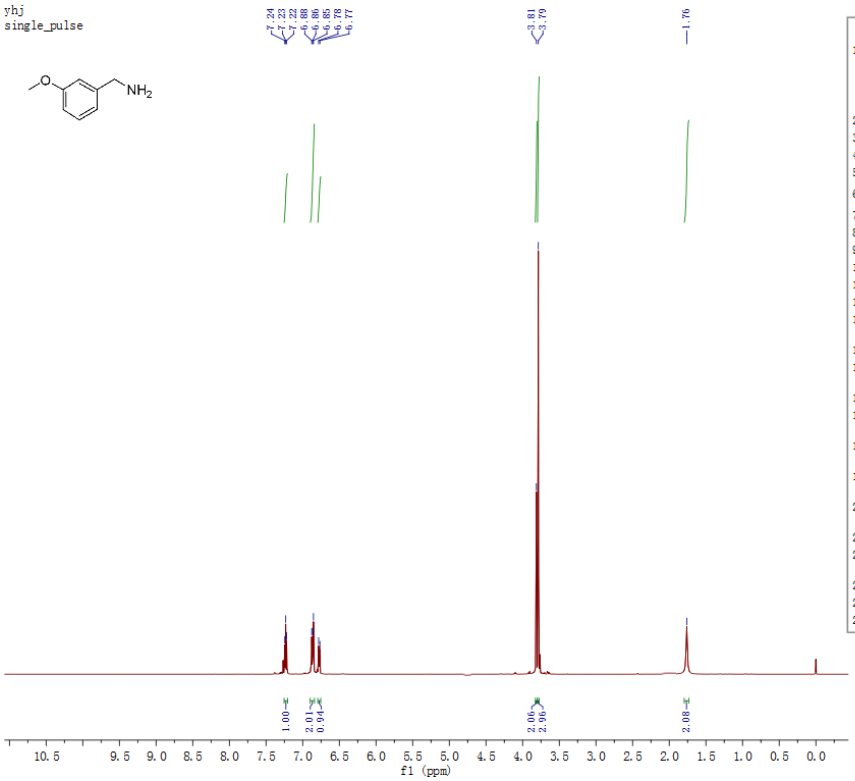

	Parameter	Value
1	Data File Name	D:/ liulei/ 艾永建-12个氢谱12个碳谱/ 艾永建-12个氢谱12个碳谱/ lql-ayj-180515-13xia-H-single_pulse-2.jdf
2	Title	yhj
3	Comment	single_pulse
4	Origin	JEOL
5	Owner	
6	Site	
7	Spectrometer	ECA 600
8	Author	HappyNMR
9	Solvent	CHLOROFORM-D
10	Temperature	24.0
11	Pulse Sequence	single_pulse.ex2
12	Experiment	1D
13	Number of Scans	16
14	Receiver Gain	28
15	Relaxation Delay	2.0000
16	Pulse Width	7.1000
17	Acquisition Time	2.9098
18	Acquisition Date	2018-05-18T16:34:51
19	Modification Date	2018-05-18T16:50:30
20	Spectrometer Frequency	600.17
21	Spectral Width	9008.5
22	Lowest Frequency	-293.5
23	Nucleus	1H
24	Acquired Size	32768
25	Spectral Size	26214

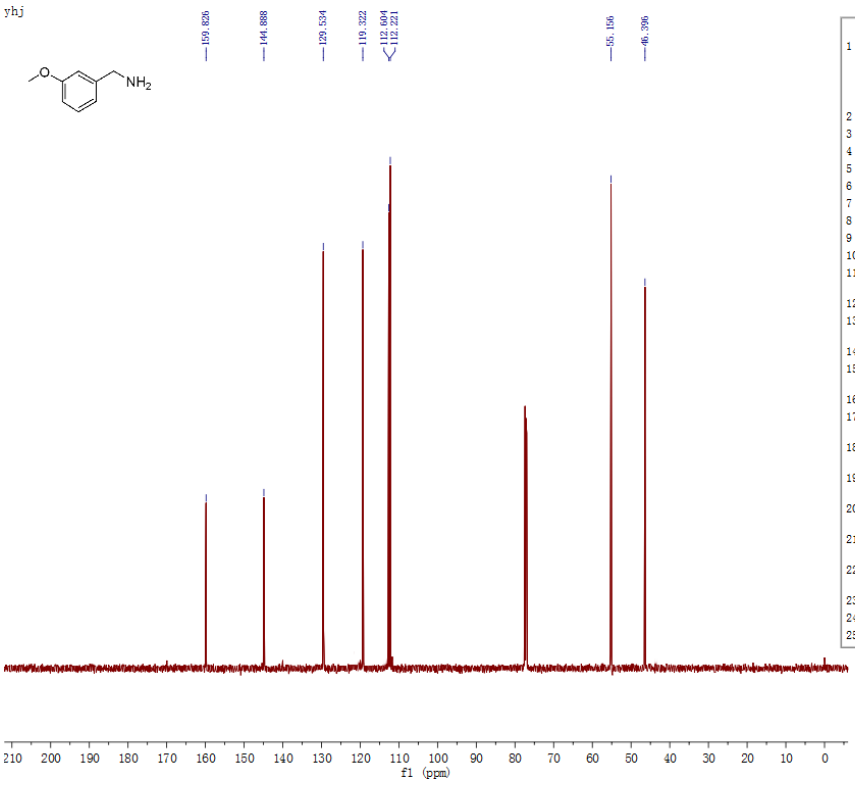

	Parameter	Value
1	Data File Name	D:/ liulei/ 艾永建-12个氢谱12个碳谱/ 艾永建-12个氢谱12个碳谱/ lql-ayj-180515-13xia-C-single_pulse_dec-3.jdf
2	Title	yhj
3	Comment	
4	Origin	JEOL
5	Owner	
6	Site	
7	Spectrometer	ECA 600
8	Author	HappyNMR
9	Solvent	CHLOROFORM-D
10	Temperature	25.0
11	Pulse Sequence	single_pulse_dec
12	Experiment	1D
13	Number of Scans	112
14	Receiver Gain	58
15	Relaxation Delay	2.0000
16	Pulse Width	4.0833
17	Acquisition Time	0.6921
18	Acquisition Date	2018-05-18T16:40:30
19	Modification Date	2018-05-18T16:57:06
20	Spectrometer Frequency	150.91
21	Spectral Width	37876.8
22	Lowest Frequency	-3860.9
23	Nucleus	13C
24	Acquired Size	32768
25	Spectral Size	26214

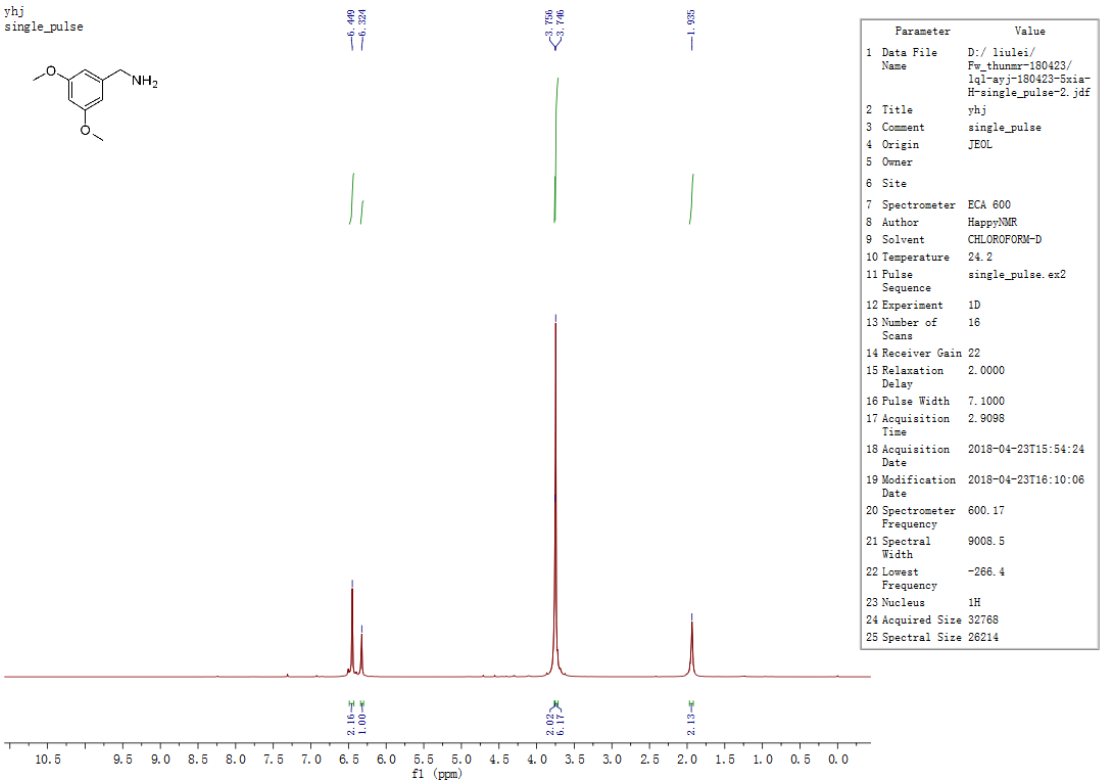

	Parameter	Value
1	Data File Name	D:/ liulei/ Fw_thunmr-180423/ lql-ayj-180423-5xia-H-single_pulse-2.jdf
2	Title	yhj
3	Comment	single_pulse
4	Origin	JEOL
5	Owner	
6	Site	
7	Spectrometer	ECA 600
8	Author	HappyNMR
9	Solvent	CHLOROFORM-D
10	Temperature	24.2
11	Pulse Sequence	single_pulse.ex2
12	Experiment	1D
13	Number of Scans	16
14	Receiver Gain	22
15	Relaxation Delay	2.0000
16	Pulse Width	7.1000
17	Acquisition Time	2.9098
18	Acquisition Date	2018-04-23T15:54:24
19	Modification Date	2018-04-23T16:10:06
20	Spectrometer Frequency	600.17
21	Spectral Width	9008.5
22	Lowest Frequency	-266.4
23	Nucleus	1H
24	Acquired Size	32768
25	Spectral Size	26214

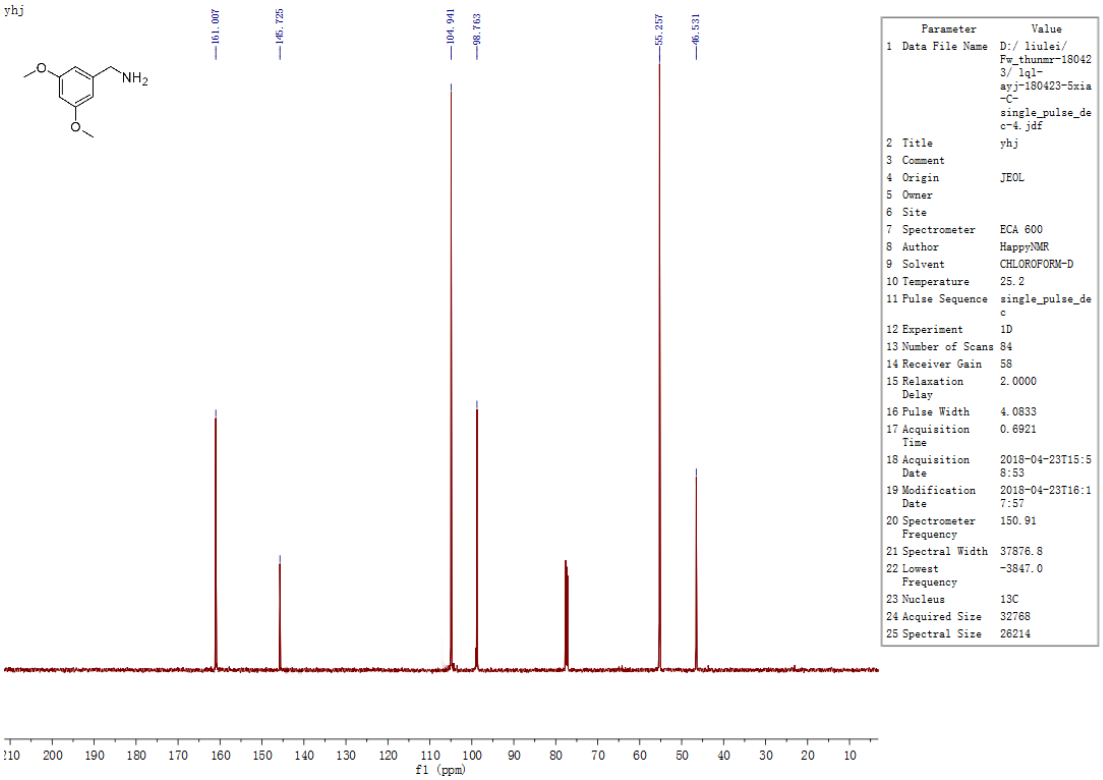

	Parameter	Value
1	Data File Name	D:/ liulei/ Fw_thunmr-18042 3/ lql-ayj-180423-5xia -C-single_pulse_dec-4.jdf
2	Title	yhj
3	Comment	
4	Origin	JEOL
5	Owner	
6	Site	
7	Spectrometer	ECA 600
8	Author	HappyNMR
9	Solvent	CHLOROFORM-D
10	Temperature	25.2
11	Pulse Sequence	single_pulse_dec
12	Experiment	1D
13	Number of Scans	84
14	Receiver Gain	58
15	Relaxation Delay	2.0000
16	Pulse Width	4.0833
17	Acquisition Time	0.6921
18	Acquisition Date	2018-04-23T15:58:53
19	Modification Date	2018-04-23T16:17:57
20	Spectrometer Frequency	150.91
21	Spectral Width	37876.8
22	Lowest Frequency	-3847.0
23	Nucleus	13C
24	Acquired Size	32768
25	Spectral Size	26214

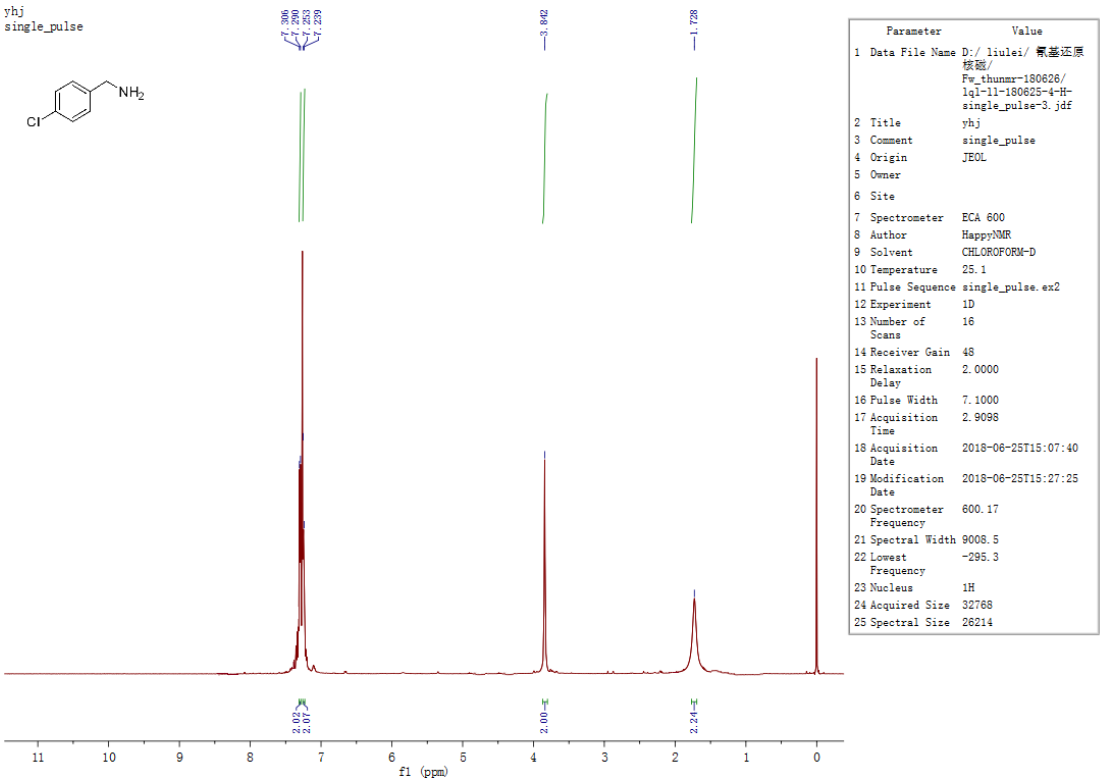

	Parameter	Value
1	Data File Name	D:/ liulei/ 氧基还原核磁/ Fw_thunmr-180626/ lql-ll-180625-4-H-single_pulse-3.jdf
2	Title	yhj
3	Comment	single_pulse
4	Origin	JEOL
5	Owner	
6	Site	
7	Spectrometer	ECA 600
8	Author	HappyNMR
9	Solvent	CHLOROFORM-D
10	Temperature	25.1
11	Pulse Sequence	single_pulse.ex2
12	Experiment	1D
13	Number of Scans	16
14	Receiver Gain	48
15	Relaxation Delay	2.0000
16	Pulse Width	7.1000
17	Acquisition Time	2.9098
18	Acquisition Date	2018-06-25T15:07:40
19	Modification Date	2018-06-25T15:27:25
20	Spectrometer Frequency	600.17
21	Spectral Width	9008.5
22	Lowest Frequency	-295.3
23	Nucleus	1H
24	Acquired Size	32768
25	Spectral Size	26214

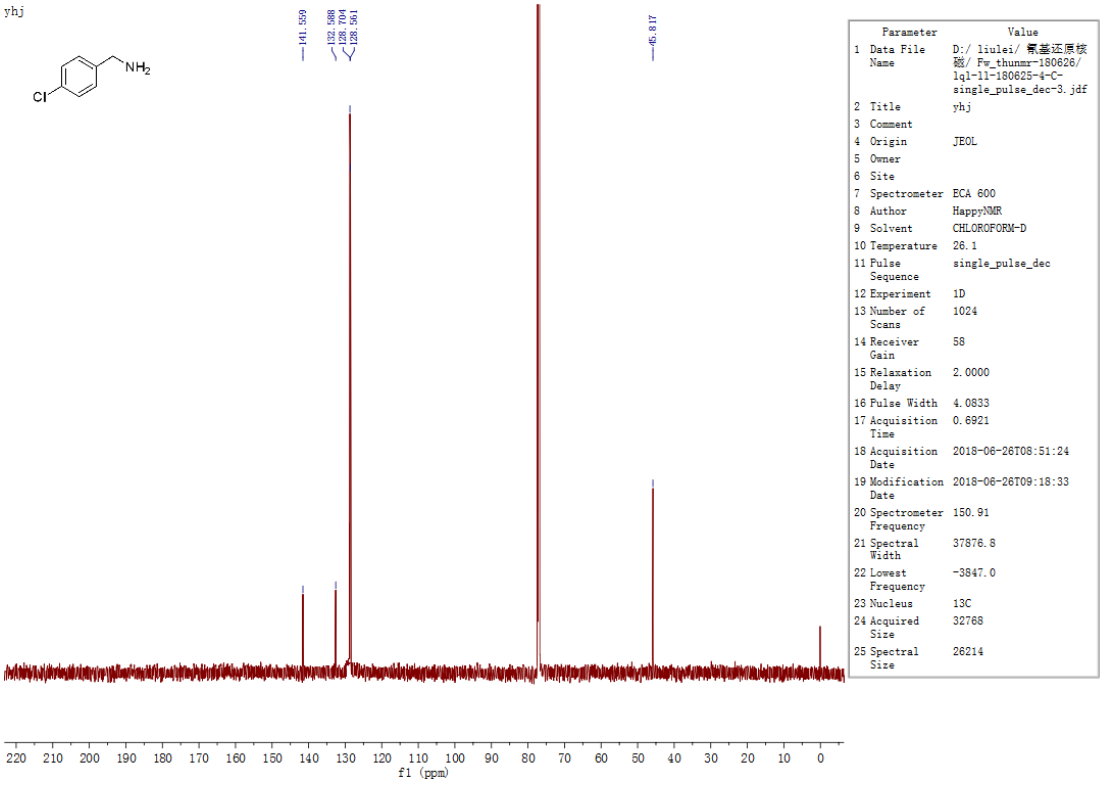

	Parameter	Value
1	Data File Name	D:/ liulei/ 氧基还原核磁/ Fw_thunmr-180626/ lql-ll-180625-4-C-single_pulse_dec-3.jdf
2	Title	yhj
3	Comment	
4	Origin	JEOL
5	Owner	
6	Site	
7	Spectrometer	ECA 600
8	Author	HappyNMR
9	Solvent	CHLOROFORM-D
10	Temperature	26.1
11	Pulse Sequence	single_pulse_dec
12	Experiment	1D
13	Number of Scans	1024
14	Receiver Gain	58
15	Relaxation Delay	2.0000
16	Pulse Width	4.0833
17	Acquisition Time	0.6921
18	Acquisition Date	2018-06-26T08:51:24
19	Modification Date	2018-06-26T09:18:33
20	Spectrometer Frequency	150.91
21	Spectral Width	37876.8
22	Lowest Frequency	-3847.0
23	Nucleus	13C
24	Acquired Size	32768
25	Spectral Size	26214

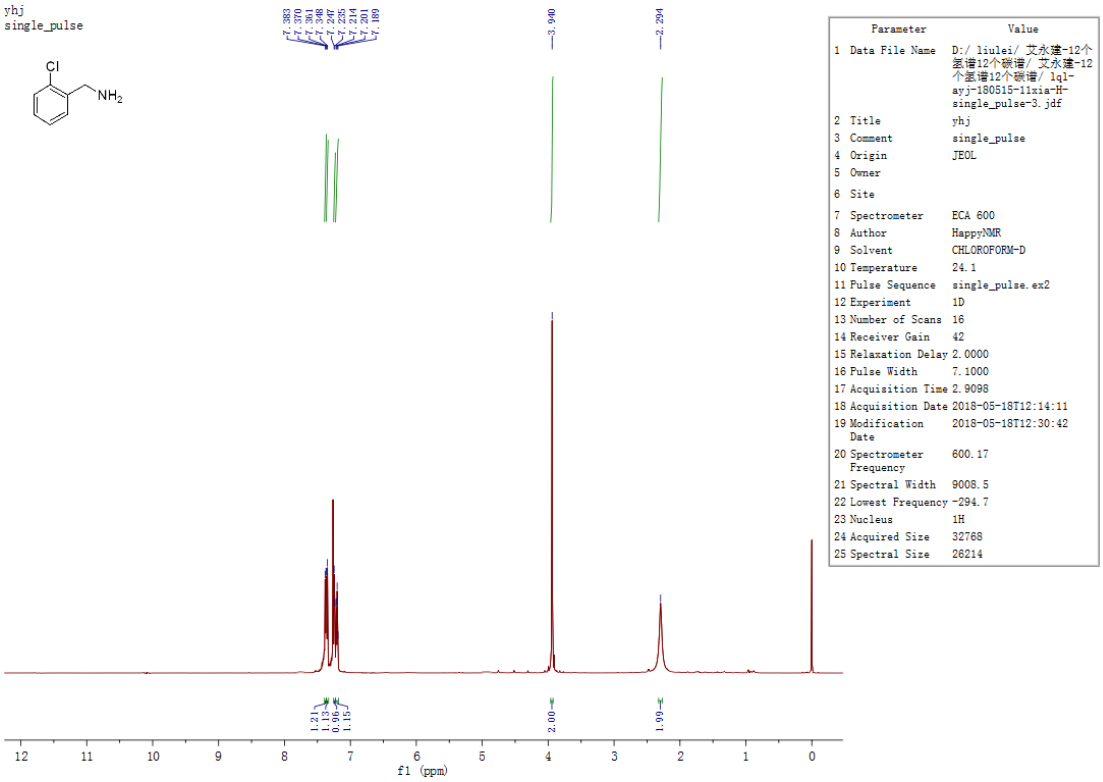

	Parameter	Value
1	Data File Name	D:/ liulei/ 艾永建-12个氢谱12个碳谱/ 艾永建-12个氢谱12个碳谱/ lql-ayj-180515-11xia-H-single_pulse-3.jdf
2	Title	yhj
3	Comment	single_pulse
4	Origin	JEOL
5	Owner	
6	Site	
7	Spectrometer	ECA 600
8	Author	HappyNMR
9	Solvent	CHLOROFORM-D
10	Temperature	24.1
11	Pulse Sequence	single_pulse.ex2
12	Experiment	1D
13	Number of Scans	16
14	Receiver Gain	42
15	Relaxation Delay	2.0000
16	Pulse Width	7.1000
17	Acquisition Time	2.9098
18	Acquisition Date	2018-05-18T12:14:11
19	Modification Date	2018-05-18T12:30:42
20	Spectrometer Frequency	600.17
21	Spectral Width	9008.5
22	Lowest Frequency	-294.7
23	Nucleus	1H
24	Acquired Size	32768
25	Spectral Size	26214

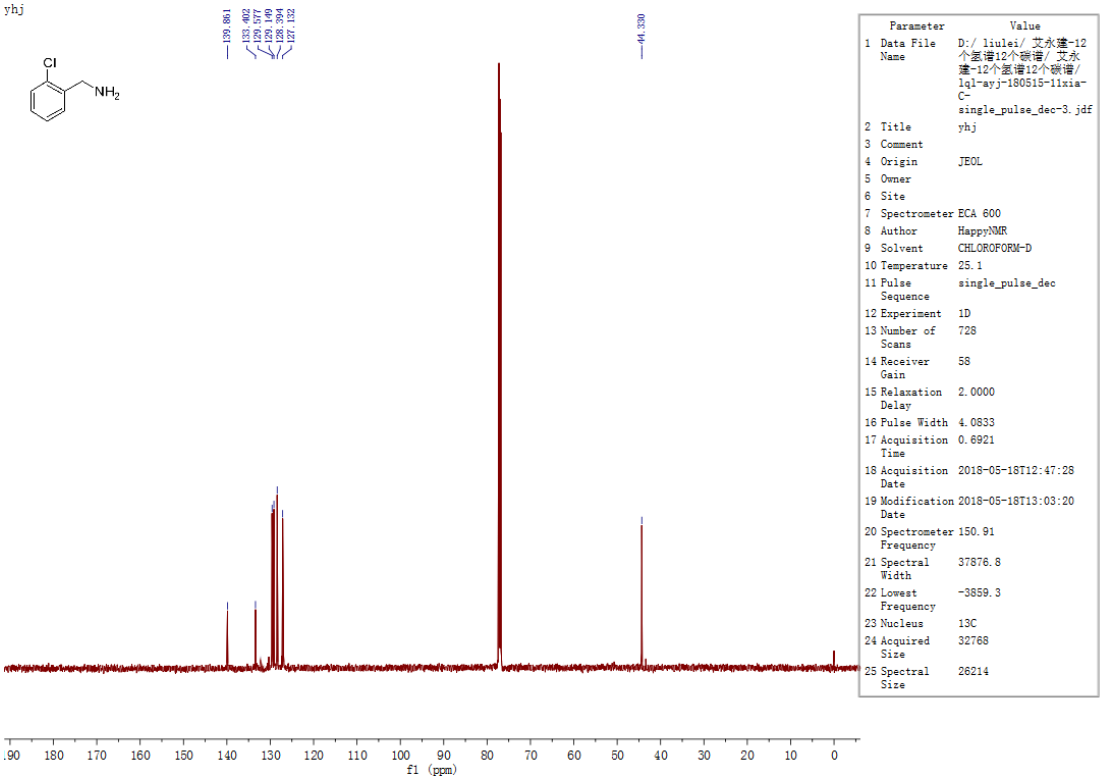

	Parameter	Value
1	Data File Name	D:/ liulei/ 艾永建-12个氢谱12个碳谱/ 艾永建-12个氢谱12个碳谱/ lql-ayj-180515-11xia-C-single_pulse_dec-3.jdf
2	Title	yhj
3	Comment	
4	Origin	JEOL
5	Owner	
6	Site	
7	Spectrometer	ECA 600
8	Author	HappyNMR
9	Solvent	CHLOROFORM-D
10	Temperature	25.1
11	Pulse Sequence	single_pulse_dec
12	Experiment	1D
13	Number of Scans	728
14	Receiver Gain	58
15	Relaxation Delay	2.0000
16	Pulse Width	4.0833
17	Acquisition Time	0.6921
18	Acquisition Date	2018-05-18T12:47:28
19	Modification Date	2018-05-18T13:03:20
20	Spectrometer Frequency	150.91
21	Spectral Width	37876.8
22	Lowest Frequency	-3859.3
23	Nucleus	13C
24	Acquired Size	32768
25	Spectral Size	26214

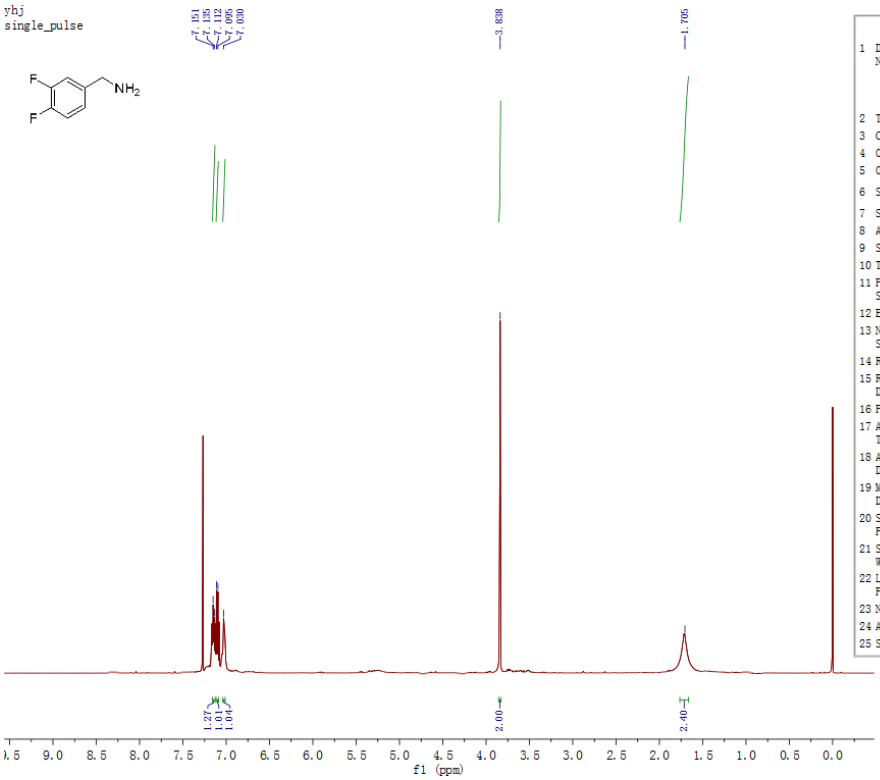

	Parameter	Value
1	Data File Name	D:/ liulei/ 刘磊-12个氢谱12个碳谱/ 刘磊-12个氢谱12个碳谱/ lql-ll-180521-17xia-H-single_pulse-3.jdf
2	Title	yhj
3	Comment	single_pulse
4	Origin	JEOL
5	Owner	
6	Site	
7	Spectrometer	ECA 600
8	Author	HappyNMR
9	Solvent	CHLOROFORM-D
10	Temperature	23.7
11	Pulse Sequence	single_pulse.ex2
12	Experiment	1D
13	Number of Scans	16
14	Receiver Gain	42
15	Relaxation Delay	2.0000
16	Pulse Width	7.1000
17	Acquisition Time	2.9098
18	Acquisition Date	2018-05-24T14:48:14
19	Modification Date	2018-05-24T15:04:32
20	Spectrometer Frequency	600.17
21	Spectral Width	9008.5
22	Lowest Frequency	-292.3
23	Nucleus	1H
24	Acquired Size	32768
25	Spectral Size	26214

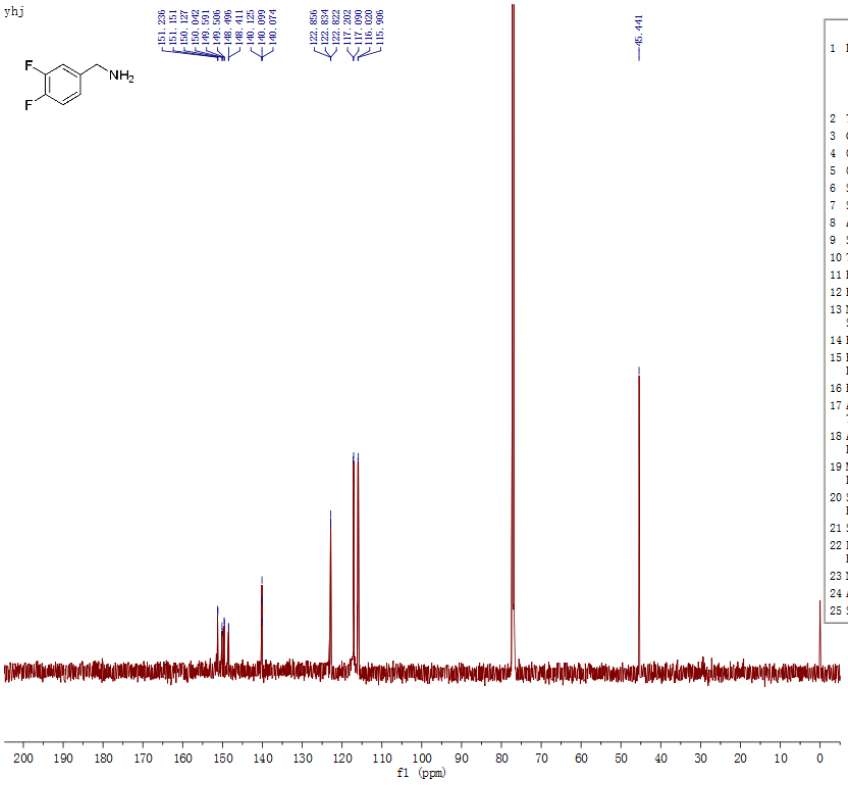

	Parameter	Value
1	Data File Name	D:/ liulei/ 氧基还原核磁/ 刘磊-12个氢谱12个碳谱/ 刘磊-12个氢谱12个碳谱/ lql-ll-180521-17xia-C-single_pulse_dec-3.jdf
2	Title	yhj
3	Comment	
4	Origin	JEOL
5	Owner	
6	Site	
7	Spectrometer	ECA 600
8	Author	HappyNMR
9	Solvent	CHLOROFORM-D
10	Temperature	24.7
11	Pulse Sequence	single_pulse_dec
12	Experiment	1D
13	Number of Scans	1024
14	Receiver Gain	58
15	Relaxation Delay	2.0000
16	Pulse Width	4.0833
17	Acquisition Time	0.6921
18	Acquisition Date	2018-05-24T15:35:18
19	Modification Date	2018-05-24T15:52:26
20	Spectrometer Frequency	150.91
21	Spectral Width	37876.8
22	Lowest Frequency	-3855.3
23	Nucleus	13C
24	Acquired Size	32768
25	Spectral Size	26214

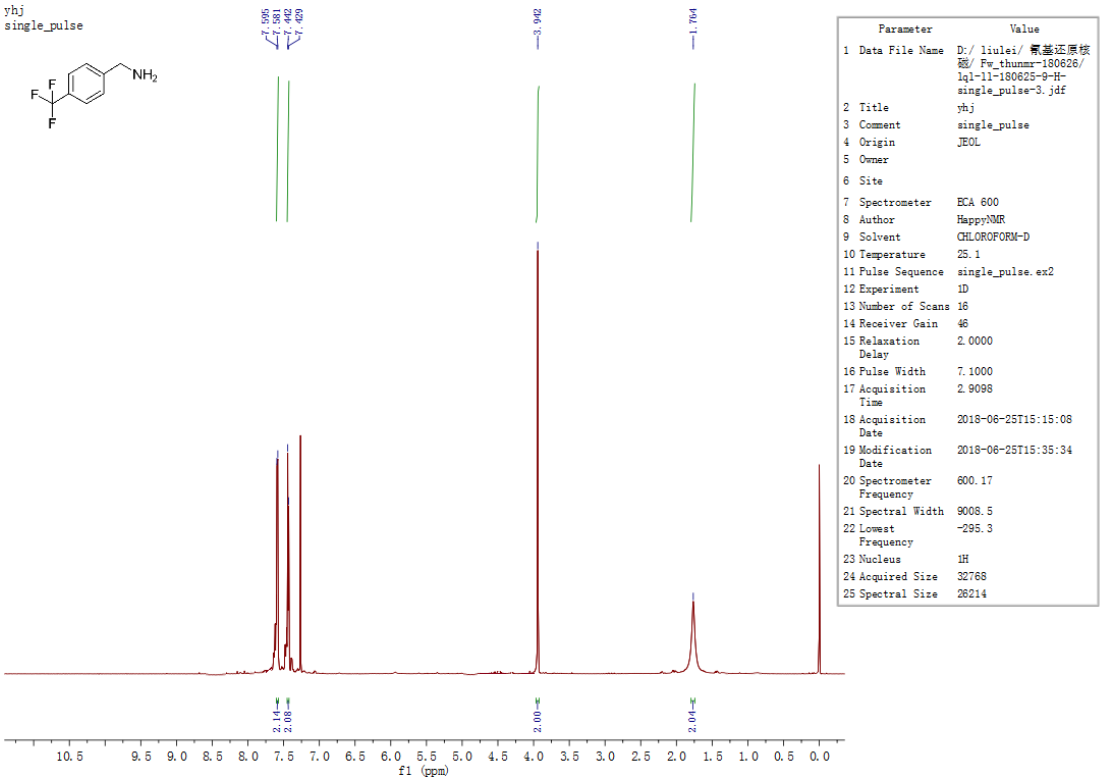

	Parameter	Value
1	Data File Name	D:/ liulei/ 氧基还原核磁/ Fw_thunmr-180626/ lql-11-180625-9-H-single_pulse-3.jdf
2	Title	yhj
3	Comment	single_pulse
4	Origin	JEOL
5	Owner	
6	Site	
7	Spectrometer	ECA 600
8	Author	HappyNMR
9	Solvent	CHLOROFORM-D
10	Temperature	25.1
11	Pulse Sequence	single_pulse.ex2
12	Experiment	1D
13	Number of Scans	16
14	Receiver Gain	46
15	Relaxation Delay	2.0000
16	Pulse Width	7.1000
17	Acquisition Time	2.9098
18	Acquisition Date	2018-06-25T15:15:08
19	Modification Date	2018-06-25T15:35:34
20	Spectrometer Frequency	600.17
21	Spectral Width	9008.5
22	Lowest Frequency	-295.3
23	Nucleus	1H
24	Acquired Size	32768
25	Spectral Size	26214

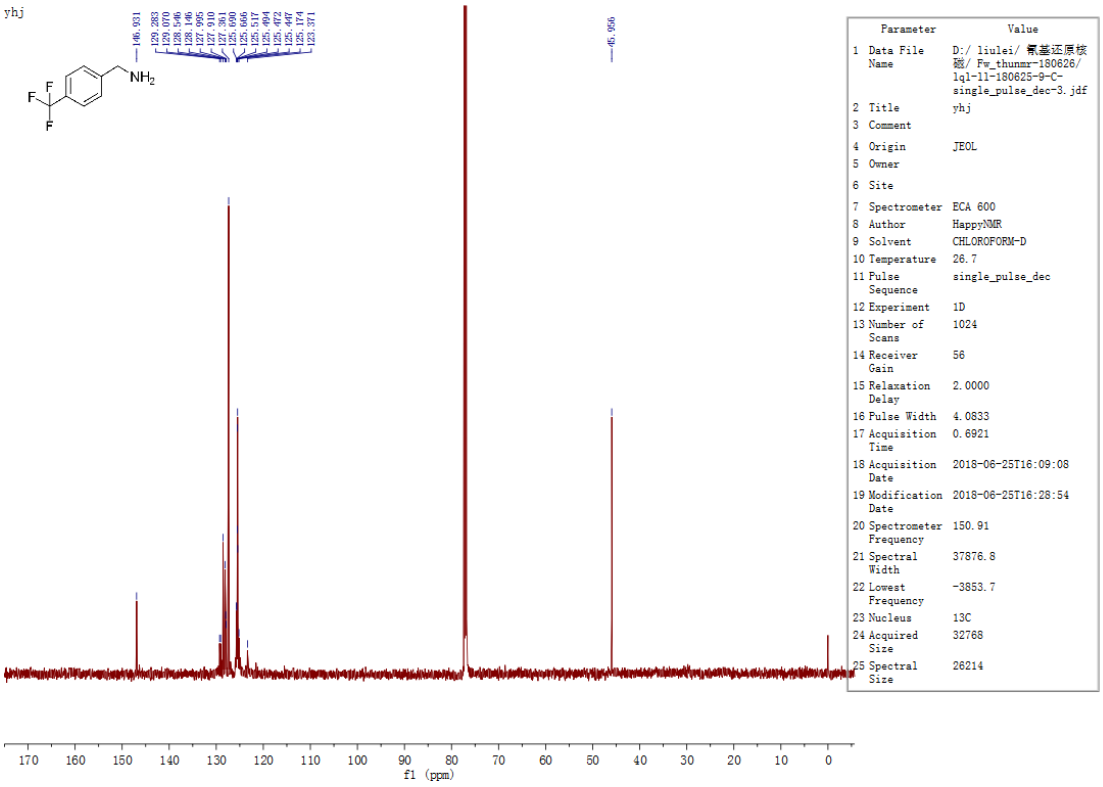

	Parameter	Value
1	Data File Name	D:/ liulei/ 氧基还原核磁/ Fw_thunmr-180626/ lql-11-180625-9-C-single_pulse_dec-3.jdf
2	Title	yhj
3	Comment	
4	Origin	JEOL
5	Owner	
6	Site	
7	Spectrometer	ECA 600
8	Author	HappyNMR
9	Solvent	CHLOROFORM-D
10	Temperature	26.7
11	Pulse Sequence	single_pulse_dec
12	Experiment	1D
13	Number of Scans	1024
14	Receiver Gain	56
15	Relaxation Delay	2.0000
16	Pulse Width	4.0833
17	Acquisition Time	0.6921
18	Acquisition Date	2018-06-25T16:09:08
19	Modification Date	2018-06-25T16:28:54
20	Spectrometer Frequency	150.91
21	Spectral Width	37876.8
22	Lowest Frequency	-3853.7
23	Nucleus	13C
24	Acquired Size	32768
25	Spectral Size	26214

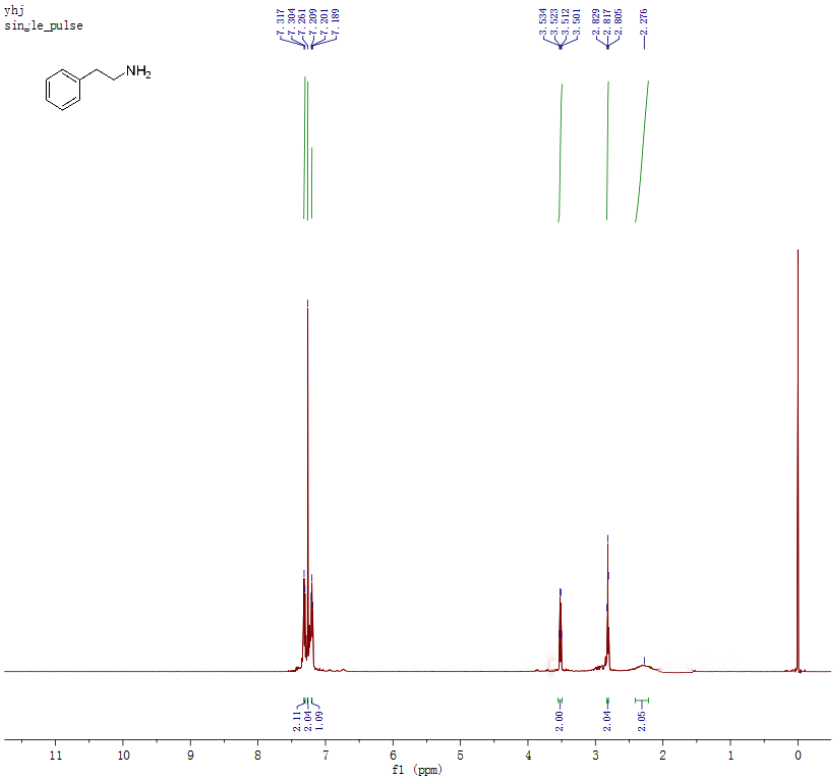

	Parameter	Value
1	Data File Name	D:/ liulei/ 刘磊-12个氢谱12个碳谱/ 刘磊-12个氢谱12个碳谱/ lql-11-180521-16xia-H-single_pulse-3.jdf
2	Title	yhj
3	Comment	single_pulse
4	Origin	JEOL
5	Owner	
6	Site	
7	Spectrometer	ECA 600
8	Author	HappyNMR
9	Solvent	CHLOROFORM-D
10	Temperature	23.1
11	Pulse Sequence	single_pulse.ex2
12	Experiment	1D
13	Number of Scans	16
14	Receiver Gain	44
15	Relaxation Delay	2.0000
16	Pulse Width	7.1000
17	Acquisition Time	2.9098
18	Acquisition Date	2018-05-23T12:53:32
19	Modification Date	2018-05-23T13:17:17
20	Spectrometer Frequency	600.17
21	Spectral Width	9008.5
22	Lowest Frequency	-296.5
23	Nucleus	1H
24	Acquired Size	32768
25	Spectral Size	26214

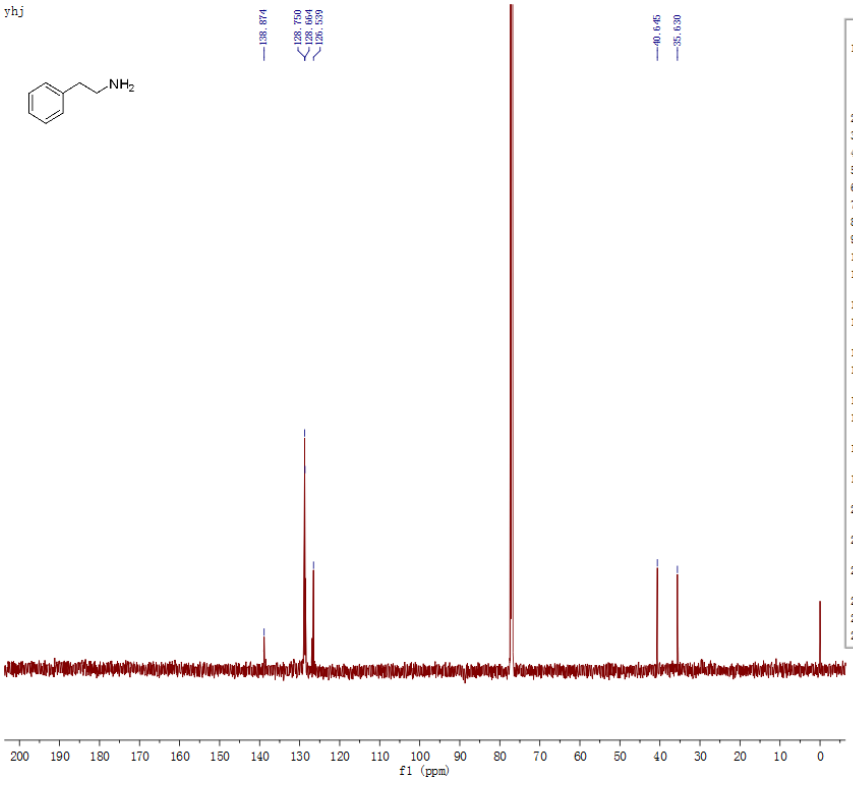

	Parameter	Value
1	Data File Name	D:/ liulei/ 刘磊-12个氢谱12个碳谱/ 刘磊-12个氢谱12个碳谱/ lql-11-180521-16xia-C-single_pulse_dec-3.jdf
2	Title	yhj
3	Comment	
4	Origin	JEOL
5	Owner	
6	Site	
7	Spectrometer	ECA 600
8	Author	HappyNMR
9	Solvent	CHLOROFORM-D
10	Temperature	24.5
11	Pulse Sequence	single_pulse_dec
12	Experiment	1D
13	Number of Scans	1024
14	Receiver Gain	58
15	Relaxation Delay	2.0000
16	Pulse Width	4.0833
17	Acquisition Time	0.6921
18	Acquisition Date	2018-05-23T13:40:06
19	Modification Date	2018-05-23T13:56:50
20	Spectrometer Frequency	150.91
21	Spectral Width	37876.8
22	Lowest Frequency	-3859.1
23	Nucleus	13C
24	Acquired Size	32768
25	Spectral Size	26214

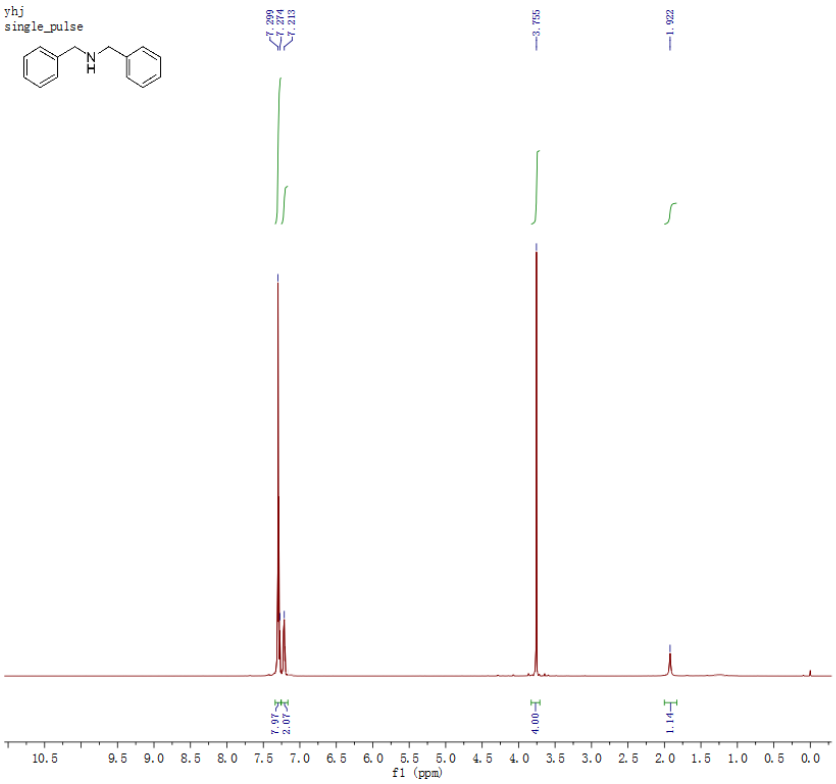

	Parameter	Value
1	Data File Name	D:/ liulei/ Fw_thunmr-180423/ lql-ayj-180420-1shang-H-single_pulse-2.jdf
2	Title	yhj
3	Comment	single_pulse
4	Origin	JEOL
5	Owner	
6	Site	
7	Spectrometer	ECA 600
8	Author	HappyNMR
9	Solvent	CHLOROFORM-D
10	Temperature	25.6
11	Pulse Sequence	single_pulse.ex2
12	Experiment	1D
13	Number of Scans	16
14	Receiver Gain	30
15	Relaxation Delay	2.0000
16	Pulse Width	7.1000
17	Acquisition Time	2.9098
18	Acquisition Date	2018-04-20T15:03:04
19	Modification Date	2018-04-20T15:18:47
20	Spectrometer Frequency	600.17
21	Spectral Width	9008.5
22	Lowest Frequency	-377.5
23	Nucleus	1H
24	Acquired Size	32768
25	Spectral Size	26214

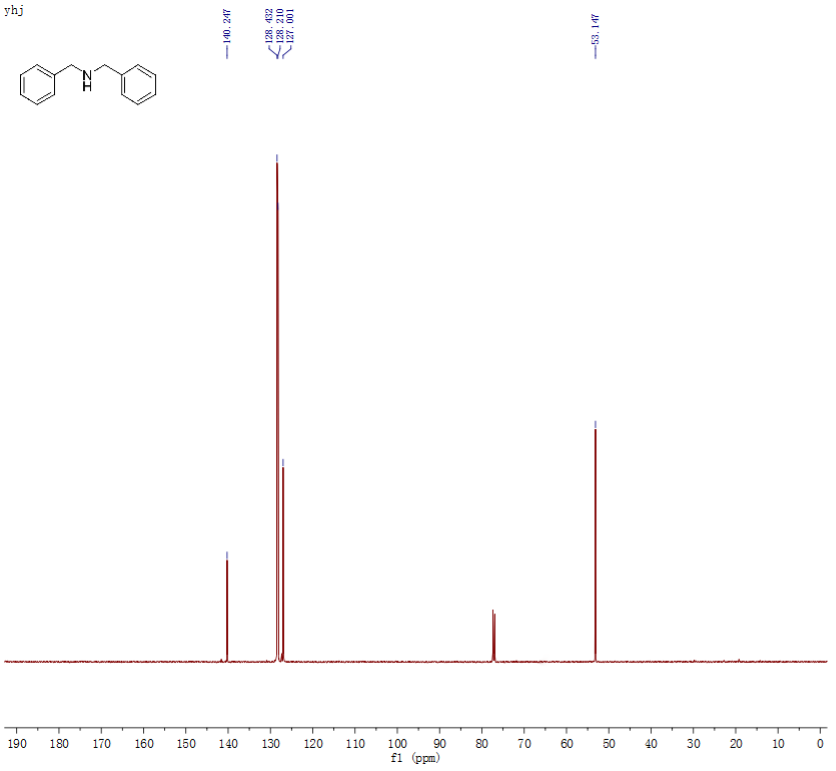

	Parameter	Value
1	Data File Name	D:/ liulei/ Fw_thunmr-180423/ lql-ayj-180420-1shang-C-single_pulse_dec-2.jdf
2	Title	yhj
3	Comment	
4	Origin	JEOL
5	Owner	
6	Site	
7	Spectrometer	ECA 600
8	Author	HappyNMR
9	Solvent	CHLOROFORM-D
10	Temperature	26.7
11	Pulse Sequence	single_pulse_dec
12	Experiment	1D
13	Number of Scans	162
14	Receiver Gain	56
15	Relaxation Delay	2.0000
16	Pulse Width	4.0833
17	Acquisition Time	0.6921
18	Acquisition Date	2018-04-20T15:11:28
19	Modification Date	2018-04-20T15:27:10
20	Spectrometer Frequency	150.91
21	Spectral Width	37876.8
22	Lowest Frequency	-3847.0
23	Nucleus	13C
24	Acquired Size	32768
25	Spectral Size	26214

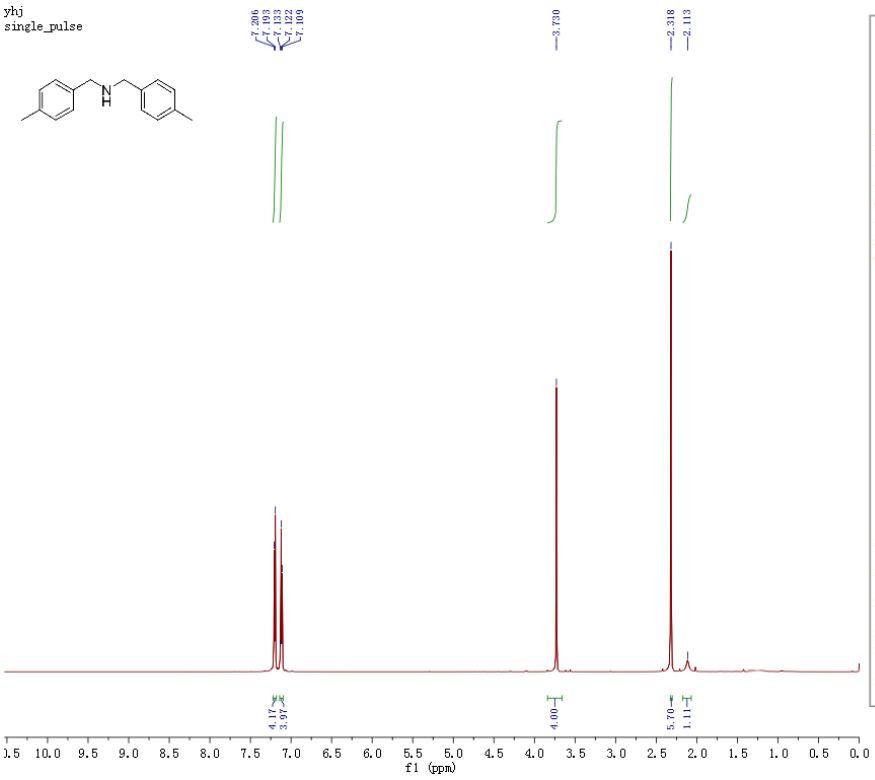

	Parameter	Value
1	Data File Name	D:/ liulei/ Fw_thunmr-180423/ lql-ayj-180420-2shang-H-single_pulse-3.jdf
2	Title	yhj
3	Comment	single_pulse
4	Origin	JEOL
5	Owner	
6	Site	
7	Spectrometer	ECA 600
8	Author	HappyNMR
9	Solvent	CHLOROFORM-D
10	Temperature	25.8
11	Pulse Sequence	single_pulse.ex2
12	Experiment	1D
13	Number of Scans	16
14	Receiver Gain	30
15	Relaxation Delay	2.0000
16	Pulse Width	7.1000
17	Acquisition Time	2.9098
18	Acquisition Date	2018-04-20T15:46:24
19	Modification Date	2018-04-20T16:05:34
20	Spectrometer Frequency	600.17
21	Spectral Width	9008.5
22	Lowest Frequency	-340.3
23	Nucleus	1H
24	Acquired Size	32768
25	Spectral Size	26214

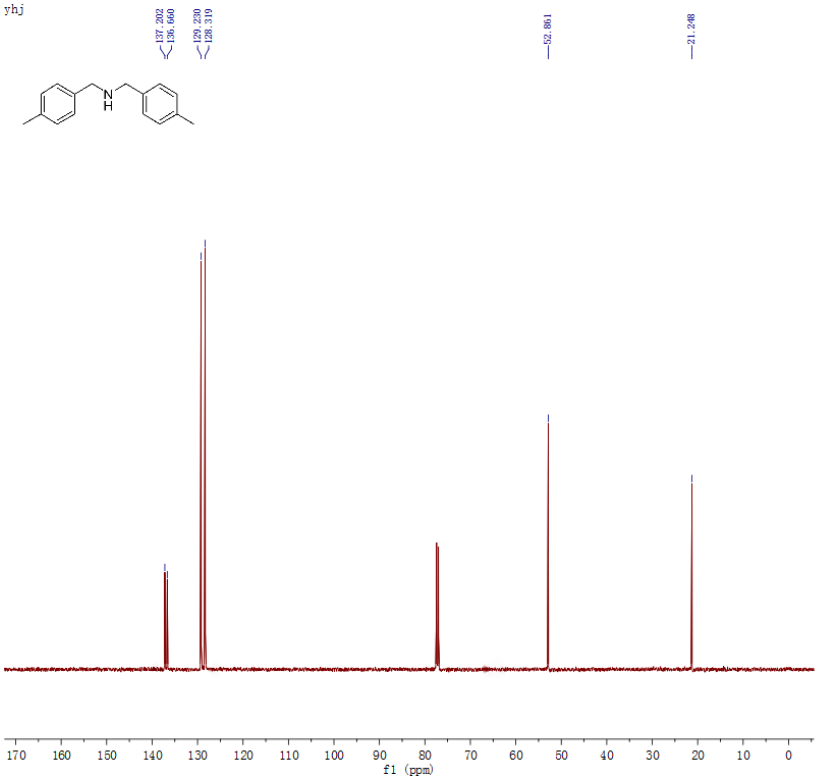

	Parameter	Value
1	Data File Name	D:/ liulei/ Fw_thunmr-180423/ lql-ayj-180420-2shang-C-single_pulse_dec-2.jdf
2	Title	yhj
3	Comment	
4	Origin	JEOL
5	Owner	
6	Site	
7	Spectrometer	ECA 600
8	Author	HappyNMR
9	Solvent	CHLOROFORM-D
10	Temperature	26.8
11	Pulse Sequence	single_pulse_dec
12	Experiment	1D
13	Number of Scans	123
14	Receiver Gain	56
15	Relaxation Delay	2.0000
16	Pulse Width	4.0833
17	Acquisition Time	0.6921
18	Acquisition Date	2018-04-20T15:52:42
19	Modification Date	2018-04-20T16:09:04
20	Spectrometer Frequency	150.91
21	Spectral Width	37876.8
22	Lowest Frequency	-3847.0
23	Nucleus	13C
24	Acquired Size	32768
25	Spectral Size	26214

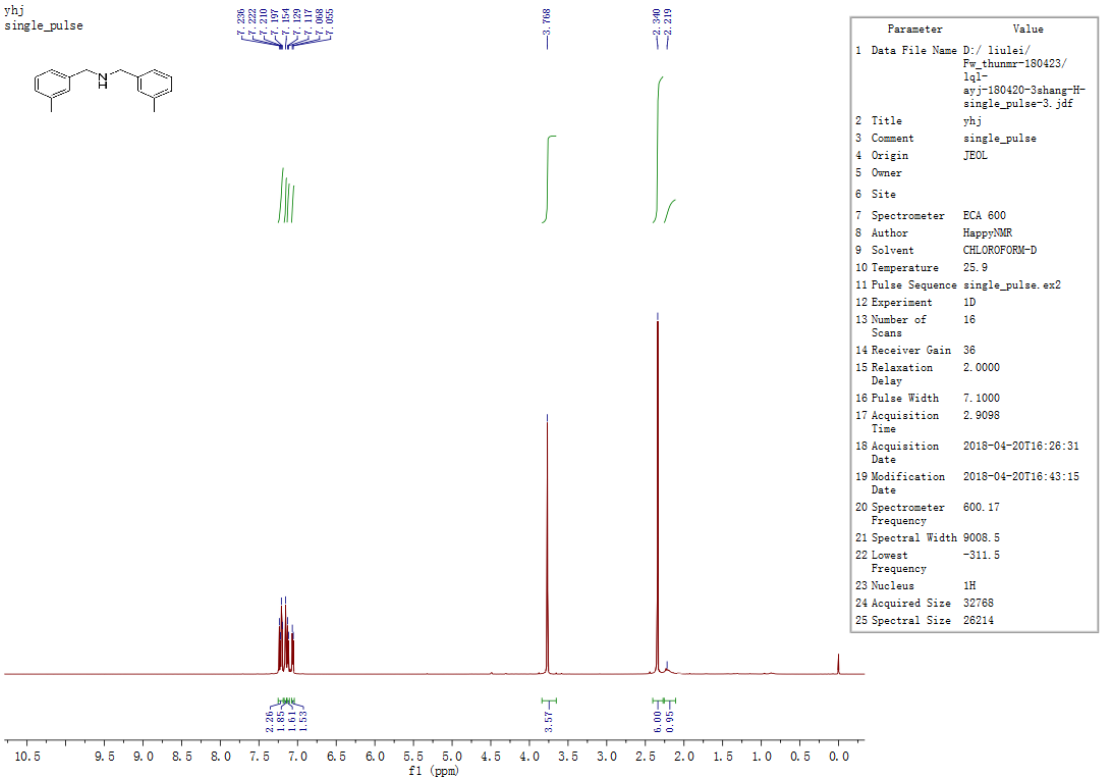

	Parameter	Value
1	Data File Name	D:/ liulei/ Fw_thunmr-180423/ lql-ayj-180420-3shang-H-single_pulse-3.jdf
2	Title	yhj
3	Comment	single_pulse
4	Origin	JEOL
5	Owner	
6	Site	
7	Spectrometer	ECA 600
8	Author	HappyNMR
9	Solvent	CHLOROFORM-D
10	Temperature	25.9
11	Pulse Sequence	single_pulse.ex2
12	Experiment	1D
13	Number of Scans	16
14	Receiver Gain	36
15	Relaxation Delay	2.0000
16	Pulse Width	7.1000
17	Acquisition Time	2.9098
18	Acquisition Date	2018-04-20T16:26:31
19	Modification Date	2018-04-20T16:43:15
20	Spectrometer Frequency	600.17
21	Spectral Width	9008.5
22	Lowest Frequency	-311.5
23	Nucleus	1H
24	Acquired Size	32768
25	Spectral Size	26214

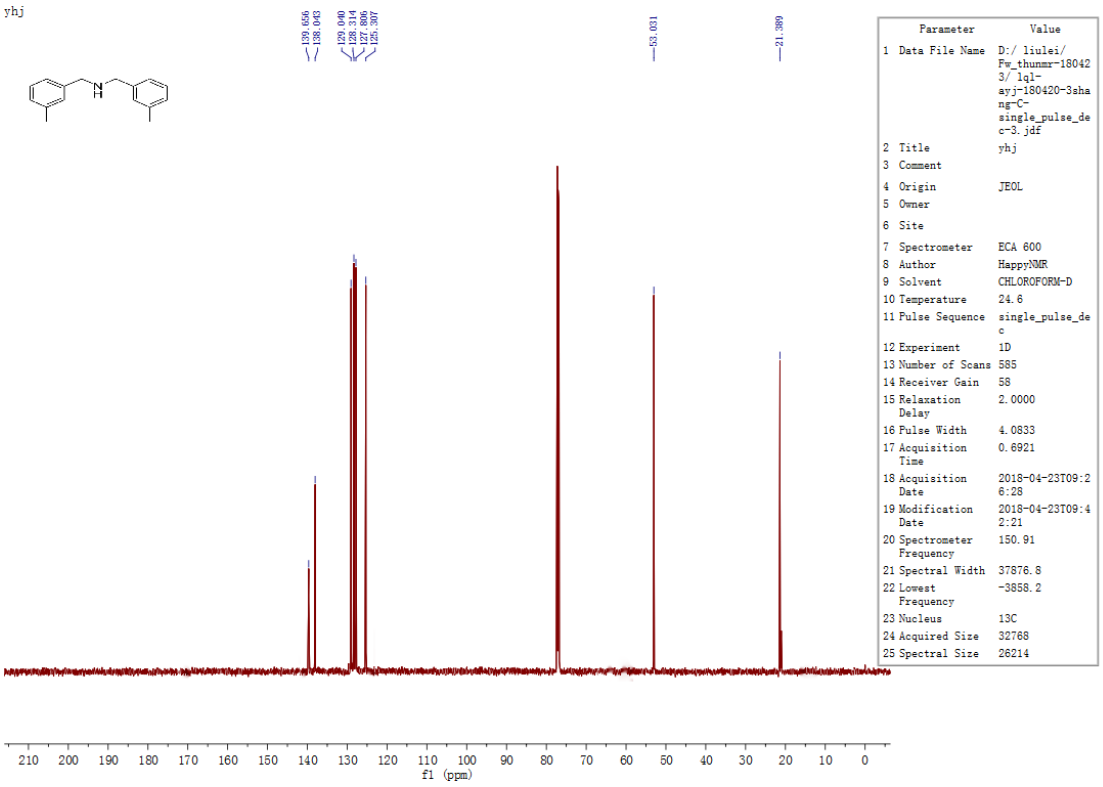

	Parameter	Value
1	Data File Name	D:/ liulei/ Fw_thunmr-180423/ lql-ayj-180420-3shang-C-single_pulse_dec-3.jdf
2	Title	yhj
3	Comment	
4	Origin	JEOL
5	Owner	
6	Site	
7	Spectrometer	ECA 600
8	Author	HappyNMR
9	Solvent	CHLOROFORM-D
10	Temperature	24.6
11	Pulse Sequence	single_pulse_dec
12	Experiment	1D
13	Number of Scans	585
14	Receiver Gain	58
15	Relaxation Delay	2.0000
16	Pulse Width	4.0833
17	Acquisition Time	0.6921
18	Acquisition Date	2018-04-23T09:26:28
19	Modification Date	2018-04-23T09:42:21
20	Spectrometer Frequency	150.91
21	Spectral Width	37876.8
22	Lowest Frequency	-3858.2
23	Nucleus	13C
24	Acquired Size	32768
25	Spectral Size	26214

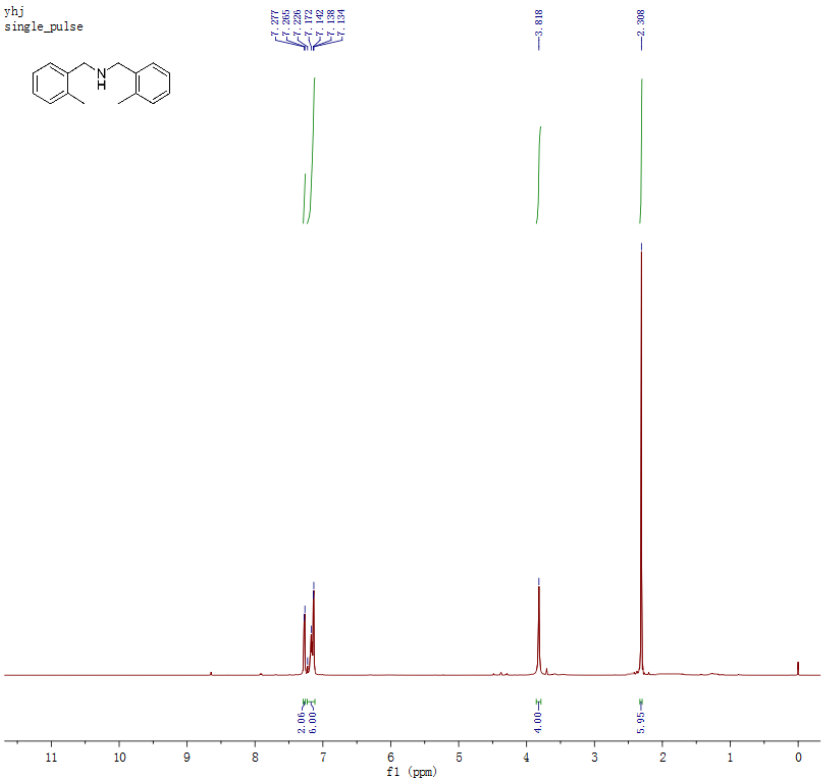

	Parameter	Value
1	Data File Name	D:/ liulei/ 刘磊-12个氢谱12个碳谱/ 刘磊-12个氢谱12个碳谱/ lql-11-180521-6shang-H-single_pulse-3.jdf
2	Title	yhj
3	Comment	single_pulse
4	Origin	JEOL
5	Owner	
6	Site	
7	Spectrometer	ECA 600
8	Author	HappyNMR
9	Solvent	CHLOROFORM-D
10	Temperature	23.7
11	Pulse Sequence	single_pulse.ex2
12	Experiment	1D
13	Number of Scans	16
14	Receiver Gain	28
15	Relaxation Delay	2.0000
16	Pulse Width	7.1000
17	Acquisition Time	2.9098
18	Acquisition Date	2018-05-21T13:58:54
19	Modification Date	2018-05-21T14:14:53
20	Spectrometer Frequency	600.17
21	Spectral Width	9008.5
22	Lowest Frequency	-317.5
23	Nucleus	1H
24	Acquired Size	32768
25	Spectral Size	26214

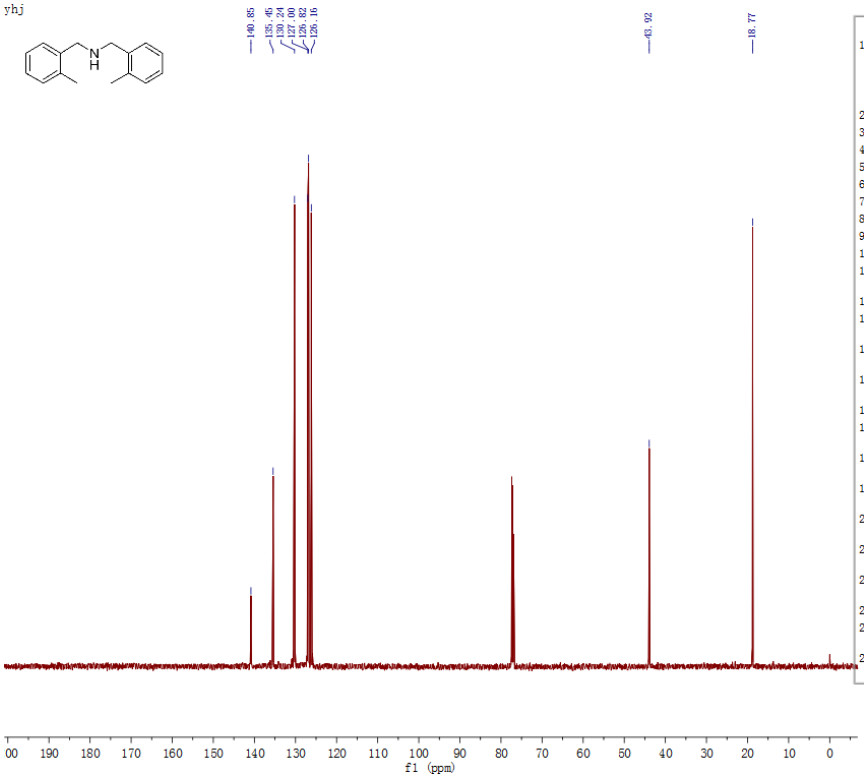

	Parameter	Value
1	Data File Name	D:/ liulei/ 刘磊-12个氢谱12个碳谱/ 刘磊-12个氢谱12个碳谱/ lql-11-180521-6shang-C-single_pulse_dec-3.jdf
2	Title	yhj
3	Comment	
4	Origin	JEOL
5	Owner	
6	Site	
7	Spectrometer	ECA 600
8	Author	HappyNMR
9	Solvent	CHLOROFORM-D
10	Temperature	24.7
11	Pulse Sequence	single_pulse_dec
12	Experiment	1D
13	Number of Scans	195
14	Receiver Gain	58
15	Relaxation Delay	2.0000
16	Pulse Width	4.0833
17	Acquisition Time	0.6921
18	Acquisition Date	2018-05-21T14:08:17
19	Modification Date	2018-05-21T14:26:38
20	Spectrometer Frequency	150.91
21	Spectral Width	37876.8
22	Lowest Frequency	-3866.8
23	Nucleus	13C
24	Acquired Size	32768
25	Spectral Size	26214

yhj
single_pulse

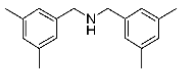

Parameter	Value
1 Data File Name	D:/ liulei/ 艾永建-12个氢谱12个碳谱/ 艾永建-12个氢谱12个碳谱/ lql-ayj-180515-8shang-H-single_pulse-2.jdf
2 Title	yhj
3 Comment	single_pulse
4 Origin	JEOL
5 Owner	
6 Site	
7 Spectrometer	ECA 600
8 Author	HappyNMR
9 Solvent	CHLOROFORM-D
10 Temperature	23.9
11 Pulse Sequence	single_pulse.ex2
12 Experiment	1D
13 Number of Scans	16
14 Receiver Gain	30
15 Relaxation Delay	2.0000
16 Pulse Width	7.1000
17 Acquisition Time	2.9098
18 Acquisition Date	2018-05-18T14:57:53
19 Modification Date	2018-05-18T15:13:32
20 Spectrometer Frequency	600.17
21 Spectral Width	9008.5
22 Lowest Frequency	-334.3
23 Nucleus	1H
24 Acquired Size	32768
25 Spectral Size	26214

yhj

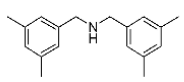

Parameter	Value
1 Data File Name	D:/ liulei/ 艾永建-12个氢谱12个碳谱/ 艾永建-12个氢谱12个碳谱/ lql-ayj-180515-8shang-C-single_pulse_dec-3.jdf
2 Title	yhj
3 Comment	
4 Origin	JEOL
5 Owner	
6 Site	
7 Spectrometer	ECA 600
8 Author	HappyNMR
9 Solvent	CHLOROFORM-D
10 Temperature	24.9
11 Pulse Sequence	single_pulse_dec
12 Experiment	1D
13 Number of Scans	160
14 Receiver Gain	58
15 Relaxation Delay	2.0000
16 Pulse Width	4.0833
17 Acquisition Time	0.6921
18 Acquisition Date	2018-05-18T15:06:15
19 Modification Date	2018-05-18T15:23:02
20 Spectrometer Frequency	150.91
21 Spectral Width	37876.8
22 Lowest Frequency	-3869.7
23 Nucleus	13C
24 Acquired Size	32768
25 Spectral Size	26214

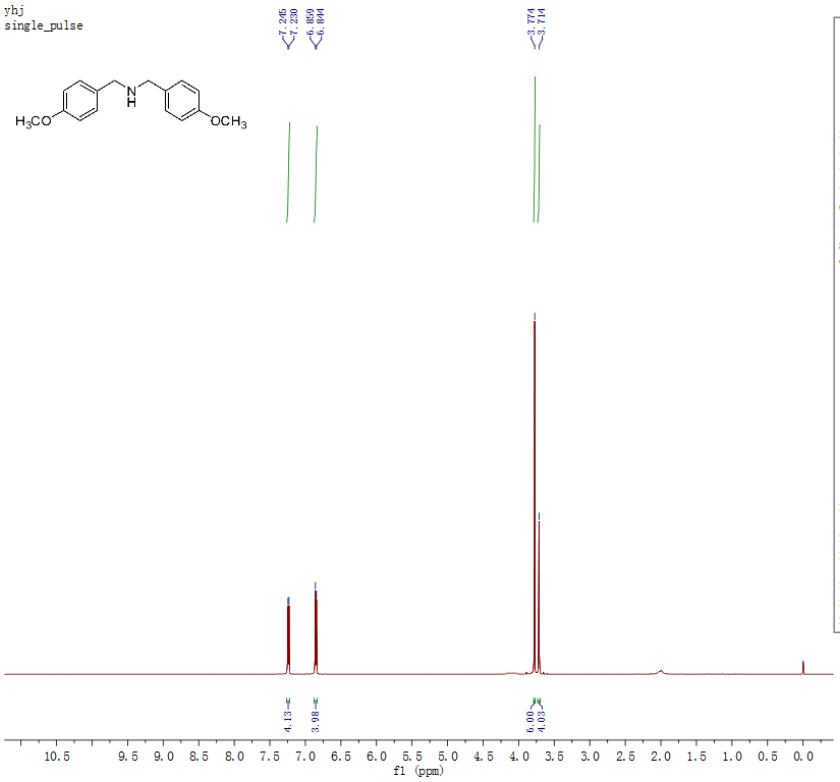

	Parameter	Value
1	Data File Name	D:/ liulei/ 艾永建-12个氢谱12个碳谱/ 艾永建-12个氢谱12个碳谱/ lql-ayj-180515-12shang-H-single_pulse-3.jdf
2	Title	yhj
3	Comment	single_pulse
4	Origin	JEOL
5	Owner	
6	Site	
7	Spectrometer	ECA 600
8	Author	HappyNMR
9	Solvent	CHLOROFORM-D
10	Temperature	23.9
11	Pulse Sequence	single_pulse.ex2
12	Experiment	1D
13	Number of Scans	16
14	Receiver Gain	28
15	Relaxation Delay	2.0000
16	Pulse Width	7.1000
17	Acquisition Time	2.9098
18	Acquisition Date	2018-05-18T15:37:47
19	Modification Date	2018-05-18T15:55:07
20	Spectrometer Frequency	600.17
21	Spectral Width	9008.5
22	Lowest Frequency	-308.5
23	Nucleus	1H
24	Acquired Size	32768
25	Spectral Size	26214

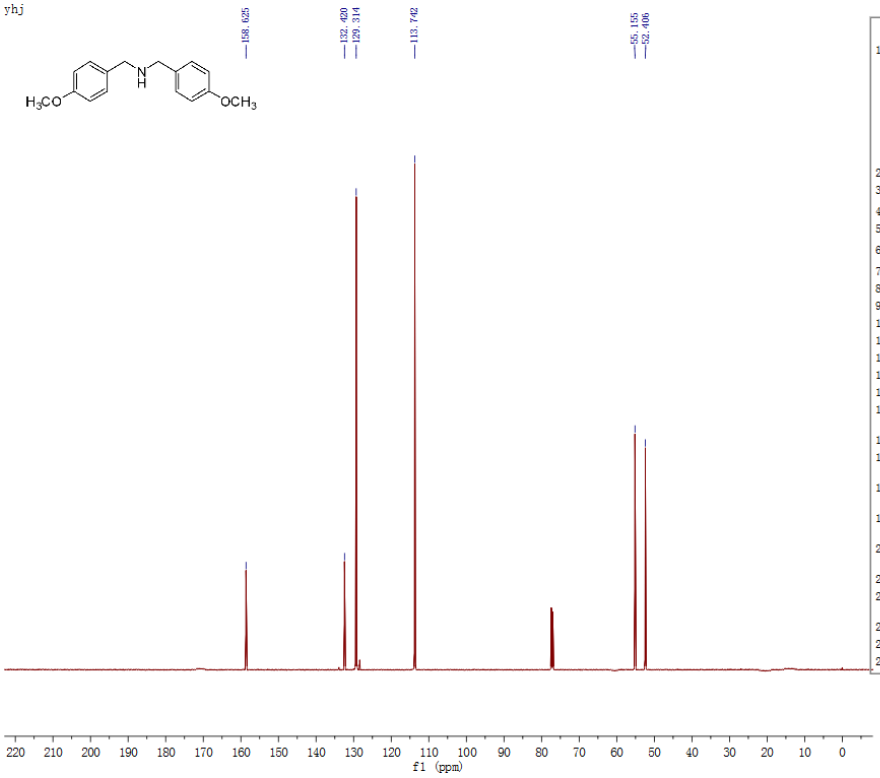

	Parameter	Value
1	Data File Name	D:/ liulei/ 艾永建-12个氢谱12个碳谱/ 艾永建-12个氢谱12个碳谱/ lql-ayj-180515-12shang-C-single_pulse_dec-2.jdf
2	Title	yhj
3	Comment	
4	Origin	JEOL
5	Owner	
6	Site	
7	Spectrometer	ECA 600
8	Author	HappyNMR
9	Solvent	CHLOROFORM-D
10	Temperature	25.1
11	Pulse Sequence	single_pulse_dec
12	Experiment	1D
13	Number of Scans	377
14	Receiver Gain	58
15	Relaxation Delay	2.0000
16	Pulse Width	4.0833
17	Acquisition Time	0.6921
18	Acquisition Date	2018-05-18T16:18:10
19	Modification Date	2018-05-18T16:33:48
20	Spectrometer Frequency	150.91
21	Spectral Width	37876.8
22	Lowest Frequency	-3865.1
23	Nucleus	13C
24	Acquired Size	32768
25	Spectral Size	26214

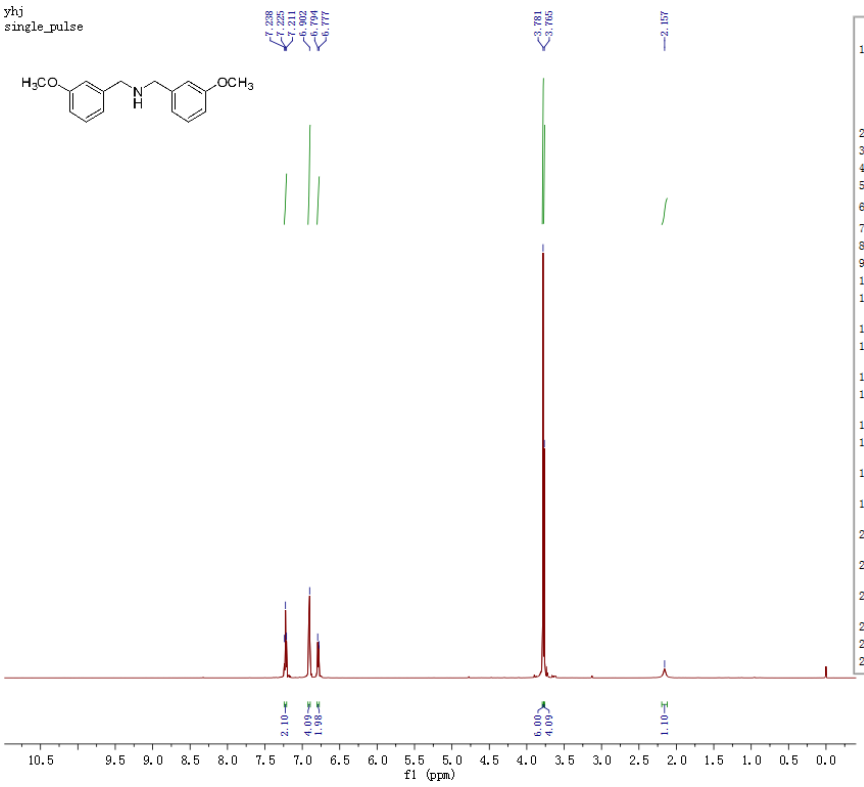

	Parameter	Value
1	Data File Name	D:/ liulei/ 艾永建-12个氢谱12个碳谱/ 艾永建-12个氢谱12个碳谱/ lql-ayj-180515-13shang-H-single_pulse-3.jdf
2	Title	yhj
3	Comment	single_pulse
4	Origin	JEOL
5	Owner	
6	Site	
7	Spectrometer	ECA 600
8	Author	HappyNMR
9	Solvent	CHLOROFORM-D
10	Temperature	24.0
11	Pulse Sequence	single_pulse.ex2
12	Experiment	1D
13	Number of Scans	16
14	Receiver Gain	28
15	Relaxation Delay	2.0000
16	Pulse Width	7.1000
17	Acquisition Time	2.9098
18	Acquisition Date	2018-05-18T16:45:16
19	Modification Date	2018-05-18T17:01:45
20	Spectrometer Frequency	600.17
21	Spectral Width	9008.5
22	Lowest Frequency	-321.7
23	Nucleus	1H
24	Acquired Size	32768
25	Spectral Size	26214

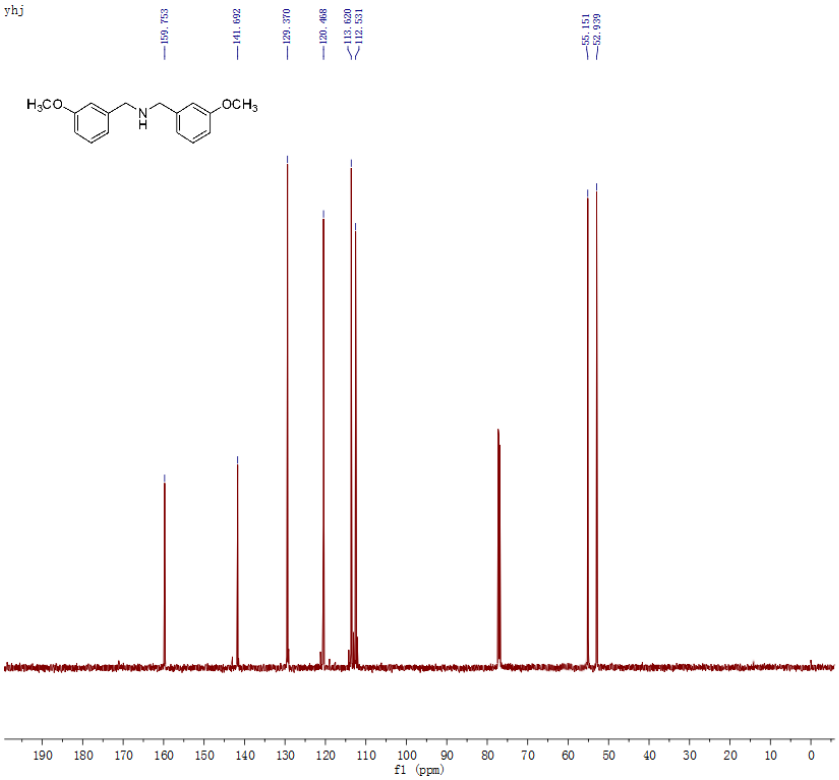

	Parameter	Value
1	Data File Name	D:/ liulei/ 艾永建-12个氢谱12个碳谱/ 艾永建-12个氢谱12个碳谱/ lql-ayj-180515-13shang-C-single_pulse_dec-3.jdf
2	Title	yhj
3	Comment	
4	Origin	JEOL
5	Owner	
6	Site	
7	Spectrometer	ECA 600
8	Author	HappyNMR
9	Solvent	CHLOROFORM-D
10	Temperature	25.0
11	Pulse Sequence	single_pulse_dec
12	Experiment	1D
13	Number of Scans	110
14	Receiver Gain	58
15	Relaxation Delay	2.0000
16	Pulse Width	4.0833
17	Acquisition Time	0.6921
18	Acquisition Date	2018-05-18T16:28:55
19	Modification Date	2018-05-18T16:45:44
20	Spectrometer Frequency	150.91
21	Spectral Width	37876.8
22	Lowest Frequency	-3868.0
23	Nucleus	13C
24	Acquired Size	32768
25	Spectral Size	26214

yhj
single_pulse

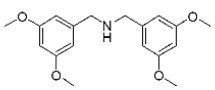

	Parameter	Value
1	Data File Name	D:/ liulei/ Fw_thunmr-180423/ lql-ayj-180423-5shang-H-single_pulse-2.jdf
2	Title	yhj
3	Comment	single_pulse
4	Origin	JEOL
5	Owner	
6	Site	
7	Spectrometer	ECA 600
8	Author	HappyNMR
9	Solvent	CHLOROFORM-D
10	Temperature	24.3
11	Pulse Sequence	single_pulse.ex2
12	Experiment	1D
13	Number of Scans	16
14	Receiver Gain	20
15	Relaxation Delay	2.0000
16	Pulse Width	7.1000
17	Acquisition Time	2.9098
18	Acquisition Date	2018-04-23T15:42:44
19	Modification Date	2018-04-23T15:58:26
20	Spectrometer Frequency	600.17
21	Spectral Width	9008.5
22	Lowest Frequency	-315.1
23	Nucleus	1H
24	Acquired Size	32768
25	Spectral Size	26214

yhj

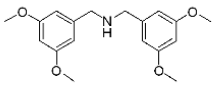

	Parameter	Value
1	Data File Name	D:/ liulei/ Fw_thunmr-180423/ lql-ayj-180423-5shang-C-single_pulse_dec-3.jdf
2	Title	yhj
3	Comment	
4	Origin	JEOL
5	Owner	
6	Site	
7	Spectrometer	ECA 600
8	Author	HappyNMR
9	Solvent	CHLOROFORM-D
10	Temperature	25.2
11	Pulse Sequence	single_pulse_dec
12	Experiment	1D
13	Number of Scans	115
14	Receiver Gain	58
15	Relaxation Delay	2.0000
16	Pulse Width	4.0833
17	Acquisition Time	0.6921
18	Acquisition Date	2018-04-23T15:48:30
19	Modification Date	2018-04-23T16:04:28
20	Spectrometer Frequency	150.91
21	Spectral Width	37876.8
22	Lowest Frequency	-3847.0
23	Nucleus	13C
24	Acquired Size	32768
25	Spectral Size	26214

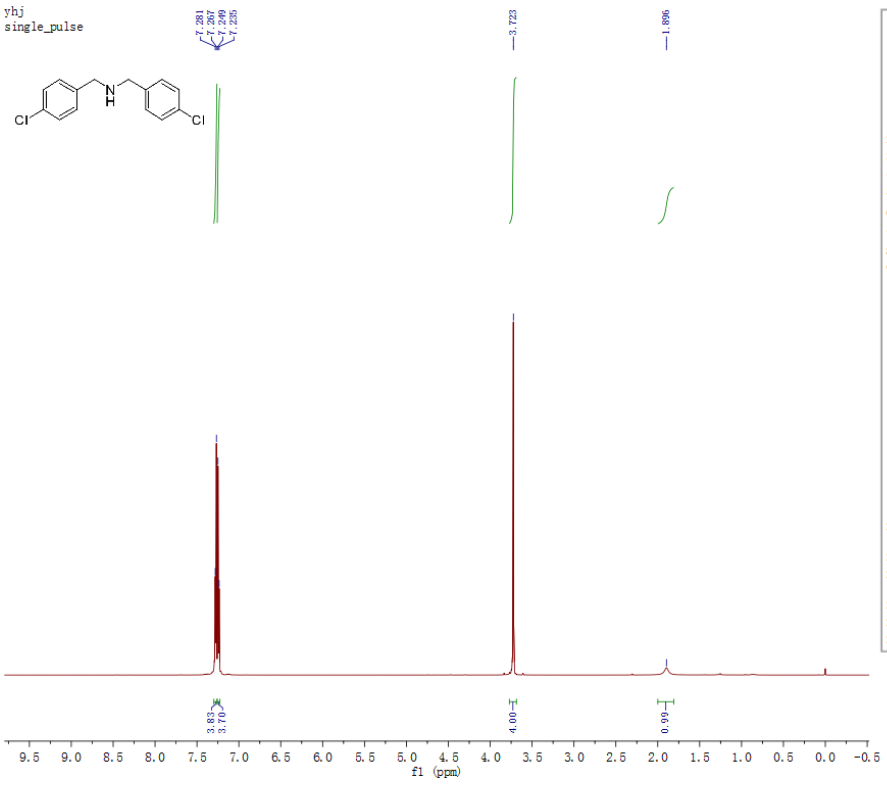

	Parameter	Value
1	Data File Name	D:/ liulei/ Fw_thunmr-180423/ lql-ayj-180423-4shang-H-single_pulse-3.jdf
2	Title	yhj
3	Comment	single_pulse
4	Origin	JEOL
5	Owner	
6	Site	
7	Spectrometer	ECA 600
8	Author	HappyNMR
9	Solvent	CHLOROFORM-D
10	Temperature	24.1
11	Pulse Sequence	single_pulse.ex2
12	Experiment	1D
13	Number of Scans	16
14	Receiver Gain	30
15	Relaxation Delay	2.0000
16	Pulse Width	7.1000
17	Acquisition Time	2.9098
18	Acquisition Date	2018-04-23T15:20:36
19	Modification Date	2018-04-23T15:36:49
20	Spectrometer Frequency	600.17
21	Spectral Width	9008.5
22	Lowest Frequency	-315.1
23	Nucleus	1H
24	Acquired Size	32768
25	Spectral Size	26214

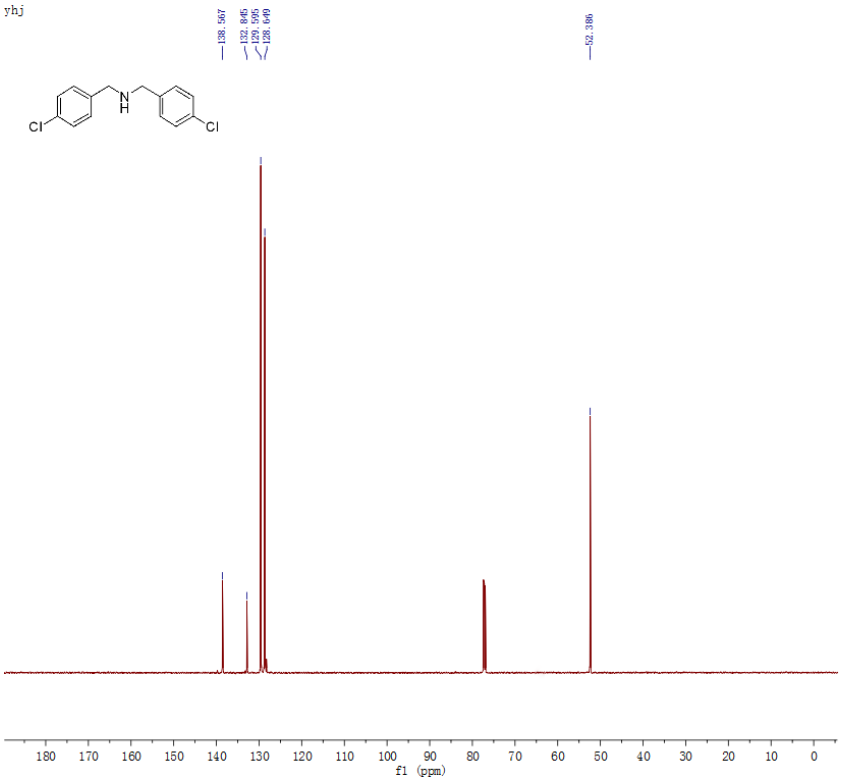

	Parameter	Value
1	Data File Name	D:/ liulei/ Fw_thunmr-180423/ lql-ayj-180423-4shang-C-single_pulse_dec-2.jdf
2	Title	yhj
3	Comment	
4	Origin	JEOL
5	Owner	
6	Site	
7	Spectrometer	ECA 600
8	Author	HappyNMR
9	Solvent	CHLOROFORM-D
10	Temperature	25.3
11	Pulse Sequence	single_pulse_dec
12	Experiment	1D
13	Number of Scans	343
14	Receiver Gain	56
15	Relaxation Delay	2.0000
16	Pulse Width	4.0833
17	Acquisition Time	0.6921
18	Acquisition Date	2018-04-23T15:36:54
19	Modification Date	2018-04-23T15:52:37
20	Spectrometer Frequency	150.91
21	Spectral Width	37876.8
22	Lowest Frequency	-3847.0
23	Nucleus	13C
24	Acquired Size	32768
25	Spectral Size	26214

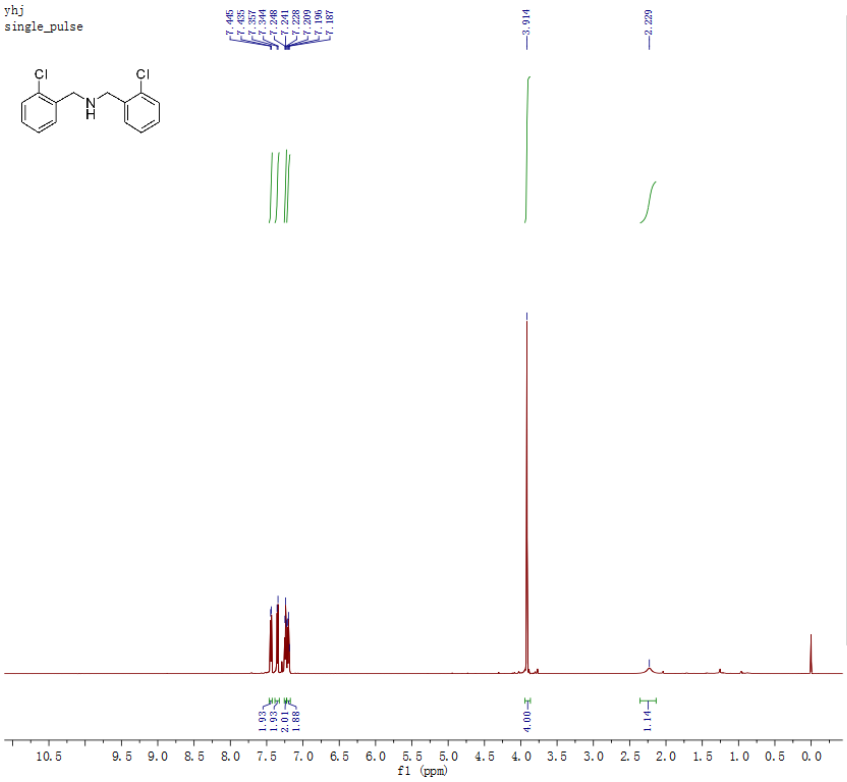

	Parameter	Value
1	Data File Name	D:/ liulei/ 艾永建-12个氢谱12个碳谱/ 艾永建-12个氢谱12个碳谱/ lql-ayj-180515-11shang-H-single_pulse-2.jdf
2	Title	yhj
3	Comment	single_pulse
4	Origin	JEOL
5	Owner	
6	Site	
7	Spectrometer	ECA 600
8	Author	HappyNMR
9	Solvent	CHLOROFORM-D
10	Temperature	23.9
11	Pulse Sequence	single_pulse.ex2
12	Experiment	1D
13	Number of Scans	16
14	Receiver Gain	40
15	Relaxation Delay	2.0000
16	Pulse Width	7.1000
17	Acquisition Time	2.9098
18	Acquisition Date	2018-05-18T11:21:36
19	Modification Date	2018-05-18T11:37:15
20	Spectrometer Frequency	600.17
21	Spectral Width	9008.5
22	Lowest Frequency	-304.3
23	Nucleus	1H
24	Acquired Size	32768
25	Spectral Size	26214

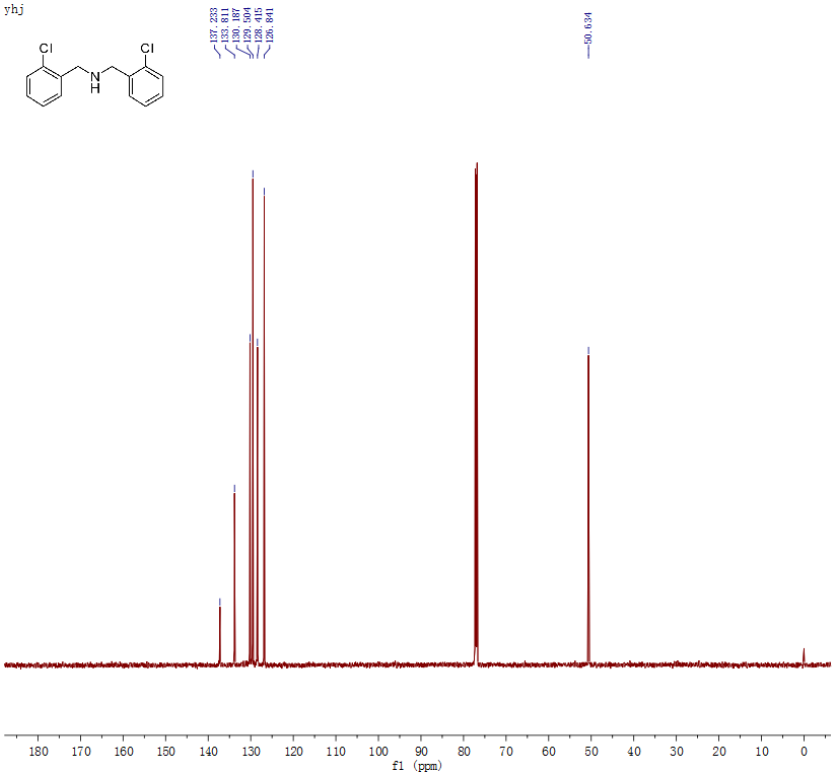

	Parameter	Value
1	Data File Name	D:/ liulei/ 艾永建-12个氢谱12个碳谱/ 艾永建-12个氢谱12个碳谱/ lql-ayj-180515-11shang-C-single_pulse_dec-3.jdf
2	Title	yhj
3	Comment	
4	Origin	JEOL
5	Owner	
6	Site	
7	Spectrometer	ECA 600
8	Author	HappyNMR
9	Solvent	CHLOROFORM-D
10	Temperature	25.2
11	Pulse Sequence	single_pulse_dec
12	Experiment	1D
13	Number of Scans	1024
14	Receiver Gain	58
15	Relaxation Delay	2.0000
16	Pulse Width	4.0833
17	Acquisition Time	0.6921
18	Acquisition Date	2018-05-18T12:08:10
19	Modification Date	2018-05-18T12:25:15
20	Spectrometer Frequency	150.91
21	Spectral Width	37876.8
22	Lowest Frequency	-3862.4
23	Nucleus	13C
24	Acquired Size	32768
25	Spectral Size	26214

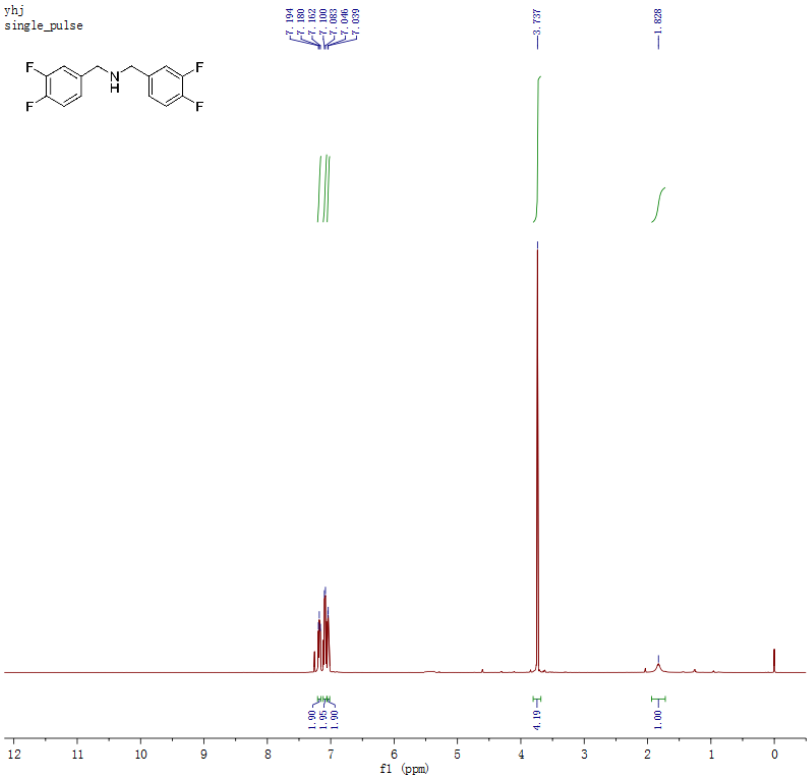

	Parameter	Value
1	Data File Name	D:/ liulei/ 氧基还原核磁/ 刘磊-12个氢谱12个碳谱/ 刘磊-12个氢谱12个碳谱/ lql-11-180521-17shang-H-single_pulse-4.jdf
2	Title	yhj
3	Comment	single_pulse
4	Origin	JEOL
5	Owner	
6	Site	
7	Spectrometer	ECA 600
8	Author	HappyNMR
9	Solvent	CHLOROFORM-D
10	Temperature	23.7
11	Pulse Sequence	single_pulse.ex2
12	Experiment	1D
13	Number of Scans	16
14	Receiver Gain	30
15	Relaxation Delay	2.0000
16	Pulse Width	7.1000
17	Acquisition Time	2.9098
18	Acquisition Date	2018-05-23T14:42:23
19	Modification Date	2018-05-23T15:12:36
20	Spectrometer Frequency	600.17
21	Spectral Width	9008.5
22	Lowest Frequency	-300.7
23	Nucleus	1H
24	Acquired Size	32768
25	Spectral Size	26214

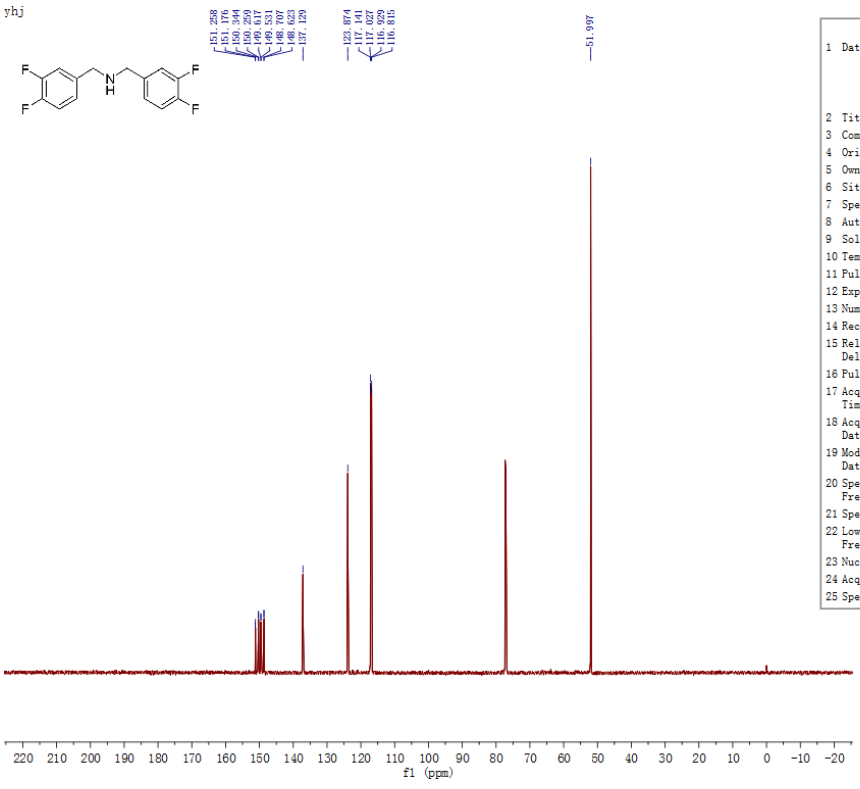

	Parameter	Value
1	Data File Name	D:/ liulei/ 氧基还原核磁/ 刘磊-12个氢谱12个碳谱/ 刘磊-12个氢谱12个碳谱/ lql-11-180521-17shang-C-single_pulse_dec-3.jdf
2	Title	yhj
3	Comment	
4	Origin	JEOL
5	Owner	
6	Site	
7	Spectrometer	ECA 600
8	Author	HappyNMR
9	Solvent	CHLOROFORM-D
10	Temperature	24.4
11	Pulse Sequence	single_pulse_dec
12	Experiment	1D
13	Number of Scans	344
14	Receiver Gain	58
15	Relaxation Delay	2.0000
16	Pulse Width	4.0833
17	Acquisition Time	0.6921
18	Acquisition Date	2018-05-23T14:58:27
19	Modification Date	2018-05-23T15:14:22
20	Spectrometer Frequency	150.91
21	Spectral Width	37876.8
22	Lowest Frequency	-3851.0
23	Nucleus	13C
24	Acquired Size	32768
25	Spectral Size	26214

yhj
single_pulse

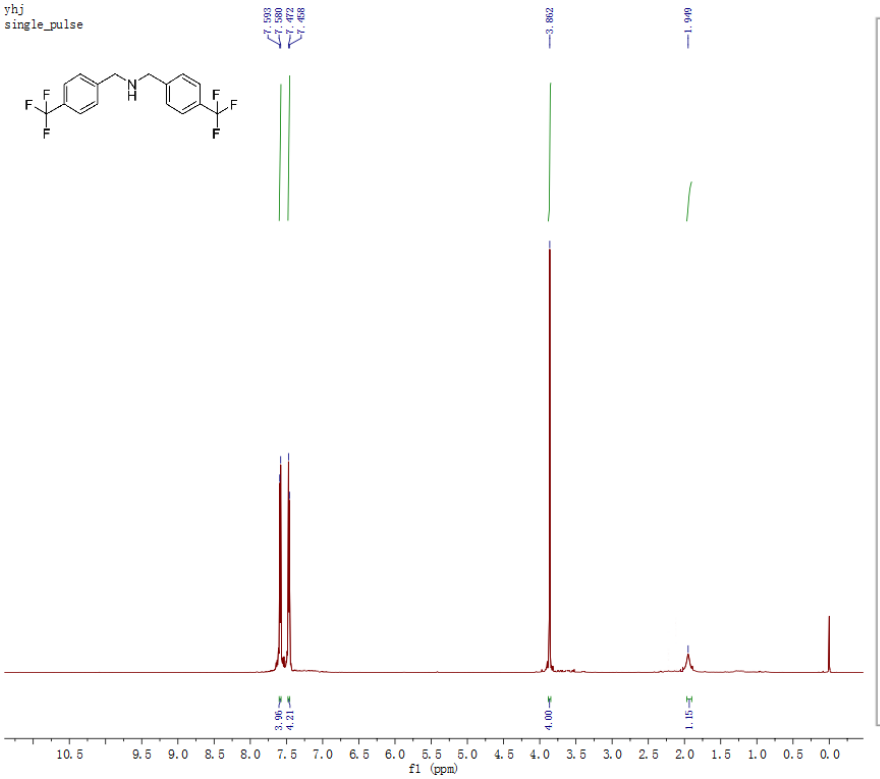

	Parameter	Value
1	Data File Name	D:/ liulei/ 艾永建-12个氢谱12个碳谱/ 艾永建-12个氢谱12个碳谱/ lql-ayj-180515-9shang-H-single_pulse-3.jdf
2	Title	yhj
3	Comment	single_pulse
4	Origin	JEOL
5	Owner	
6	Site	
7	Spectrometer	ECA 600
8	Author	HappyNMR
9	Solvent	CHLOROFORM-D
10	Temperature	23.8
11	Pulse Sequence	single_pulse.ex2
12	Experiment	1D
13	Number of Scans	16
14	Receiver Gain	36
15	Relaxation Delay	2.0000
16	Pulse Width	7.1000
17	Acquisition Time	2.9098
18	Acquisition Date	2018-05-18T13:17:12
19	Modification Date	2018-05-18T13:33:37
20	Spectrometer Frequency	600.17
21	Spectral Width	9008.5
22	Lowest Frequency	-302.5
23	Nucleus	1H
24	Acquired Size	32768
25	Spectral Size	26214

yhj

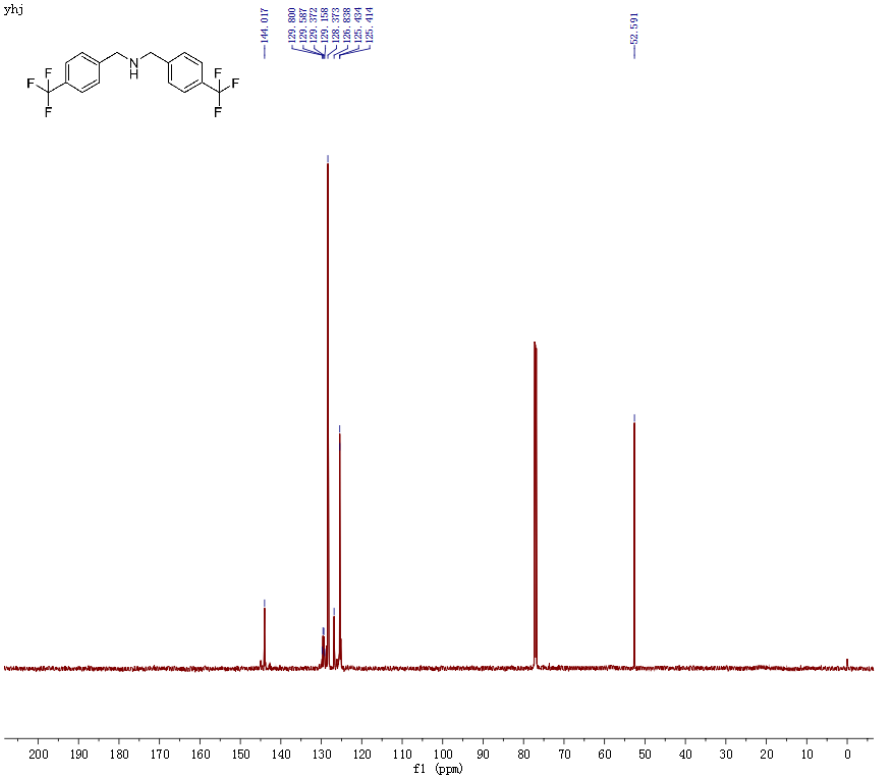

	Parameter	Value
1	Data File Name	D:/ liulei/ 艾永建-12个氢谱12个碳谱/ 艾永建-12个氢谱12个碳谱/ lql-ayj-180515-9shang-C-single_pulse_dec-3.jdf
2	Title	yhj
3	Comment	
4	Origin	JEOL
5	Owner	
6	Site	
7	Spectrometer	ECA 600
8	Author	HappyNMR
9	Solvent	CHLOROFORM-D
10	Temperature	25.0
11	Pulse Sequence	single_pulse_dec
12	Experiment	1D
13	Number of Scans	522
14	Receiver Gain	58
15	Relaxation Delay	2.0000
16	Pulse Width	4.0833
17	Acquisition Time	0.6921
18	Acquisition Date	2018-05-18T13:41:14
19	Modification Date	2018-05-18T13:58:02
20	Spectrometer Frequency	150.91
21	Spectral Width	37876.8
22	Lowest Frequency	-3852.3
23	Nucleus	13C
24	Acquired Size	32768
25	Spectral Size	26214

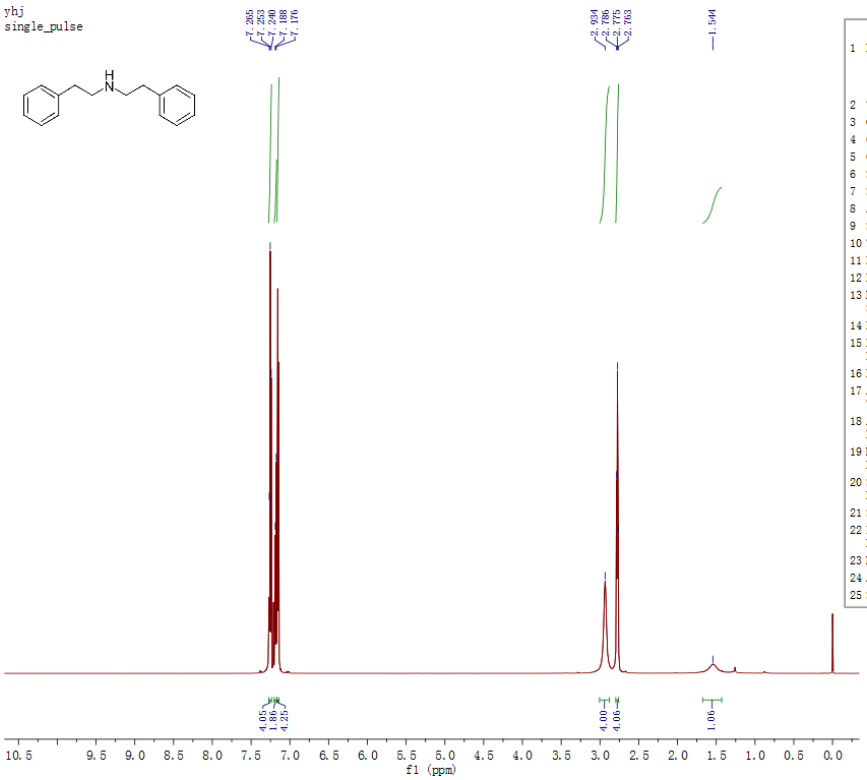

	Parameter	Value
1	Data File Name	D:/ liulei/ 氰基还原核磁/ lql-11-180704-16shang-H-single_pulse-3.jdf
2	Title	yhj
3	Comment	single_pulse
4	Origin	JEOL
5	Owner	
6	Site	
7	Spectrometer	ECA 600
8	Author	HappyNMR
9	Solvent	CHLOROFORM-D
10	Temperature	26.1
11	Pulse Sequence	single_pulse.ex2
12	Experiment	1D
13	Number of Scans	16
14	Receiver Gain	30
15	Relaxation Delay	2.0000
16	Pulse Width	7.1000
17	Acquisition Time	2.9098
18	Acquisition Date	2018-07-04T15:18:16
19	Modification Date	2018-07-04T15:40:12
20	Spectrometer Frequency	600.17
21	Spectral Width	9008.5
22	Lowest Frequency	-327.1
23	Nucleus	1H
24	Acquired Size	32768
25	Spectral Size	26214

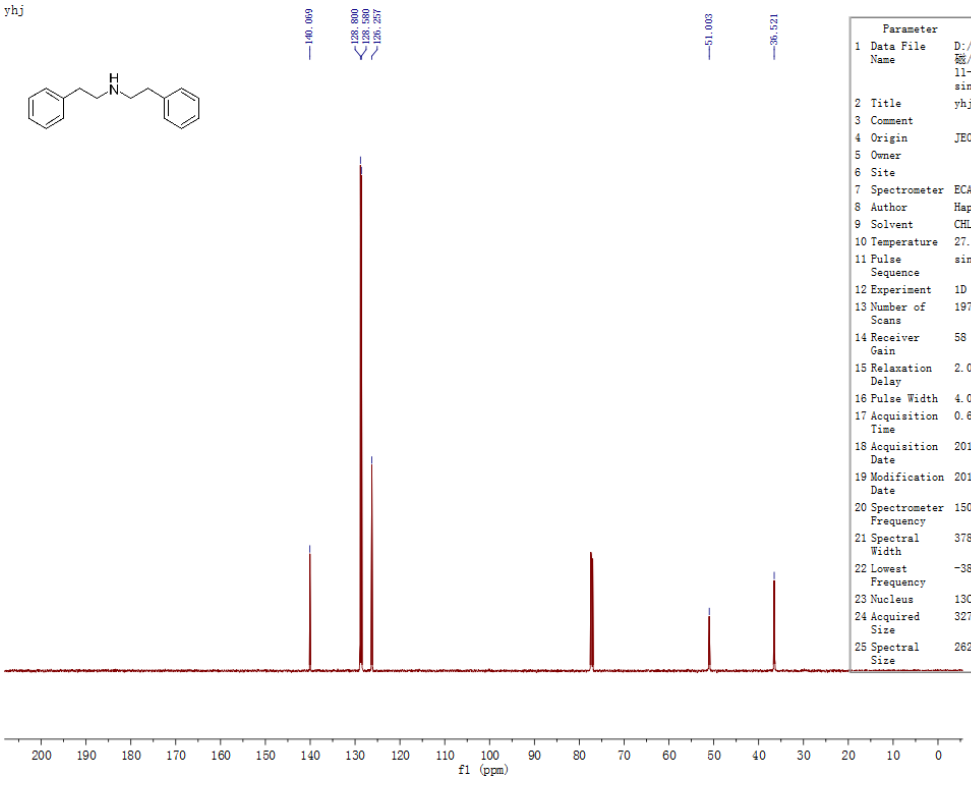

	Parameter	Value
1	Data File Name	D:/ liulei/ 氰基还原核磁/ lql-11-180704-16shang-C-single_pulse_dec-2.jdf
2	Title	yhj
3	Comment	
4	Origin	JEOL
5	Owner	
6	Site	
7	Spectrometer	ECA 600
8	Author	HappyNMR
9	Solvent	CHLOROFORM-D
10	Temperature	27.1
11	Pulse Sequence	single_pulse_dec
12	Experiment	1D
13	Number of Scans	197
14	Receiver Gain	58
15	Relaxation Delay	2.0000
16	Pulse Width	4.0833
17	Acquisition Time	0.6921
18	Acquisition Date	2018-07-04T15:27:53
19	Modification Date	2018-07-04T15:47:13
20	Spectrometer Frequency	150.91
21	Spectral Width	37876.8
22	Lowest Frequency	-3847.0
23	Nucleus	13C
24	Acquired Size	32768
25	Spectral Size	26214

Reference

Adam, R., Alberico, E., Baumann, W., Drexler, H.-J., Jackstell, R., Junge, H. & Beller, M. (2016). NNP-Type Pincer Imidazolylphosphine Ruthenium Complexes: Efficient Base-Free Hydrogenation of Aromatic and Aliphatic Nitriles under Mild Conditions. *Chem. Eur. J.,* 22**,** 4991-5002.

Adam, R., Bheeter, C. B., Cabrero-Antonino, J. R., Junge, K., Jackstell, R. & Beller, M. (2017). Selective Hydrogenation of Nitriles to Primary Amines by using a Cobalt Phosphine Catalyst. *Chemsuschem,* 10**,** 842-846.

Lu, S., Wang, J., Cao, X., Li, X. & Gu, H. (2014). Selective synthesis of secondary amines from nitriles using Pt nanowires as a catalyst. *Chem. Commun.,* 50**,** 3512-3515.

Mukherjee, A., Srimani, D., Ben-David, Y. & Milstein, D. (2017). Low-Pressure Hydrogenation of Nitriles to Primary Amines Catalyzed by Ruthenium Pincer Complexes. Scope and mechanism. *Chemcatchem,* 9**,** 559-563.

Shao, Z., Fu, S., Wei, M., Zhou, S. & Liu, Q. (2016). Mild and Selective Cobalt-Catalyzed Chemodivergent Transfer Hydrogenation of Nitriles. *Angew. Chem. Int. Edit.,* 55**,** 14653-14657.

Zen, Y.-F., Fu, Z.-C., Liang, F., Xu, Y., Yang, D.-D., Yang, Z., Gan, X., Lin, Z.-S., Chen, Y. & Fu, W.-F. (2017). Robust Hydrogenation of Nitrile and Nitro Groups to Primary Amines Using Ni2P as a Catalyst and Ammonia Borane under Ambient Conditions. *Asian. J. Org. Chem.,* 6**,** 1589-1593.